GENESIS OF GOLD MINERALIZATION IN ATTAPPADI, SOUTHERN GRANULITE TERRAIN, INDIA

A THESIS

Submitted in partial fulfilment of the requirements for the award of the degree of

DOCTOR OF PHILOSOPHY

in

EARTH SCIENCES

by

PRADEEPKUMAR T

DEPARTMENT OF EARTH SCIENCES
INDIAN INSTITUTE OF TECHNOLOGY ROORKEE
ROORKEE - 247 667 (INDIA)

OCTOBER, 2008

INDIAN INSTITUTE OF TECHNOLOGY ROORKEE
ROORKEE

CANDIDATE'S DECLARATION

I hereby certify that the work which is being presented in this thesis entitled **GENESIS OF GOLD MINERALIZATION IN ATTAPPADI, SOUTHERN GRANULITE TERRAIN, INDIA** in partial fulfillment of the requirements for the award of the Degree of Doctor of Philosophy and submitted in the Department of Earth Sciences, Indian Institute of Technology Roorkee, Roorkee is an authentic record of my own work carried out during a period from July 2004 to October 2008 under the supervision of Dr. R. Krishnamurthi, Associate Professor, Department of Earth Sciences, Indian Institute of Technology Roorkee, Roorkee.

The matter presented in this thesis has not been submitted by me for the award of any other degree of this or any other University/Institute.

(PRADEEPKUMAR T)

This is to certify that the above statement made by the candidate is correct to the best of my knowledge.

(R.Krishnamurthi)
Supervisor

Date: 16/10/2008

The Ph.D. Viva-Voce Examination of **Mr. Pradeepkumar T**, Research Scholar, has been held on 20/9/2010.

Signature of Supervisor

Signature of External Examiner
20/9/10

Acknowledgements

This project was conceived by Dr.R.Krishanamurthi who recognized the significance of the Attappadi supracrustals in addressing Genesis of gold mineralization. I hope that this thesis goes some way towards answering the questions that occupied so many of our discussions. Thanks for your encouragement, advice and belief.

I would like to thank Dr.Rajesh Sharma, Wadia institute of Himalayan Geology for allowing me to use his fluid inclusion lab for analyzing and discussing the data. I also convey my deep and sincere gratitude and indebtness to Dr.V.Ravikantth for his constructive suggestions, motivation and support as and when required. His sincerity and helping nature shall always be remembered with gratitude and respect. I would like to thank Dr.R.V.G Nair at Geological Survey of India for his involvement and supervision in the field. I also would like to thank Dr.S.Balakrishanan, for discussing geochemical data and for giving valuable information from his special field of study.I also convey my deep and sincere gratitude and indebtness to Dr. A. K. Sen, Associate Professor, Earth Sciences Department, Indian Institute of Technology, Roorkee for his day to day involvement and supervision from day one till end of the research work. I would like to thank all my committee members for their comment and suggestions. Additional thanks to Dr.K.L Puruseth for who graciously filled a vacancy on my committee at the last moment.

I extend my profound gratitude to Prof. R.P.Gupta, Head of the Department, Earth Sciences IIT Roorkee for his administrative help for successful completion of this thesis.

I have been greatly assisted during my studies by many of the technical staff at IIT Roorkee. A special thanks to "Nair ettan "who shared the wonderful days in Roorkee. You do not get to do good research, or for that matter anything, if you do not have good friends around you. I am lucky to have several of them who had propelled me to whosoever I am with their constant love and encouragement Gadhi, Fahd, Saju, Vivek, Sony, Kiran, Varun, , Ebin, Sajin, Anish, Rahul Jainet, Manoj,Emjee Gautham, Jomi, Manish, Nibu, Anand, Purushothaman, Deepthy, Ritu, Smitha, Dhanya, Anitha chichi, Ambili chechi and many others, I thank you all for being with me always.

I have been blessed with enduring support from my family during this long journey. My wife, Nisha and sweet little daughter Sreelakshmi have been incredibly patient and been unending source of encouragement. My Amma, achan, chettan, chechi, karthikuttan have also been extemly generous and supportive. With out their help, this long journey would not have ended. I will keep their endeavors in my dreams for ever.

The financial support I received from Ministry of Human Resource development (MHRD), India duly acknowledged.

Place: Roorkee

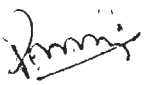

Date: 16-10-2008 (PRADEEPKUMAR T)

List of Figures

List of Tables

List of Abbreviations

EPMA	- Electron Probe Micro Analyzer
HREE	- Heavy Rare Earth Elements
IIT	- Indian Institute of Technology
ICP-MS	- Inductively Coupled Plasma-Atomic Emission Spectrometer
LILE	- Light Ion Lithophile Elements
LREE	- Light Rare Earth Elements
Ma	- Million years
MHRD	- Ministry of Human Resource development
REE	- Rare Earth Elements
XRF	- X-ray Fluorescence Sequential Spectrometer

Abstract

In India more than 99 percentage of the total primary gold is from a vast expanse of over 4,0000 sq.km area covering major part of Karnataka, Andhra Predesh, Tamil Nadu and Kerala. Therefore, it is imperative to fully assess the gold potential of the gold fertile land of southern India. Traditionally, high grade metamorphic settings have been regarded as unfavorable for hosting gold deposits. As a result, exploration as well as research has been biased towards amphibolite facies and lower grade metamorphic settings in Precambrian terrains. However, now it is becoming increasingly clear that gold deposits do occur in granulite facies terrains and these areas are unexplored. This is an attempt to look at the evolutionary history of gold deposits in Southern Granulite Terrain using geochemical, fluid inclusion study and taking into consideration of the existing knowledge from published structural and geochronological studies.

Metavolcanics and metasedimentary rocks designated as 'Attappadi supracrustals' occur as enclaves and remnants within the gneisses exposed in the crustal scale Bhavani shear zone. The assemblage of rock types such as metapyroxinite, talc-tremolite-actinolite schist, amphibolites, Banded Iron Formations (BIF), sillimanite/kyanite bearing quartzite and *fuchsite* quartzite in Attappadi represents a greenstone belt setup. Geochemical studies of metavolcanics show that the Attappadi greenstone belt consists of Fe-rich tholeiites. This metavolcanics (tholeiitic composition) intercalated Algoma type BIF. The chondrite-normalized REE patterns of low K-tholeiite of Attappdi exhibit enrichments in LREE with respect to HREE. The possible reasons for overall enrichment of LREE reflect the composition of an enriched source EMORB or related to metasomatic enrichment in a hydrothermal system. The BIFs show LREE enrichment

with a striking positive Eu anomaly. Possible source materials of positive Eu anomaly of BIF have been attributed to a hydrothermal activity in oceanic environment.

Considering various criteria like lithological assemblages, geological setting and geochemistry it is proposed that at least a major part of the volcanism of the Attappadi supracrustal sequence must have evolved in a spreading center tectonic setting. The protoliths of gneisses in Attappadi are of monzodioritic in composition, they are intruded into the Attappadi supracrustals during the melting of lower crust in a convergent tectonic setting and crustal thickening possibly associated with a subduction related processes, during the late stage of greenstone belt deformation have provided a favorable geochemical environment for gold mineralization under the conditions of deformation and metamorphism.

The mineralized zones typically occur within or in the vicinity of regional, crustal-scale deformation zones with a brittle to ductile type of deformation.The veins are concentrated in a 20-to 30-km wide 30-km long, linear NE-SW trending zone. The regional-scale sigmoidal pattern of the vein arrays strongly suggests that this broad zone acted as a regional scale shear zone. Gold is intimately associated with sulfide minerals, including pyrite, pyrrhotite chalcopyrite and galena in quartz veins. One or possibly two mineralizing events appear to have deposited gold in Attappadi greenstone belt. The first stage gave rise to a mineral assemblage consisting of simultaneous pyrite and gold deposition and followed by a late stage deposition of chalcopyrite and galena filling microfractures in quartz. Fe-rich tholeiite possibly under different physical conditions must have provided required sulfur and gold to hydrothermal fluid in Attappadi greenstone belt.

Fluid inclusion study of gold-quartz veins in Attappadi area provide good evidence of fluid chemistry, depositional environment, and origin of mineralizing fluids in this deformed terrain. The mineralizing fluids have relatively low salinity (3-6wt%NaCl eq.), consistent density of CO_2 (0.6-0.7 g/cm^3) and H_2-O-CO_2 rich. During the late stage of Attappadi greenstone belt deformation and metamorphism, the circulating hydrothermal fluids (H_2O-CO_2 fluid) were responsible for the breakdown of ferromagnesian minerals and release of silica which along with gold from the tholeiite rocks formed the quartz veins within the shear zones. This is correlated to the higher gold content available in the mafic rocks and also corroborated by the spatial proximity of the auriferous quartz veins to them. Alternatively magmatic fluid can also be considered as possible source for vein-type gold deposit in Attappadi, mainly because of the widespread distribution of granitic intrusive in the supracrustals. However, less saline and H_2O-CO_2 fluids in inclusions present in quartz veins have relatively consistent composition throughout Attappadi region suggesting a regional uniform, homogeneous fluid source related to metamorphism.

The combination of the fluid inclusion and other data suggest a pressure-temperature range of ore formation of the order of 250-300°C and 2.5 kb. The close association of gold with sulfide minerals within quartz veins indicates that gold was transported as bi-sulfide complexes. The phase separation due to the lowering of lithostatic pressure during regional upliftment caused fluid immiscibility which has been proposed as the principle mechanism for gold deposition in Attappadi greenstone belt.

Summing up the source of fluids, the Attappadi greenstone belt constitutes orogenic gold deposits that formed by metamorphic fluids from accretionary processes

and generated by prograde metamorphism and thermal re-equilibration of subducted volcano-sedimentary terrains.

Contents

CHAPTER 1

Introduction

INTRODUCTION

Gold is relatively scarce in the earth, but it occurs in different types of rocks and in many different geological environments. Though scarce, gold is concentrated by geological processes to form commercial deposits of two principal types: lode (primary) deposits and placer (secondary) deposits. Lode deposits are the targets for the "hardrock" prospector seeking gold at the site of its deposition from mineralizing solutions, are important class of deposits whose total gold production is second only to that of the Witwatersrand palaeoplacer deposit. Lode gold deposits also called as mesothermal gold, metamorphic gold, gold-only, shear-zone hosted, structurally-controlled deposits (Misra, 2000) and recently, the term orogenic gold deposits has been proposed (Groves et al., 1998). This type of deposits occurs primarily in greenstone belts of Archaean cratons such as those in Australia, Brazil, Canada, India and South Africa, as well as Mesozoic and Cenozoic age rocks in orogenic belts like the North American Cordillera (Goldfarb et al., 2001). Lode gold deposits are present in metamorphic terrains of various ages, displaying variable degrees of deformation. The host geological environments include volcano-plutonic and clastic sedimentary terrains. The host rocks have been characteristically metamorphosed up to greenschist facies conditions, and locally to amphibolite or granulite facies conditions. The gold deposits typically occur within or in the vicinity of regional, crustal-scale deformation zones with a brittle to ductile type of deformation. The geological structures generally indicate compressional to transpressional tectonic settings (Phillips et al., 1993; Groves et al., 2003).

Detailed studies on lode gold deposits of Archaean greenstone belts in different continents have resulted in certain general consensus on host rocks,

metamorphism, structural setting (regional and deposit scale), style of mineralization, hydrothermal alteration and P-T conditions of formation. But there is still a considerable debate on the source of ore fluid-metals and concentration mechanisms responsible for mineralization (Groves et al., 2003). From fluid inclusion studies, it has been observed that the presence of CO_2 rich fluid is entirely consistent in Archaean lode gold deposits (Pandalai et al., 2003; Mao et al., 2008), and is quite distinct with respect to fluids encountered in other major classes of ore types. Because of the difficulties in defining a unique source of gold-fluid, a number of genetic models have been proposed (the proposed models are discussed in detail in chapter 2). Thus gold deposits must have formed by a variety of process involving different source rocks during the evolution of greenstone belts. In order to understand the Archaean gold metallogeny better, individual deposits and their associated rocks need to be studied in detail.

In India, gold mineralization of economic importance is restricted to greenstone-type lithostratigraphic sequences (amphibolite facies) occurring in western and eastern parts of Dharwar Craton (DC) of South India (Radhakrishana and Curtis, 1999). Few lesser known gold occurrences have also been reported from Moyar and Bhavani shear zones (Figure 1.1) within Southern Granulite Terrain (SGT). Since time immemorial, the Wynad within Moyar Shear Zone (MSZ) and adjoining regions in SGT were known for gold occurrences (Santosh et al., 1990), where as, gold mineralization in Bhavani Shear Zone (BSZ) in Attappadi area is a recent discovery (Nair, 1993). There have been significant studies from Wynad gold field on ore petrography, fluid inclusions and isotopic signatures to understand the genesis of gold mineralization (Sawarkar, 1980; Nair et al., 1987; Binu-Lal et al., 2003; Malathi and Srikantappa, 2005). But for Attappadi gold mineralization no unequivocal evidence

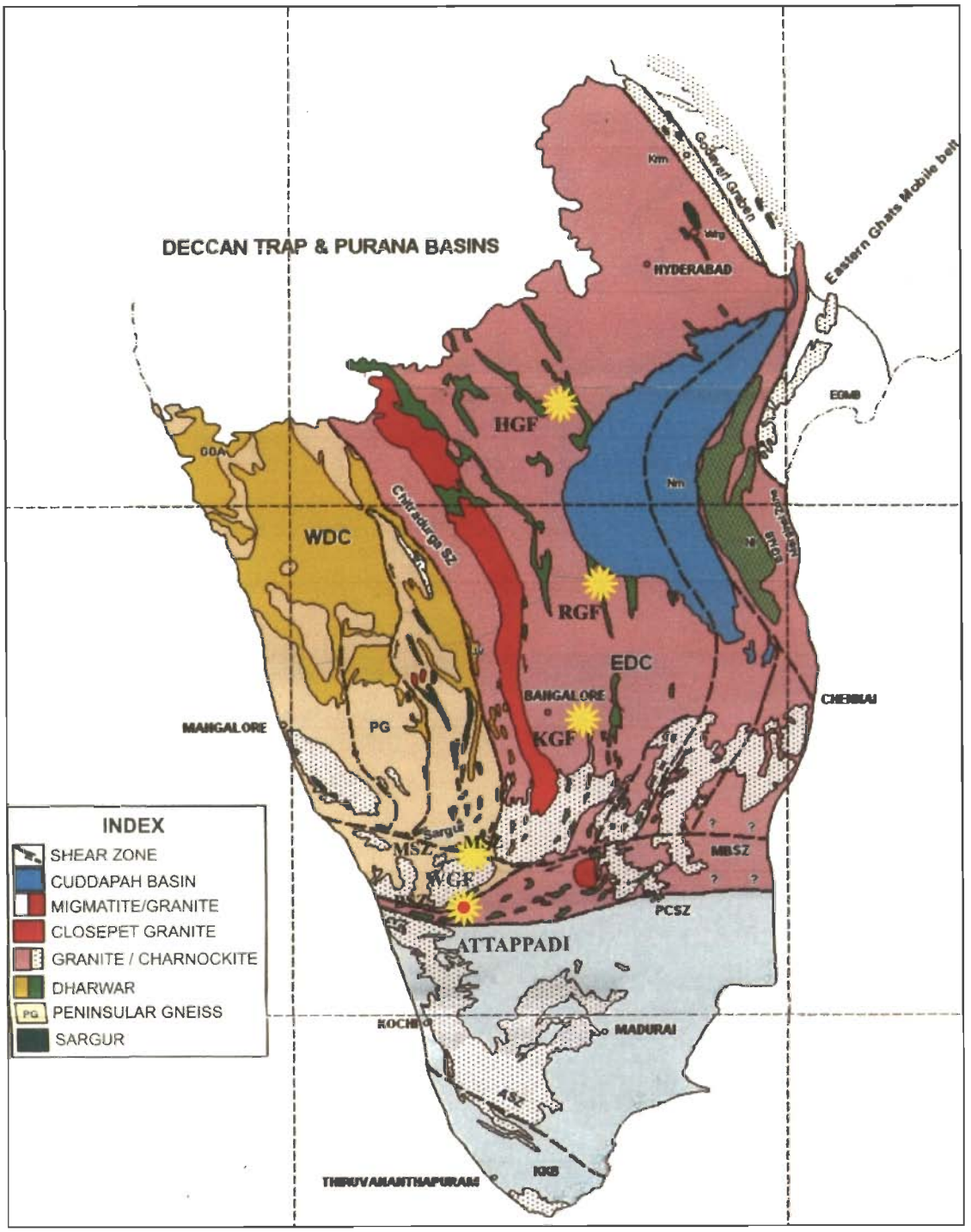

Figure 1.1 Locality of major gold fields in Peninsular India plotted on a simplified geological map taken from Ramakrishnan and Vaidyanadhan (2008) HGF-Hutti Gold field,RGF-Ramagiri Gold field,Kolar Gold field, WGF-Wyanad Gold field

was suggested for source of gold/ hydrothermal fluids and the processes that operated to concentrate the gold in quartz veins. So far, no integrated work has been carried out involving field, petrographic, ore microscopic, fluid inclusion and geochemical studies to arrive at a conceptual model for gold mineralization in Attappadi.

The formation of epigenetic gold mineralization in greenstone belts is generally explained by the metamorphic secretion theory. This theory is based on the assumption that the source of the gold may be komatiitic or tholeiitic lavas, chemical or clastic sediments and even granitic rocks from which, as a result of regional metamorphic overprinting, gold was extracted and concentrated in suitable structures (Saager et al., 1982). In any metallogenic concept based on metamorphic secretion the availability and, therefore, the siting of gold in potential source rocks is of great importance. For this reason, the mineralogical sitting of gold in various types of potential source rocks has been discussed by a number of workers (Boyle 1979; Gottfried et al., 1972; Tilling et al., 1973; Crocket 1974; Ramdohr 1975; Keays and Scott 1976; Saager et al., 1982). In most papers a preferential association of gold with sulfides is suggested. The present study area Attappadi also not an exception where, gold is associated with sulfides of different generation (Nair et al., 1996), in order to understand the metallogenic episodes in BSZ detailed ore microscopic studies were carried out.

An assessment of contribution to total gold production shows that mafic volcanic rocks are by far the most important source rocks in several regions (Kolar, Ramagiri, Hutti schist belt in the DC, South India, Siva Siddaiah and Rajamani 1984, Zachariah et al., 1992; Girithran and Rajamani, 1998, Yilgramm block, Grooves and Phillips, 1987, Zimbabwe Craton, Foster, 1995). The Attappadi gold deposit also shows a marked volcanic host rock control. The petrogenetic study of host

metavolcanics in the DC unraveled a genetic link between the high iron tholeiite and gold mineralization (Giritharan and Rajamani, 1998). Thus, the petrogenetic study of the host rocks (metavolcanics, gneisses and BIF) associated with the auriferous quartz vein becomes more important and inspired the present study.

The second major goal of this dissertation has been to reconstruct as much as possible the geochemical and PVTX conditions of hydrothermal system responsible for gold mineralization. The basic questions to be addressed are: What is the source for gold and concentration mechanism responsible for mineralization in Bhavani shear zone? What was the nature of aqueous species dissolved the gold? What caused the deposition of gold in Attappadi area of Bhavani shear zone?

Fluid inclusion microthermometry has been abundantly used to define fluid composition, processes, pressure-temperature and ore forming conditions of lode gold deposits. Based on this study it has been proposed that the ore forming fluids were H_2O-CO_2, normally with 10-25 mol % CO_2, low salinity ($\leq$10 wt% NaCl equivalent), and moderate density (0.9 g/cm^3). The combination of the fluid inclusion and other data suggest a pressure-temperature range of ore formation of 1-3 kb and 250-350°C. Some shallow deposits must have formed as low as 0.5 kb and 150°C, and deeper deposits under higher pressures up to 5 kb and higher temperatures of 700°C (Hagemann and Brown, 1996).

Problems associated to fluid inclusion studies in syntectonic, orogenic gold deposits are their possible reequilibration due to overprinting deformation and uplift/exhumation following formation of the deposits. The gold mineralization in Attappadi is spatially and or genetically related to reactivated BSZ. The Archaean-Proterozoic rock units hosted Attappadi gold mineralization occurs in very different regional and geological setting. Thus the fluid inclusion study of this deposit is

significant to characterize the fluid chemistry and to check to some extent, the main factors controlling gold remobilization and deposition in a polyphase deformed terrain.

A corollary aim has been the construction of a probable genetic model to serve as a practical guide in further ore discovery.

In order to understand the gold mineralization in Attappadi the following research methodologies have been used:

1) Field work for this project was mainly carried out over two months in July August 2005. During this period, the author conducted a general overview of the regional geology of the study area, visited and assessed known Au occurrences, collected samples for petrographic, ore microscopic, fluid inclusion and geochemical research. A follow-up re-evaluation of selected areas was conducted in July 2006. A total of 220 samples were collected from filed in 2005 and 120 samples in 2006 including: 1) mineralized samples and host rocks, 2) samples for geochemistry, 3) regional rock types, 4) Quartz vein samples for fluid inclusion studies. The main foci for sample collection were the areas of previously recorded gold occurrences or prospects. Samples were prepared and analyzed at Department of Earth Science IIT Roorkee and Wadia Institute of Himalayan Geology Dehradun

2) Petrography and ore microscopic studies of host rock and ore samples to ascertain rock types, alteration and mineral assemblage.

3) Geochemical Studies: Major and trace element geochemical analysis were carried out on representative samples using X-ray fluorescence techniques and Inductively Coupled Plasma Mass Spectrophotometer (ICP - MS - Perkin Elmer SCIEX ELAN DRC e) at Wadia Institute of Himalayan Geology, Dehradun. The geochemical data were utilized to determine if any relationships exists between mineralization and

ultramafics or mafic lithologies present in the area and further determining the possible tectonic environments. Descriptions of analytical techniques and sample processing have been given in Chapter 5.

4) Fluid inclusion studies: Doubly polished wafers of mineralized veins and quartz biotite gneiss were prepared and fluid inclusions were characterized. Heating-freezing runs were conducted on a Linkam THMSG600 heating-freezing system fitted on to a Nikon E600 micoscope at the Wadia Institute of Himalayan Geology, Dehradun. The data has been used to determine the nature P-T conditions and potential source of the vein forming fluids, and to define any regional variations in the fluid chemistry. The details of the microthermometric studies have been given in chapter 6.

5) Major element analyses of selected minerals were carried out by Electron Probe Micro Analyzer (EPMA) (CAMECA - SX-100) at Wadia Institute of Himalayan Geology, Dehradun.

6) Analyses of separated gold grains from mineralized veins were using SEM-EDAX (QUANTA 200F) at Indian Institute of Technology Roorkee, Roorkee.

This current investigation evaluates the various gold occurrences and associated geological environment within BSZ:

1) To recognize the distribution pattern of metallic minerals in mineralized zones and their textural relationship with gold

2) To determine the geochemical characteristics of different geological units, specifically those known to host Au mineralization

3) To find out the source of gold in BSZ

4) To determine the nature, P-T conditions and source of the vein forming fluids

5) To propose a probable genetic model of gold mineralization in Attappadi greenstone belt

The following is my perception of the main "original contributions to knowledge" that are presented in this thesis:

1) This work presents the first comprehensive major and trace element data (including REE) for gneissic rocks in this region.

2) This work is a first effort to determine the trace element (including REE) data of metavolcanics in Attappadi. It is also the first application of fluid inclusion studies in Attappadi greenstone belt and the data provide the nature of ore fluid and precipitation mechanism of gold in BSZ.

This is first attempt to look at the evolutionary history of gold deposits in SGT using geochemical, fluid inclusion study and taking into consideration of the existing knowledge from published structural and geochronological studies.

CHAPTER 2

Greenstone-hosted lode gold deposits

GREENSTONE-HOSTED LODE GOLD DEPOSITS

2.1 Introduction

Gold mineralization in Archaean granite-greenstone environments, especially gold-quartz veins, contributes considerably to the world's gold production. Gold-quartz veins with a close spatial link to Archaean greenstones are known to occur on a world-wide scale, for instance in the Barberton Mountain Land- South Africa, in the Golden Mile of the Kalgoorlie district- Western Australia, in the Abitibi greenstone belt of the Superior structural province- Canada and Kolar Schist belt of South India (Kerrich and Cassidy, 1994; Goldfarb et al., 2001). Several authors have shown that these deposits formed during the late stages of evolution of the host granitoid-greenstone terrains (e.g Colvine, 1989). Several outstanding problems remain for greenstone-hosted lode gold deposits. Genetic considerations of these deposits must address some key components such as deposit-scale structural style, metamorphism of the host rocks (and associated rocks), alteration geochemistry, fluid characteristics with emphasis on transportation and deposition of gold. A comprehensive overview of the published literature pertaining to gold mineralization in greenstone-hosted lode gold deposits is given in this chapter. The following review shows that we have gained a fairly good knowledge about the descriptive aspects of lode gold deposits. It is recognised that they constitute an independent class of deposits with recurring characteristics throughout the geologic record and in different geologic environments. Geochronology has provided important constraints for fitting confidently the deposits into a regional tectonic evolution. On the other hand, despite intense research effort in the past two decades, sources of fluids and solutes are still intensely debated.

2.2 Structure

One of the most important factors controlling the distribution of Archaean lode gold deposits and the geometry of the ore shoots is the" Structure". On a regional scale, majority of the lode gold deposits are sited adjacent to major shear zones such as those in Western Australlia (Eisenloh et al., 1989), Canada (Colvine et al., 1984) and South Africa (Vearncombe et al., 1988) and the deposits are usually sited in subsidiary structures within regional faults/ shear zones that were "active" during the period immediately prior to cratonization. A variety of structures are mineralized, strike-, oblique-, reverse- and normal- slip shear zones all recorded as controlling gold mineralization (Goldfrab.et al., 2001). Steep reverse shear zones are particularly important ore-controlling structures (Sibson et al., 1988). In many regions Archaean lode gold deposits, the ore shoots have plunge sub parallel to the mineral- elongation lineations in the host rocks suggesting a fundamental structural link between dilation and the development of conduits which focused fluid flow (Groves and Foster, 1991). Most structures that control lode gold mineralization show features typical of brittle-ductile deformation.

2.3 Host rocks

On a craton scale many lithologies in Archaean greenstone belts may host gold mineralization. The deposits show a marked volcanic host rock control in the schist belts of Eastern Darwar Craton, India (Giritharan and Rajamani, 1998) and Western Australia (Phillips et al., 1984) and Fe rich tholeiite metabasalts host majority of the deposits in these areas. The tholeiite host rock appears important for two reasons. Firstly, they contain sufficient iron for formation of sulfides which show a strong spatial relationship to gold mineralization in many of the major Archaean lode gold deposits. Secondly, they become a competent lithology at amphibolite grade

metamorphism for brittle fracturing, so that focused fluid flow is possible for vein formation (Giritharan and Rajamani, 1998).

2.4 Vein Mineralogy

Veins in the lode gold deposits are dominated by quartz with subsidiary carbonate and sulfide minerals, and less abundantly, albite, chlorite, white mica (fuchsite in ultramafic host rocks), tourmaline, and scheelite. Carbonate minerals consist of calcite, dolomite and ankerite. Gold occurs in the veins and in adjacent wallrocks. Gold is usually intimately associated with sulfide minerals, including pyrite, pyrrhotite, chalcopyrite, galena, sphalerite and arsenopyrite. In volcano-plutonic settings, pyrite and pyrrhotite are the most common sulfide minerals in greenschist and amphibolite grade host rocks, respectively, while arsenopyrite is the predominant sulfide mineral in ores hosted by sedimentary rocks. Tellurides can be significant ore minerals in some deposits. Gold to silver ratios typically range between 10:1 and 5:1, less commonly 1:1. Although the vein systems can be continuous for over 1 to 2 km vertical extent, there is generally little change in ore grade, and ore and gangue mineralogy with depth (Mortiz, 2000).

2.5 Ore Chemistry

Archaean lode gold deposits are commonly termed the "gold only" deposits (Kerrich et al., 2000; Goldfarb et al., 2001; Groves et al., 2003) because of the extreme enrichment of gold relative to other metallic elements, particularly the base metals Cu, Pb, and Zn that commonly accompany Au in other deposit types (e.g. Porphyry Cu-Au, epithermal deposits, Au-rich volcanogenic massive sulfide deposits). The deposit have a characteristic metal association Au ± Ag ± As ± W ± Sb ± Te ± B with low Pb, Cu and Zn contents.

2.6 Wall rock alteration

Hydrothermal wallrock alteration in lode gold deposits is developed in a zoned pattern with a progression from proximal to distal assemblages. The alteration intensity decreases with distance with respect to the ore bodies. Scale, intensity and mineralogy of the alteration is a function of wallrock composition and crustal level (e.g. McCuaig and Kerrich, 1998).Wall rock alteration in Archaean lode gold deposits normally involves mass introduction of CO_2, K_2O, S and H_2O with either introduction of Na_2O. The timing of wall rock alteration relative to the peak metamorphism is highly controversial in the amphibolite facies domains (Phillips, 1986). However, in greenschist facies settings, several detailed studies have shown that alteration minerals overprint peak metamorphic assemblages and hence the wall rock alteration post dated peak metamorphism (Groves and Foster, 1991).

2.7 Fluid inclusion characteristics

As to the nature of the fluids responsible for gold mineralization in the Archaean lode gold deposits, it is now widely agreed that low saline, H_2O-CO_2 rich fluids with a moderate density were responsible for gold mineralization (Kerrich and Cassidy, 1994; Goldfarb et al., 2001; Binu-Lal et al., 2003; Pandalai et al., 2003; Coulibaly et al., 2008). The fluid was near neutral to slightly alkaline and normally reducing, although oxidized fluids have been recorded (Cameron and Hattori, 1987). The temperature of the fluids reported for lode gold deposits varies between 250 and 350°C and 1-3kbars pressures. Significant methane concentrations in the fluids have also been reported (Ho, 1987; Panchapakesan et al., 1996). Variable degree of phase separation are recorded (Ho, 1987) but it is only rarely that saline aqueous fluids were recogonized, for example, up to 34 wt% NaCl equivalent has been reported in the Sigma mine, Quebec (Robert and Kelly, 1987).

2.8 Transportation and Deposition

One of the most debated problems in the Archaean lode gold mineralization is that of transportation and deposition of gold. How did a noble metal particularly prized for its lack of chemical activity get dissolved and transported in solution? It was a million dollar question unresolved until 1973, with two schools of thought, one favoring gold transportation as sulfide complexes and the other favoring transportation as chloride complexes. However, many researchers argue that sulfide complexes are more ideal for gold transportation than the chloride complexes, because of the following reasons.

(i)The ores in majority of the gold deposits are characterized by high concentration of Au, Sb, Bi, Hg, As, W, and B(above background value) and strong enrichment of gold relative to Cu, Zn, Pb, and Ag.

(ii) Elemental ratios of these metals close that of crustal abundances as seen on volcanogenic massive sulfides should be typical which is not observed in many of the Archaean lode gold deposits. Thus the nature and co- elemental association, high gold: base metal ratios and commonly intimate association of gold with Fe-sulfides, all suggest gold transported as reduced sulfur complexes (Phillips and Grooves, 1983; Binu-Lal et al., 2003).

It is now believed that deposition of gold from the auriferous sulfide complexes was achieved by the interaction of the hydrothermal fluid with Fe-rich host rocks and this wallrock reactions induced instability of the reduced sulfur complexes and caused gold precipitation as suggested by Phillips and Groves (1984) which is given below:

$$FeO(\text{in silicate}) + HAu(HS)_2 \longrightarrow FeS_2 + 3/2\ H_2O + Au.$$

Although this mechanism is generally applicable to many of the larger Archaean lode gold deposits, it is not an universal mechanism, since many rocks with low Fe/ (Fe+Mg) ratios are mineralized and it is likely that other fluid-wallrock reactions might have been responsible for changes in P^H and oxygen fugacity (fO_2) of the hydrothermal fluid. Thus fluid rock interactions are important in producing large average grade deposits in Archaean. The formation of high grade ore shoots containing free gold is more problematical but there is increasing evidence that phase separation with formation of co- existing CO_2-H_2O rich fluids may change the concentration of H^+, CH_4 and H_2S within the fluid and may cause gold precipitation (Spooner et al., 1987). Craw et al (2001) attributed this phase separation to the lowering of lithostatic pressure or changes from lithostatic to hydrostatic pressure during regional uplift and erosion, related to compressional tectonics.

2.9 Geodynamic setting

Phanerozoic lode gold deposits are spatially associated with convergent plate boundaries (Nesbitt, 1991; Kerrich and Cassidy, 1994; Goldfarb et al., 1998). The tectonic setting of the Precambrian deposits remained more ambiguous until the late 1980s. Based on abundant geological similarities between the gold deposits from Phanerozoic orogenic belts and Archaean greenstone belts, a plate convergent setting is also suggested for Archaean deposits (Barley et al., 1989; Hodgson and Hamilton, 1989; Kerrich and Wyman, 1990). For instance, the Archaean Superior Province of Canada is characterized by the diachronous accretion from north to south of diverse plutonic, volcano-plutonic, and metasedimentary subprovinces between 2710 and 2670 Ma (Card, 1990). Lode gold deposits are linked in time and space to the diachronous accretion events, and typically occur after and during the later magmatic, metamorphic and deformation stages of each accretion event (Poulsen et al., 1992).

Goldfarb et al (2000) recognized a broad correlation of formation of lode gold deposits with thermal events associated to the growth of new continental crust during the evolution of our planet. Formation of lode gold deposits on a global- scale was episodic at about 3100 Ma, 2700-2500 Ma, 2100-1700 Ma, and the Phanerozoic. Lode gold deposits are found in accretionary orogens (e.g. western North and South America) and collisional orogens (e.g. Variscan, Appalachian and Alpine orogens), also called peripheral and internal orogens, respectively (Groves et al., 1998).

2.10 Isotopic characteristics

The low salinity, H_2O-CO_2 fluids that gave rise to Archaean lode gold mineralization are reported to be most compatible in composition with metamorphic fluids from amphibolite facies terrains (Crawford, 1981; Phillips and Powell, 1993) but could also be produced by mantle degassing. In order to resolve the source of the ore components and the fluids themselves, many researchers have carried out stable and radiogenic isotope studies and incompatible element ratio studies as discussed below.

Hydrogen and oxygen isotopes have been popular in the attempt at constraining the source of the fluids involved in the formation of lode gold deposits. $\delta^{18}O$ values of the fluids generally range between +6 and +11‰ (SMOW), and δ D fluid values between –30 and –80‰ (SMOW). Both metamorphic (e.g. McCuaig and Kerrich, 1998) and magmatic fluids (So and Yun, 1997; de Ronde et al., 2000) reasonably fit the observed values. $\delta^{18}O$ and δ D fluid values from a number of deposits fall outside the above mentioned "typical" ranges. In Archaean lode-gold deposits from Western Australia, such values are interpreted as incursion of surface-derived waters (Hagemann et al., 1994). Low δD values of –160 to -80‰ in Phanerozoic North American Cordilleran and Korean deposits are interpreted as

reflecting the deep circulation of meteoric waters during formation of the lode gold deposits (Nesbitt et al., 1986; Shelton et al., 1988). By contrast, other authors attribute such low δD values to fluid reaction with lode matter and reduced gas species (Peters et al.; 1990; Goldfarb et al., 1997). Goldfarb et al., (1991) mentioned that such low δD values obtained by analysis of bulk extraction of fluid inclusions are due to late generations of secondary inclusions trapping meteoric water unrelated to gold deposition.

Carbon and sufur isotope data are variable for lode gold deposits of all ages and from different districts (e.g. Nesbitt, 1991; McCuaig and Kerrich, 1998). Carbon isotope data for carbonates associated with gold mineralization implicate a $\delta^{13}C$ for CO_2 in the ore fluid of -5 ± 20 ‰ (Golding and Wilson, 1987) which is broadly compatible with a juvenile origin for the carbon with variations in individual deposits perhaps related to redox changes or mixing with local carbon reservoirs. While several authors have suggested that $\delta^{13}C$ are compatible with a magmatic origin for the CO_2 (Burrows et al., 1986; Colvine et al., 1984) many others have suggested magmatic dissolution of mantle derived carbonation zones along shear zones that also host the gold mineralization (Groves et al., 1988)

Similarly, Pb and Sr isotope systematics of different minerals from lode gold deposits have not allowed us to define a unique rock reservoir as the source of gold. In contrast, they indicate heterogeneous sources, and yield a general picture of a large-scale reservoir with a variety of rocks providing the components contained in the lode gold deposits (Nesbitt, 1991; McCuaig and Kerrich, 1998). Moreover, there is no certainty that gold originates from the same source rocks as Pb and Sr, since the radiogenic isotopic compositions may only reflect interaction with different rocks during fluid migration, thus altering the original isotopic signature of the fluid (e.g.

Moritz et al., 1990; Pettke et al., 2000). He isotopes can be used to discriminate among major fluid reservoirs such as mantle, meteoric and crust (Pettke et al., 2000).

2.11 Genetic models

Intense research effort in the past two decades related to lode gold deposits resulted in enormous data on various aspects of gold mineralization, but sources of fluids and solutes are still intensely debated. This is reflected by the disagreement about different genetic models proposed (Figure 2.1) by number of researchers.

1. Metamorphic derivation of ore fluids by greenstone belt devolatilization (Kerrich and Fryer, 1979; Phillips and Grooves, 1983, Foster, 1985; Phillips, 1993)
2. Crustal out gassing (Kerrich, 1986) and granulitization (Colvine et al., 1988; Cameron, 1988).
3. Magmatic model involving the releasing of fluids by minor felsic inclusions (Burrows and Spooner, 1987) or by Lamprophyres (Rock and Grooves, 1988; Rock et al, 1989).
4. Direct mantle degassing model for the ore fluids and ore components (Perring et al., 1987).

2.11a Crustal continuum model

There has been a tendency in the late 1980s and early 1990s to classify gold deposits located within deformation zones under a single category named mesothermal, with the understanding that they were formed by the same process regardless of their age and geographic location (Kerrich and Wyman, 1990; Nesbitt, 1991). It is clear that with such a unifying classification, the origin of some deposits has remained contentious, in particular in higher grade metamorphic settings. Some authors have ascribed a deep origin to such deposits, suggesting a syn-metamorphic

origin (e.g. Neumayr et al., 1993), therefore supporting a crustal continuum model (Fig.2.2) for the lode gold deposits (Groves, 1993; Groves et al., 1998).

Considering that the Archaean lode gold deposits formed under a range of crustal regimes (sub-greenschist to lower granulite facies) and that the isotopic data are compatible with multiple fluid sources, a more realistic genetic model may be crustal continuum model. This model is partly based on those of Colvine et al (1988), Foster (1989), and Barnicoat (1991), envisage the existence of giant, late Archaean hydrothermal systems with various potential sources of fluids and solutes at different crustal levels. The potential source includes basal portions of greenstone belt sequences (metamorphic devlotilization), deep-level intrusive granitoids (magmatic hydrothermal fluids), lower crust and upper mantle (degassing) and even subducted lithosphere. The model is consistent with the age of gold mineralization linked to the accretionary tectonic settings in the Superior province and the Yilgarn Block. It is even allows for the mixing of meteoric water or seawater in lower or sub-green schist facies settings at upper crustal levels, as has been found to be the case with shallow-level lode deposit in the Yilgarn Block (Hagemann et al., 1994) and has also been emphasized by Nesbit and Muehlenbachs (1989) for mesothermal gold deposit in the North American cordillera. A problem associated with the crustal continuum model is the timing of peak metamorphic events at the different levels of the crust, for example, a 2600 Ma age for peak metamorphism in the high grade domains and a 2630 ma for greenschist lode gold mineralization (Witt et al., 1997). The earlier timing of peak metamorphic event at upper crustal levels (greenschist domains) relative to deeper crustal levels (amphibolite and granulite facies domains) may have resulted from crustal thickening due to thrusting, but medium to high-pressure metamorphic assemblages that might be expected in an over thrust terrain have not

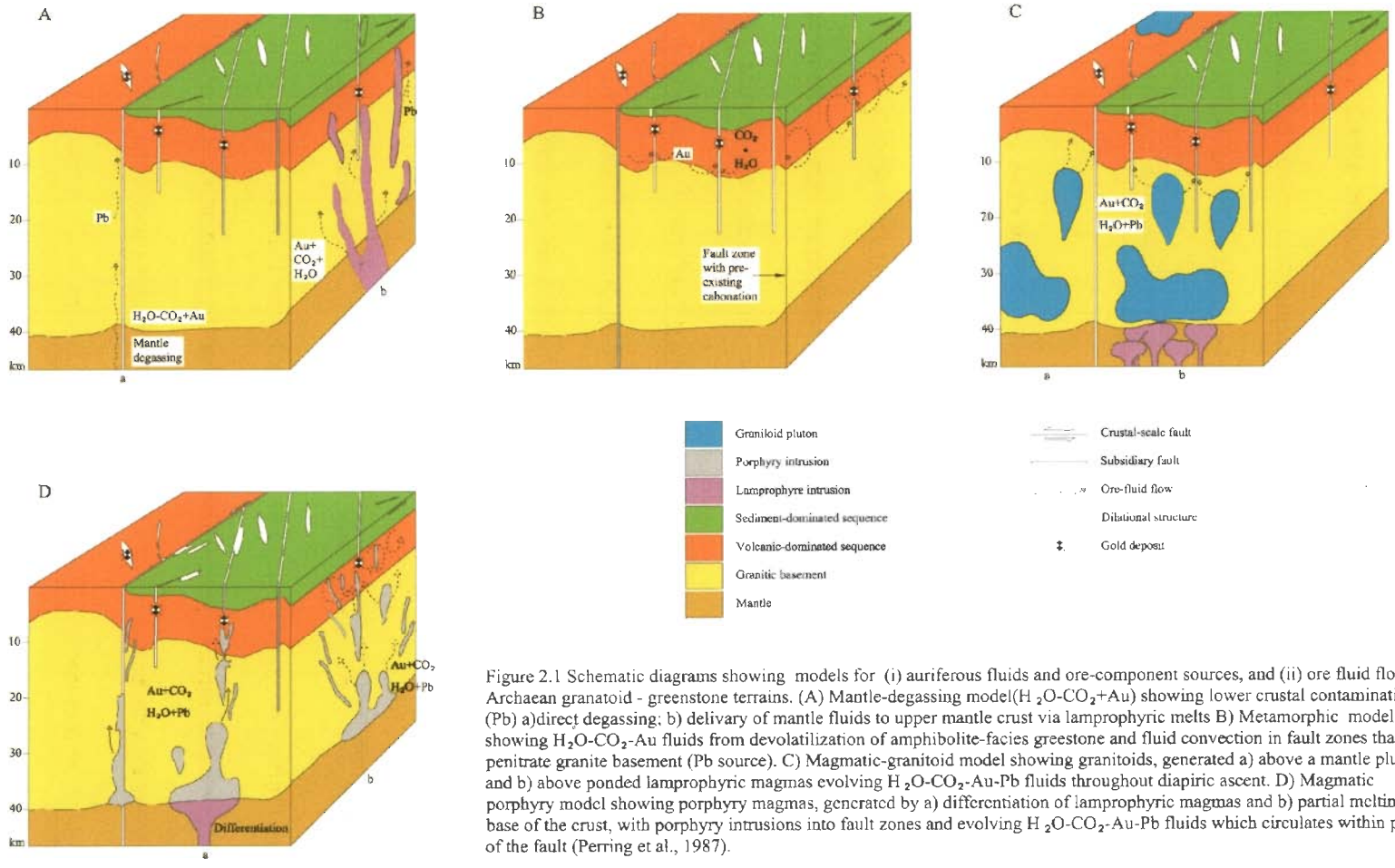

Figure 2.1 Schematic diagrams showing models for (i) auriferous fluids and ore-component sources, and (ii) ore fluid flow in Archaean granatoid - greenstone terrains. (A) Mantle-degassing model(H_2O-CO_2+Au) showing lower crustal contamination (Pb) a)direct degassing; b) delivary of mantle fluids to upper mantle crust via lamprophyric melts B) Metamorphic model showing H_2O-CO_2-Au fluids from devolatilization of amphibolite-facies greestone and fluid convection in fault zones that penitrate granite basement (Pb source). C) Magmatic-granitoid model showing granitoids, generated a) above a mantle plume and b) above ponded lamprophyric magmas evolving H_2O-CO_2-Au-Pb fluids throughout diapiric ascent. D) Magmatic porphyry model showing porphyry magmas, generated by a) differentiation of lamprophyric magmas and b) partial melting of base of the crust, with porphyry intrusions into fault zones and evolving H_2O-CO_2-Au-Pb fluids which circulates within plane of the fault (Perring et al., 1987).

been observed. In contrast, other authors favour a shallow origin for such deposits, subsequently overprinted by deformation and regional metamorphism at deeper structural levels (e.g. Morasse et al., 1995; Penzcak and Mason, 1997). Lode gold deposits hosted by upper amphibolite to granulite metamorphic grade rocks have only been recognised in Archaean terrains, and seem to be absent in Phanerozoic orogenic belts (Groves et al., 1998).

2.11b Lateral flow model

A synmetamorphic lateral flow model proposed by Witt et al. (1997) attempts to address the shortcoming in crustal continuum model, at least for the deposits in the Kalgoorlie and Norseman terrains (Yilgarn Block, Western Australlia). This model envisages a two-step process, the first driven by dominantly vertical temperature gradients, as it is postulated for the cratonization and crustal continuum models discussed above, and the second by lateral temperature gradients induced by uplift at the margins of the greenstone terrains accompanied by granitic intrusions. The first step involved the ascent of CO_2 bearing, low-K fluids from the lower part of the greenstone pile, the deep crust or mantle regions via regional shear zones during the early stage of regional metamorphism and the dispersion of these fluids through the greenstone sequence via smaller scale structures. The gold mineralization occurred from a small number of large hydrothermal systems during the later stages of regional metamorphism due to lateral flow of fluids driven by the devolatilization reactions at or near the transition from greenschist to amphibolites facies conditions. However, the model, like other symetamorphic models, does not account for lode gold deposits such as those of the val d 'Or camp (Canada), if the gold mineralization in this area was indeed emplaced 60 Ma later than peak regional metamorphism as claimed by Anglin et al. (1996).

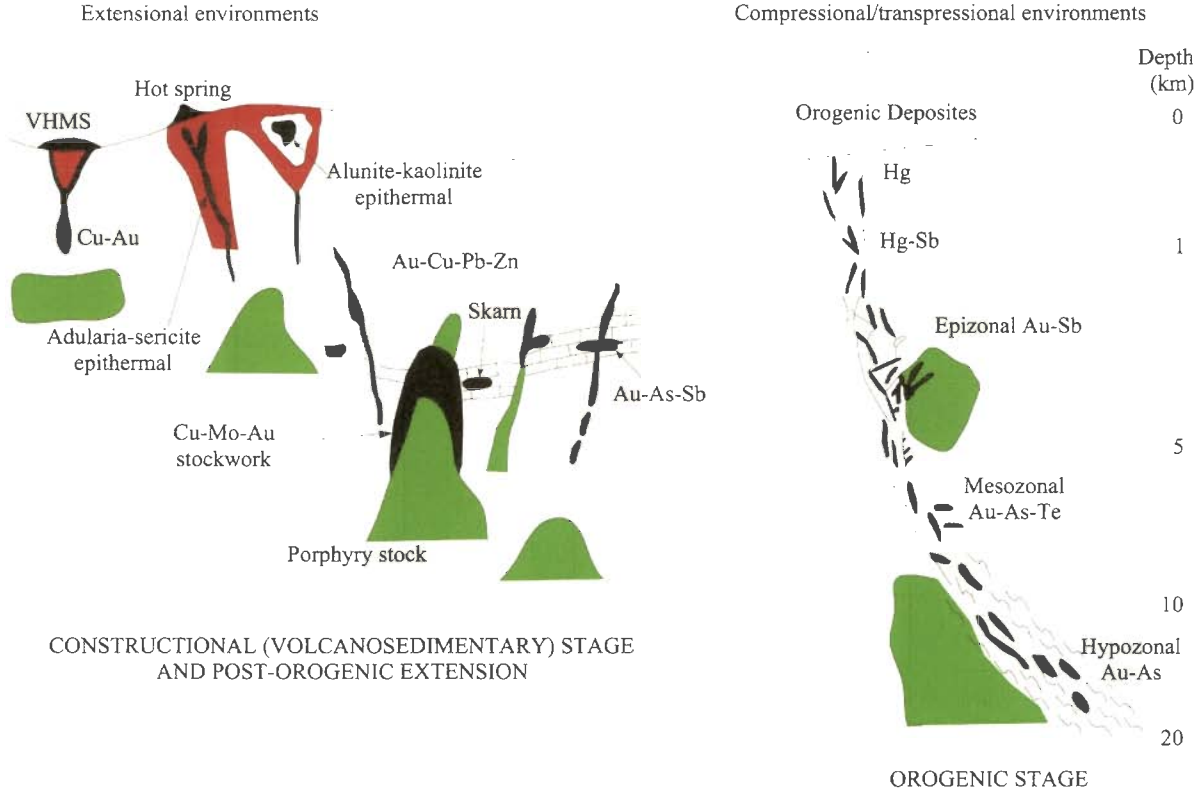

Fig. 2.2 crustal continuum model for Lode gold deposits (Groves et al., 1998)

2.12 Summary

An excellent review of the various genetic models proposed and the pros and cons of each of them has been presented by Kerrich and Cassidy (1994). Since then, Hagemann and Cassidy (2000), Kerrich et al. (2000), Ridley and Diamond (2000), Groves et al. (2003), and Goldfarb et al. (2001) among others, have also revisited the subject. A brief summary is presented here.

Gold mineralization is spatially related to transcraton shear zones, mantle-derived carbonation zones, granitioids, feldsic porphyries and lamprophyres. These associations, combined with overall similarity of isotopic data from different cratons, suggest that gold mineralization was related to a single, at least craton scale processes. This probably involved a deep seated tectono-metamorphic event incorporating melting of mantle at depth of 150 km (to produce lamprophyres, melting of the upper mantle or base of the crust (porphyries) and lower crust (granitoid),mantle degassing (regional carbonation zones), interaction of fluids with lower crust and metamorphic fluids at upper crustal levels. The stage at which gold and other ore components were added to the hydrothermal system is still to be resolved. Certainly, gold deposition commonly occurred during specific events within long-lived shear zones, and it is not clear whether this was due to structural controls or to introduction of gold from a specific source at a particular time during tectonism. Also unresolved is whether the ore fluids were mainly magmatic, mainly metamorphic or a combination of both.

Several genetic models were proposed during the last two decades without a definite consensus. Each of these models has merit, and various aspects of all or some of them are potentially involved in the formation of quartz-carbonate greenstone-hosted gold deposits in metamorphic terrains. It is largely believed that the greenstone-hosted quartz-carbonate vein deposits are related to metamorphic fluids

from accretionary processes and generated by prograde metamorphism and thermal re-equilibration of subducted volcano-sedimentary terrains. The temporal distribution of gold deposits with major peaks of hydrothermal gold mineralization in Archaean and post late Paleozoic is an indication of the importance of tectonic control and setting of these deposits. The younger deposits are almost restricted to convergent plate boundaries, which most of the deposits forming in subduction related magmatism in volcanic arc and marginal basins and continental margin orogenic belts (Groves and Foster, 1991). These indicating the possibility that the late Archaean gold mineralization may have been controlled by convergent margin tectonics. Studies in Kolar Schist belt of South India (Krogstad et al., 1989) suggest that plate tectonic process operated in the Archaean similar to the Phanerozoic convergent margin setting and the accretionary tectonics were responsible in Kolar area. Similar evidences of the accretionary tectonic terrains were also reported from other mineralized greenstone belts of South India (Zachariah et al., 1995, 1996)

The deep-seated, Au-transporting metamorphic fluid has been channelled to higher crustal levels through major crustal faults or deformation zones (Figure 2.3). Along its pathway, the fluid has dissolved various components - notably gold - from the volcano-sedimentary packages, including a potential gold-rich precursor, which will then precipitate as vein material or wallrock replacement in second and third order structures at higher crustal levels through fluid-pressure cycling process and temperature, pH and other physico-chemical variations. According to Ridley and Diamond (2000), a model based on either metamorphic devolitilization or granitoid magmatism fits best most of the geological parameters.

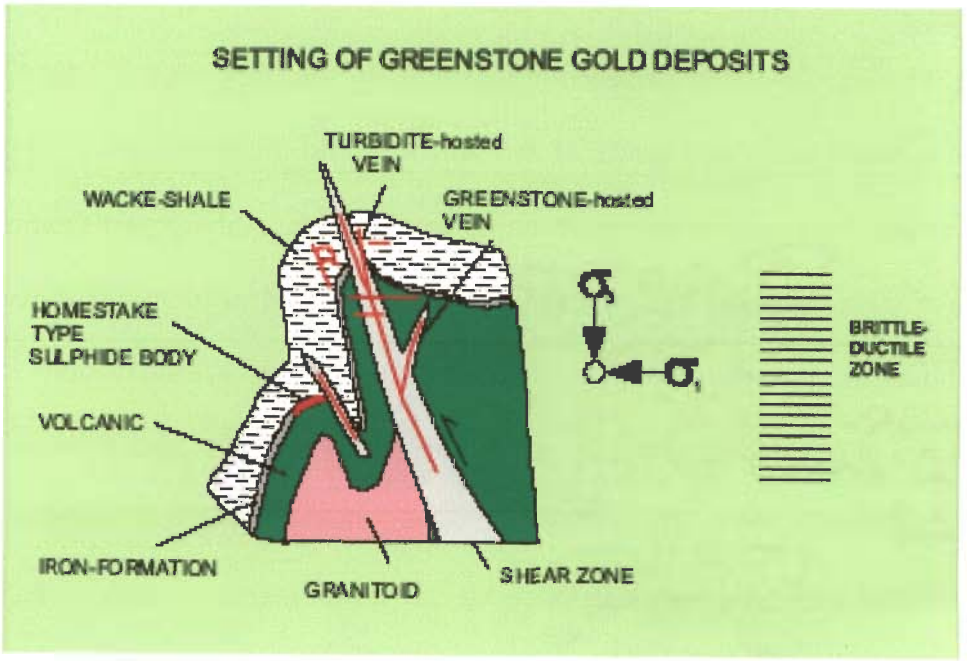

Figure: 2.3 Schematic diagram illustrating the setting of greenstone-hosted quartz-carbonate vein deposit (from Poulsen et al., 2000).

CHAPTER 3

Geological setting

GEOLOGICAL SETTING

3.1 Regional Geology

A brief outline of the nature and distribution of the major Archaean terrains and gold mineralization in Peninsular India is discussed in this chapter. Southern part of Peninsular India represents relatively low-grade granite-greenstone assemblages in the Dharwar Craton (DC), juxtaposed against high-grade granulites (Figure 3.1). A 20-35 km wide zone, known as the Transition Zone, exists between the DC and the Southern Granulite Terrain (SGT). Foliated tonalite-trondhjemite-granodiorite gneisses, metavolcanic rocks and Banded Iron Formation (BIF) form part of the DC. The DC is characterized by greenschist to amphibolite facies metamorphism and the rocks prograde into Archaean granulites of the SGT. DC is divided into two crustal blocks: the Western Dharwar Block, dominated by Archaean tonalite-trondhjemite-granodiorite gneisses of different ages (3.4 Ga to 2.5 Ga), and the Eastern Dharwar block is dominated by Neo-Archaean (2.7 Ga to 2.5 Ga) granodiorite to granitic gneisses (Radhakrishna and Naqvi, 1986; Balakrishnan et al `1990; Rogers and Giral, 1997,). These granitoid gneisses contain older Archaean supracrustal belts (greenstone belts) containing continental and oceanic-like volcano-sedimentary rocks at greenschist to amphibolite facies of metamorphism (Rogers and Giral, 1997). Integration of presently available data indicates that the entire Archaean gold mineralization of economic importance is restricted to greenstone-type lithostratigraphic sequences such as those occurring in Kolar, Hutti, Ramagiri, Gadag areas of Western and Eastern Dharwar Craton of South India (Figure 1.1). This mineralization associated with greenstone belts are of two different genetic types: (1) a structurally controlled epigenetic type related to hydrothermal solutions and (2) a

stratiform syngenetic type intimately associated with amphibolite facies host rocks (Sivasiddaiah and Rajamani,1989, Sangurmath, 2005).

Apart from greenstone hosted gold mineralization in DC, few lesser known gold occurrences are associated with quartz veins present in the high-grade SGT. Since time immemorial, the Wynad within Moyar shear zone (Figure 3.1) have been known for winning gold from the river bed (Santosh, 1995).The auriferous quartz reefs have been mined to recover primary gold for several years, starting in the latter part of the last century. Several exploration programs were undertaken by Geological Survey of India (GSI) and have demarcated potential targets for further gold recovery. This region is considered to be one of the potential sites for India's future gold mining programs (Radhakrishna and Curtis, 1999). The gold deposits of Wynad comprise three principal categories: (1) primary lode-gold mineralization in vein quartz traversing Precambrian amphibolites and granite gneisses; (2) supergene gold associated with laterites in weathering profiles; (3) placer gold associated with stream gravels (Sawarkar, 1980; Nair et al., 1987). Recent research at Wynad gold field has provided new insights into the genesis of this deposit such as possible gold source, characteristics of ore fluid and mechanism of ore deposition (Binu-Lal et al., 2003; Malathi and Srikantappa, 2005). The regional and detailed geological investigations carried out in the last ten years in the SGT resulted in the recognition of several new gold prospects including the gold mineralization reported from the Attappadi area of SGT (Nair, 1993, Nawaratne, 2001). Therefore, new information on the metallogenetic characteristics of these ancient terrains became available, only during the last decade.

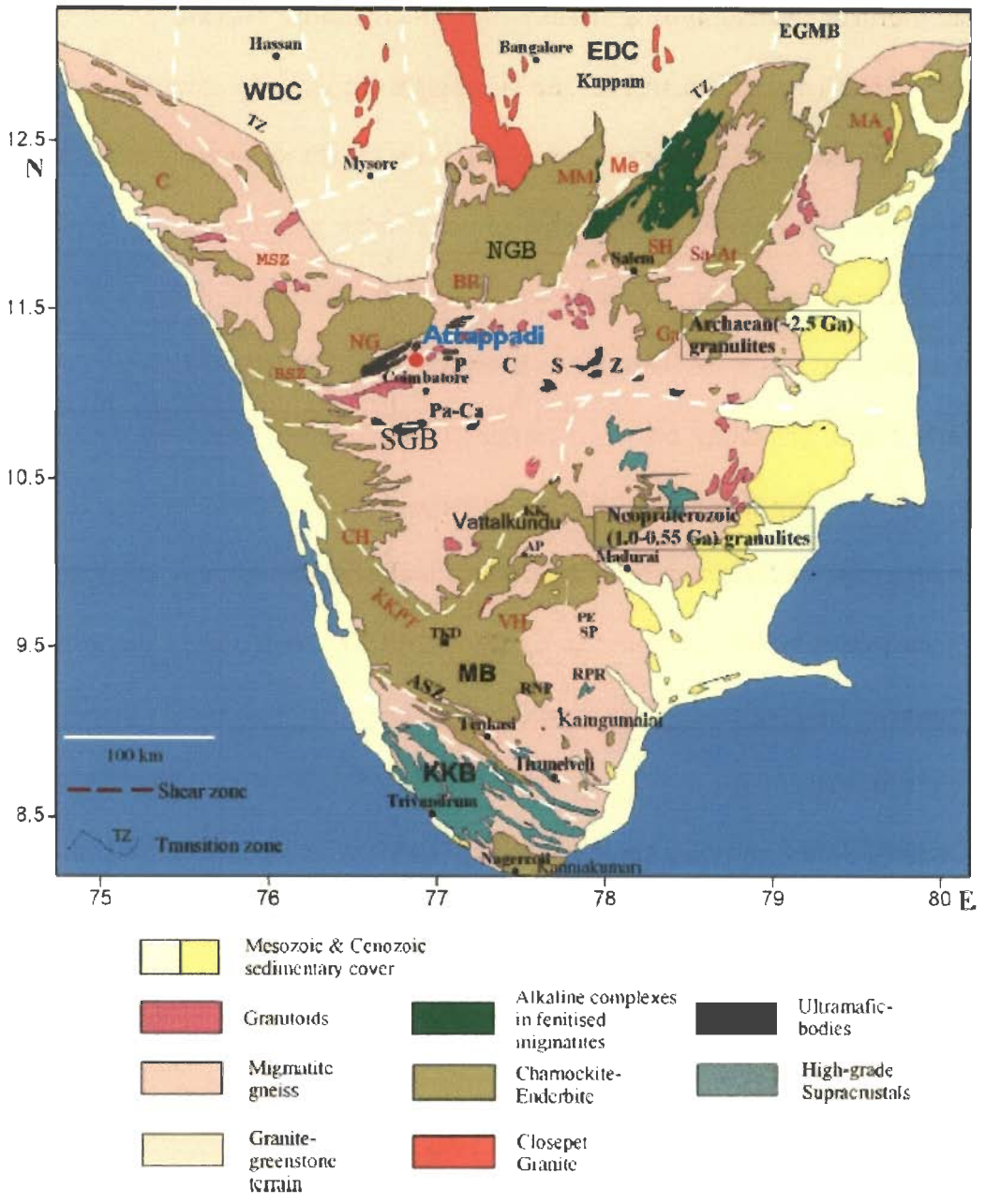

Eastern Ghat Mobile Belt (EGMB), Western and Eastern Dharwar Cratons (WDC, EDC); Madurai Block (MB) and Kerala Khondalite Belt (KKB). The High land massifs: Nilgiri (NG); Coorg (C); Biligiri Rangan (BR); Malai Mahadeswara (MM); Shevroy (SH); Kodaikanal massif (KK); Madras (MA); Cardamom (CH) and Varshunadu Hills (VH). The Palghat-Cauvery Shear Zone System (PCSZ) comprising component shear zones, Moyar (Mo); Bhavani (Bh); Mettur (Me); Palghat-Cauvery (Pa-Ca); Salem–Attur (Sa–At) and Gangavalli (Ga). Other shear zones, Karur–Kambam–Painavu–Trichur (KKPT) and Achankovil Shear Zone (ASZ). Andipatti (AP), Peraiyur (PE), Rajapalayam Road (RPR), Ramnathpuram (RNP), Sedapatti (SD), Sarvathapuram (SP), Sivakasi (SK) and Tekkadi (TKD).

Figure 3.1 Different granulite blocks and major shear zones in South India (GSI, 2001)

3.2 Current Understanding about Southern Granulite Terrain

Further south of DC the metamorphism increases to granulite facies and this region is known as Southern Granulite Terrain (SGT) and were further divided into different crustal blocks based on the regional shear zones (Figure 3.1), which criss-cross the southern peninsular India (Drury et al., 1984; Shabeer et al., 2004). According to this framework the E-W trending Palghat-Cauvery Shear Zone (PCSZ) divides the granulites into two terrains, (1) Northern Granulitic Blocks (NGB), including Coorg granulites (C) in the west and MaleMahadeshwara (MM) in the eastern part, and (2) Southern Granulitic Block (SGB) including Madurai Granulite Block (MB). In the Northwestern part of the PCSZ Shear Zone, Moyar Shear Zone separates Biligirirangan (BR) granulites to the north and Nilgiri granulites to the south, it merges with the Bhavani Shear zone to form Moyar-Bhawani Shear zone (MBSZ). In the eastern margin of PCSZ Salem-Attur Shear zone and an oblique N 45° Shear named as Gangavalli Shear Zone (Ga) (Chetty, 1996) is also present. In south, the SGB is bounded by NW-SE trending Achankovil Shear Zone (ASZ). In general the granulites are exposed from the southern margin of Archaean greenstone-granite belt of Dharwar craton to the tip of the peninsula with many regional shear zones criss-crossing the terrain. There have been several competing theories for explaining the association of granulites and shear zones. Shear zones were visualized in terms of major terrain boundaries (Bhaskar Rao et al., 2003), where as, others considered them to be ancient suture zones (Viswanathan et al., 1990). Even the plate-tectonic models proposed to explain the localization of strain and high P-T conditions, ranging from collisional tectonics with both, southward subduction and northward subduction to magma under-plating (Rai et al., 1993; Drury et. al., 1984; Chetty, 1996; Ramakrishnan, 2003; Srikantappa et al., 2003).

Drury et al. (1984) point out that the Dharwar Craton is characterized in general by greenschist to amphibolite grade of metamorphism, and that BIF and mafic-ultramafic supracrustal rocks are common but that associated calc-silicate rocks are rare. The SGT on the other hand is characterized by mainly granulite grade of metamorphism, and by extensive calc-silicate rocks but rare BIF and maficultramafic supracrustals. Drury et al. (1984) also state that the supracrustal rocks of the D C are autochthonous with respect to the gneissic granitoid basement rocks, while in the SGT the supracrustals are tectonically interleaved with charnockite and enderbite sheets. However, the spatial variation in the abundance of various lithological assemblages are not abrupt across the PCSZ; rather there is a gradual decrease in the abundance of mafic supracrustal rocks and BIF from the DC into the SGT. Accepting that in general high-grade rocks represent the SGT, and that the DC is dominated by greenschist and amphibolite grade of metamorphism, the details of the regional variations of these metamorphic facies are far more complex (Mukhopadhyay, 1986). Moreover, both SGT and the DC are poly-metamorphic terrains, so that variations in the patterns of metamorphic grades cannot be used to support the existence of separate terrains until these metamorphic events are dated and placed in structural context (Gosh et al., 2004).

3.3 Bhavani Shear Zone

The present study area, Attappadi, is situated in the western termination of Bhavani shear zone (BSZ) in the NGB. The ENE-WSW trending BSZ is the southern major constituent of the MBSZ. The Nilgiri charnockite massif (mainly garnetiferous enderbites) marks the northwest side of the Bhavani Shear Zone (Figure 3.1) and southeast margin is not well defined because of lack of exposures. BSZ characterized by a zone of intense mylonite, in turn overprinted by late brittle- to brittle ductile

structures (Gosh et al., 2004). Sheared gneisses are steeply dipping with sparse subvertical stretching lineations. The BSZ, although well within the Northern block of SGT, is largely made up of reworked gneisses which have been retrogressed from earlier charnockites (Srikantappa et al., 2003). The crustal blocks which have escaped the shearing are preserved as charnockites massifs in the Nilgiri, Kolli and Shevroy hills (Raith et al 1999). The BSZ is dominated by ENE-WSW trending hornblende-biotite gneiss, highly deformed quartz biotite schist and augen gneiss with mylonitic fabric. Ghosh et al. (1996), dated the charnockite occurring in BSZ as 2.5 Ga which is similar to the age of Nilgiri granulite massif 2.5 Ga (Crawford, 1969). Undeformed dolerite dykes of Attappadi was dated and gave K-Ar date of 2030±65 Ma (Radhakrishna, 1995) and indicates a shearing episode in the Bhavani Belt much older than 2.0 Ga and younger than 2.5 Ga. A recent research carried out by Ghosh et al. (2004) showed granite/pegmatite veins within BSZ that were syn-kinematic with respect to the late brittle-ductile deformation, and dated the hydrothermal zircon from undeformed quartz vein within the granite at ≈600 Ma by U-Pb method. Thus Ghosh et al. (2004) proposed the last shearing activity was of Neo-Proterozoic age. Furthermore, according to Meissner et al. (2002) the last shearing activity in the BSZ occurred ≈ 513Ma. The geochronological data support multiple episodes of deformation, metamorphism and fluid flow in Neo-Proterozoic BSZ. The geochronologies, structural and metamorphic history of BSZ have been studied extensively for the last four decades, but not much attention was given to elucidate the structural and petrological framework of the gold mineralization.

3.4 Geology of Attappadi

As shown on the map (Figure 3.2) gneisses are the predominant rocks in the study area. All rock types of Attappadi other than supracrustals could be categorized

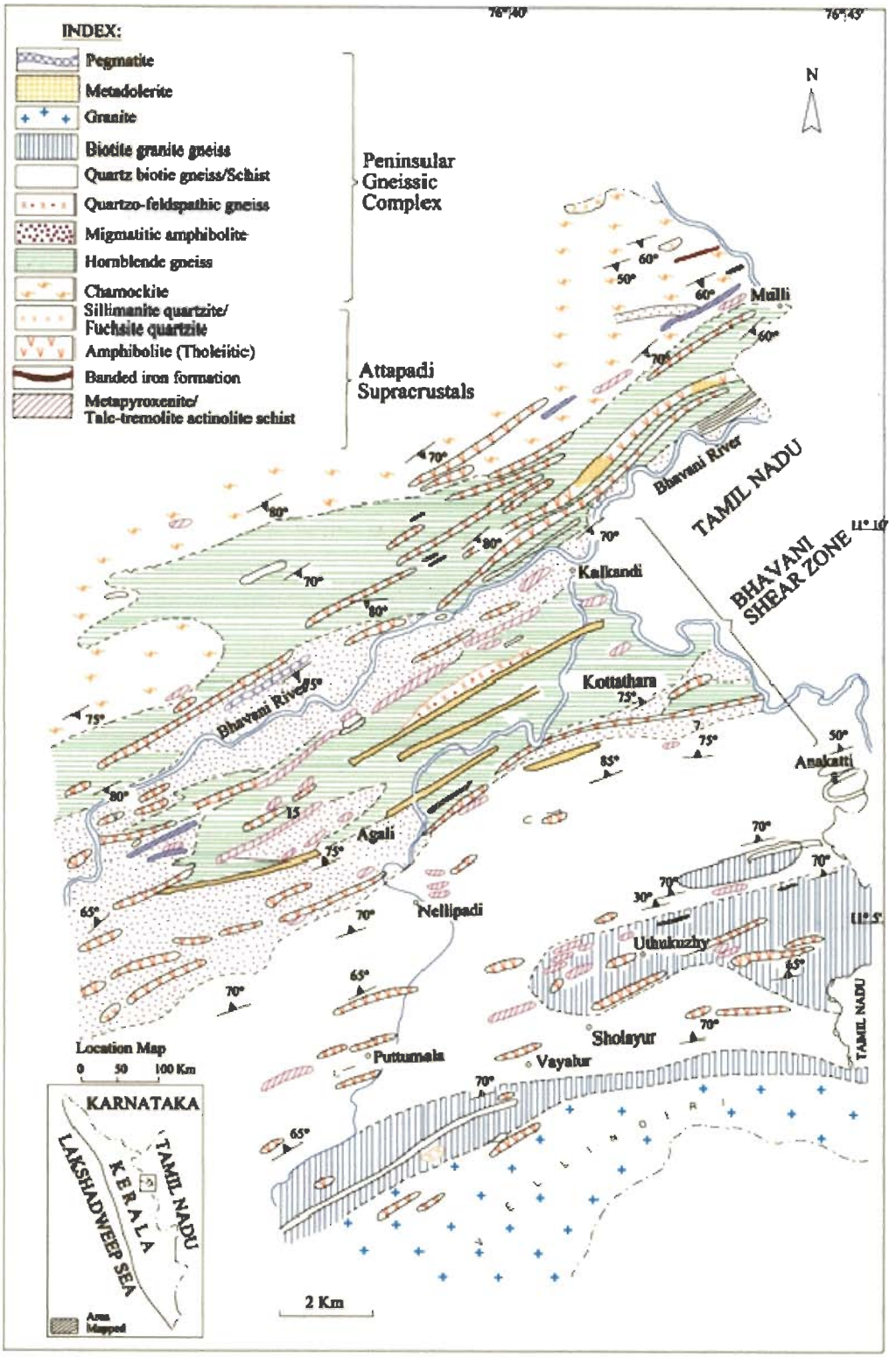

Figure 3.2 Geological map of Attappadi Nair et al. (2005)

into seven broad types. They are charnockite, hornblende gneiss, migmaititic ambhibolite, quartz biotite gneiss, quartz-feldspathic gneiss, biotite granite gneiss and pegmatite. According to Nair et al. (2005), among the rock types charnockite, hornblende gneiss , migmatitic amphibolite, quartz biotite gneiss , quartz-feldspathic gneiss and biotite granite gneiss have been identified that belong to the Peninsular Gneissic Complex (PGC).The granite and pegmatite of Attappadi represent the post kinematic intrusives. Many dolerite dykes also have been reported from this area. The bands and layers of ultramafics and mafic rocks (Ultramafic and mafic rocks represented by metapyroxinite, talc-tremolite-actinolite schist and amphibolites) of varying dimension, BIF, sillimamite/kyanite bearing quartzite and fuchsite quartzite occurring within the PGC of Attappadi area designated as Attappadi Supracrustals (AS) by Nair et al. (2004).The tentative stratigraphy of the Attappadi supracrustals as is given by Nair et al. (2005) shown below;

Sillimanite quartzite/fuchsite quartzite
Amphibolite (Tholeiitic)
Banded Iron Formations
} Attappadi supracrustals
Metapyroxenite/Talc-tremolite-actinolite schist

Remnants and enclaves of Attappadi supracrustals occur within the gneisses. BIF is another important rock type occurring in close association with the metapyroxinite and amphibolites. The high grade rocks of the Sathyamangalam Group (regarded as equivalents of the Sargur Group by Ramakrishnan, 1993) form the northern extension of the Attappadi supracrustals (Nair and Nair, 2001). Attappadi is unique in that, a number of rock types varying in composition from ultramafic to

metapelites occur as supracrustals. The metapelites are of granulite facies and the ultramafics are of greenschist facies and the enclosing gneisses represent amphibolites facies (Nair et al., 2004).

The area had undergone polyphase deformation (Figure 3.3). The planar S_0, is defined by the layering within chemogenic precipitate (BIF). The earliest folds F_1, apart from being tight and appressed occur in intrafolial positions and also constitute the rootless folds. This folding has given rise to an axial planar penetrative foliation and is defined mainly by hornblende and to a lesser extend by chlorite and is co-parallel to the lithoboundaries identified as S_0. S_1 schistosity is defined by hornblende and chlorite, and this mineralogical association suggests that the deformation occurred under upper greenschist to lower amphibolite facies conditions. The subsequent F_2 resulted in refolding of S_1 and transposition of S_1 subparallel to the F_2 axial trace. The most prominent planar structures are the discrete mylonitic foliation S_2 attributed the regional NE-SW trending Bhavani shear. Mylonite development, biotitization, chloritization and microgranulation are found associated with these surfaces (Nair and Nair, 2004).

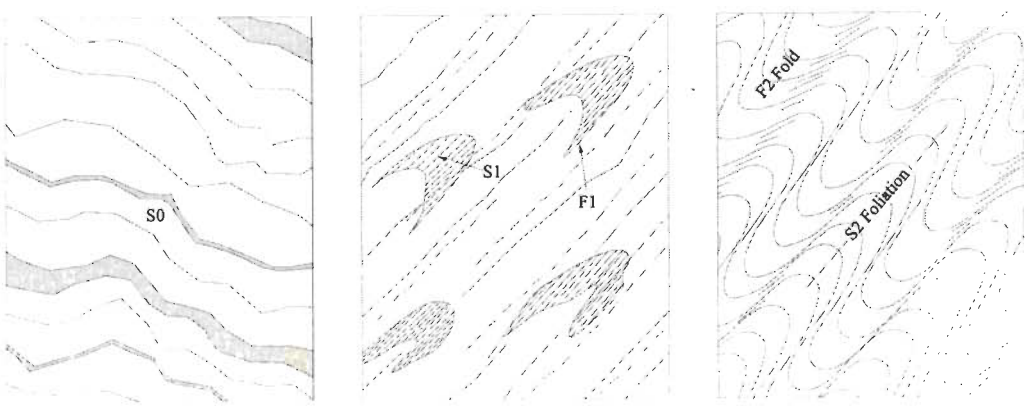

Figure 3.3 Schematic reprentaion of deforamational stages developed in Atatppadi

3.5 Gold Mineralization

Mani (1965) reported the panning for gold by local miners in Siruvani River of Attappadi. Detailed studies to assess the economic potential of Attappadi area was carried out subsequently by Nambiar (1982 and Nair and Rao (1990). However, no primary gold prospects were identified. (Nair 1993) carried out the geomorphologic mapping combined with panning of Siruvani River which led to the discovery of primary gold mineralization in epigenetic quartz vein in Puttumala. The veining, mineralization and associated lithology of this deposit appear to be typical of greenstone-hosted lode gold deposit. The observations of numerous GSI geologists are summarized and given in Table 3.1. On the basis of mode of occurrence two types of gold mineralization are recognized in Attappadi, (1) Primary gold mineralization is associated with quartz veins intruding to AS and PGC. (2) Placer deposit along the bank of Siruvani River.

The Geological Survey of India has confirmed the high gold bearing potentiality of the rocks in the 834sq km area of the Attappadi. Gold mineralization is known from Kottathara, Puttumala, Pothupadi, Mundaiyur and Kariyur-Vannathorai Prospects of Attappadi. Gold occurs in quartz veins traversing in BIF, metavolcanics, and hornblende and biotite gneiss. Deccan Gold Mines Limited later confirmed the earlier reported gold grades and have given the following values,

Kottathara prospect: Three zones have been delineated and the prospect has an ore resource of 60,000 tonnes grading 13.63g/t gold according to Geological survey of India. While tracing the NE extension of Kottathara prospect, stringers of quartz analyzing 9 g/t 35 g/t and 49g/t gold have been picked up in stream beds.

Table.3.1 Previous studies in Attappadi

Mani, 1965	The geological mapping of Attappadi was carried out initially .Recognized a regional shear zone parallel to the course of Bhavani River over a length of 20 km and extending eastward into Tamil Nadu with an average width of 10 km. Also reported the panning for gold by local miners in Siruvani River of Attappadi
Nambiar, 1982;	Completed mapping as part of a project by Geological survey of India .The major lithounit hornblende gneisses in this shear zone represents retrograde product of charnockites/mafic granulite
Nair, 1993	The remnants and enclaves of supracrustal like rocks represented by sillimanite quartzite/fuchsite quartzite, tholeiitic amphibolite, banded iron formations, metapyroxenite/talc-tremolite-actinolite schist are found within hornblende gneiss/ biotite gneiss in Attappadi area. Also reported the primary gold mineralization in quartz veins associated with these rocks.
Nair and Maji,1995	Systematic panning of alluvial sediments of the first -order and higher order streams of Bhavani and Siruvani fluvial regime resulted in the delineation of three sub parallel auriferous zones in Attappadi. Scout panning and grab sampling further established as anomalous area, the Pothupadi- Puttumala ridge. Epigenetic quartz veins/ veinlets traversing amphibolites and granite gneiss of this ridge was found to host galena, pyrite and chalcopyrite. Puttumala area was subjected to detailed mapping, soil sampling and trenching to establish the dimension, structure and grade of the ore body. Geochemical anomaly in E –W to NE-SW direction. Trenches substantiated the occurrence of a mineralized zone over a width of 2 meter and strike length of 350 meter and reported the structural control for the localization of gold mineralization.
Nair et al. 1996	Structural studies have revealed that the area has undergone polyphase deformation and metamorphism. The earliest fold F_1 is tight appressed asymmetrical folds which have developed on mezoscopic scale and also occur in intrafolial position. They have led to the development of axial plane cleavage. The second generation fold F_2 is open symmetrical post folial folds which have developed on a regional scale. The F_3 folds on F_2 axial traces are broad wraps in N-S direction. The most prominent penetrative planar structure is the fracture cleavage attributed to the regional NE-SW trending Bhavani shear.
Nair and Nair, 2001	Reported the auriferous nature of banded iron formation. Subsurface techniques used to establish the quartz veins and their boundary. Geophysical studies carried out in Kottathara area. The IP surveys in Kottathara prospect had brought out the chargeability anomaly along the mineralized shear zone. Delineated four parallel zones in the northern part of Kottathara.
Nair et al. 2004	Report the preserved pillow and ocelli structures in metaultramafite. REE geochemical data of BIF and their possible Precambrian a age. The Komatiitic and tholeiitic nature of ultramafic rocks based on major element geochemistry. Named this supracrustal rock as Attappadi Supracrustals and given the stratigraphy of Attappadi supracrustals, and reported a possible occurrence of relict green stone belt within SGT.
Nair et al. 2005	Preliminary appraisal of Kottathara prospect. Suggested the multistage mineralization based on field, ore microscopy and preliminary geochemical study.

Puttumala prospect: A 60 cm sample of vein quartz carrying galena (lead sulfide) from old trenches showed high spot values of gold up to 21g/t.

Pothupadi Prospect: A sample of vein quartz traversing amphibolite assayed 4 g/t gold.

Mundaiyur Prospect: Gold occurs in quartz veins over a length of 300 m with gold-bearing sulphides enveloping the quartz veins.

Kariyur-Vannathorai Prospect: Samples of vein quartz have shown gold contents ranging from 3 to 20 g/t.

In Attappadi region gold grains are found only in native state and occur in different shapes and sizes. Visible specks of gold were noticed in the samples collected from veins, particularly where the associated sulphides have been subjected to weathering and leaching resulting in the formation of limonite. Gold grains with maximum dimension of 2 mm were reported. Pyrite is the dominant sulfide phase within the quartz lodes (occurring as stringers and fracture fillings). Chalcopyrite, covellite, chalcocite and galena are commonly observed in the mineral assemblage (Nair et al., 1996).

CHAPTER 4

Field study, Petrography and Mineralogy

FIELD STUDY, PETROGRAPHY AND MINERALOGY

4.1 Location and Accessibility

Attappadi is located in Palakkadu district of Kerala state in Peninsular India (Figure 4.1). The study area is accessible from Mannarkkadu, Coimbatore and Pattambi by road. Attappadi is a part of Western Ghats, and is physiographically an undulating terrain with elongated ridges trending in NE-SW direction. The area under investigation falls between11° 00' to 11° 15' N latitude and 76° 35' to 76° 60' E longitude on Survey of India toposheet No. 58 A/12.

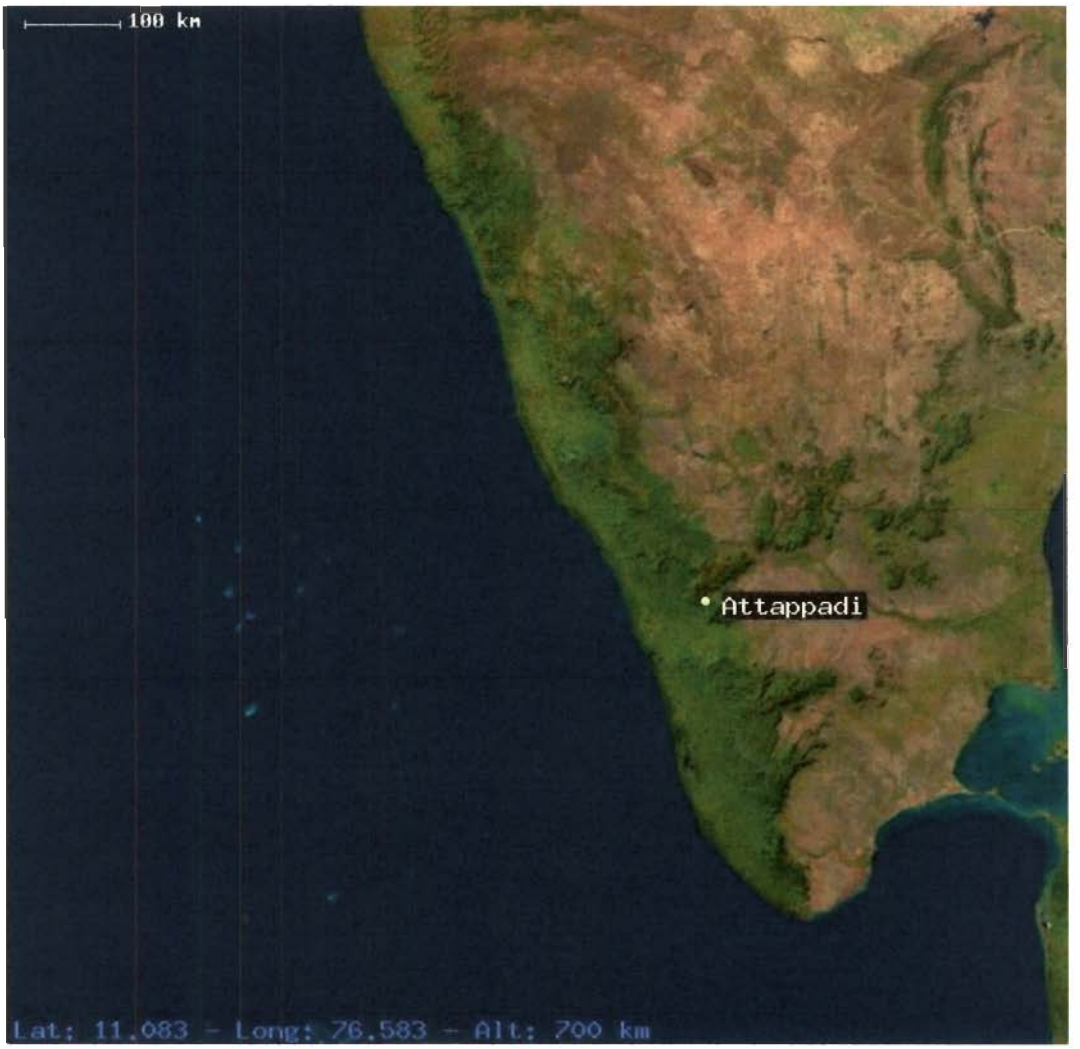

Figure 4.1 Google map showing the study area

4.2 Field Study

Field work was carried out along several traverses all run through locations of mainly reported gold occurrences with Agali as the base camp.

1. Agali-Kattuvalavu
2. Agali -Vannathorai
3. Agali –Puttumala
4. Agali -Narasimukku
5. Agali -Anaikatti-Sholayur
6. Agali -Kottathara-Bhuthavazhi

Objectives of field study:

- Classify different rock types present in Attappadi and decipher the yet undefined contact relationship between the Attappadi Supracrustals and Peninsular Gneissic Complex
- Collect representative samples for petrographic, ore microscopic, fluid inclusion and geochemical studies to understand the nature and petrogenesis of the mineralized zones

The sampling locations are shown in Figure 4.2. The spatial distribution of the various lithounits of Attappadi is described in the previous chapter (section 3.4). Representative samples were collected and the following rock descriptions are organized to follow the above GSI map and nomenclature.

4.2.1 Metavolcanics

The metavolcanics belonging to the Attappadi supracrustals are represented by two varieties i) Metaultramafic/talc-tremolite-actinolite schist and ii) amphibolites. These rocks occur as bands conformable to the foliation of the enclosing gneisses with width varying from few cm to 50 meter and length extending up to 1500 meter.

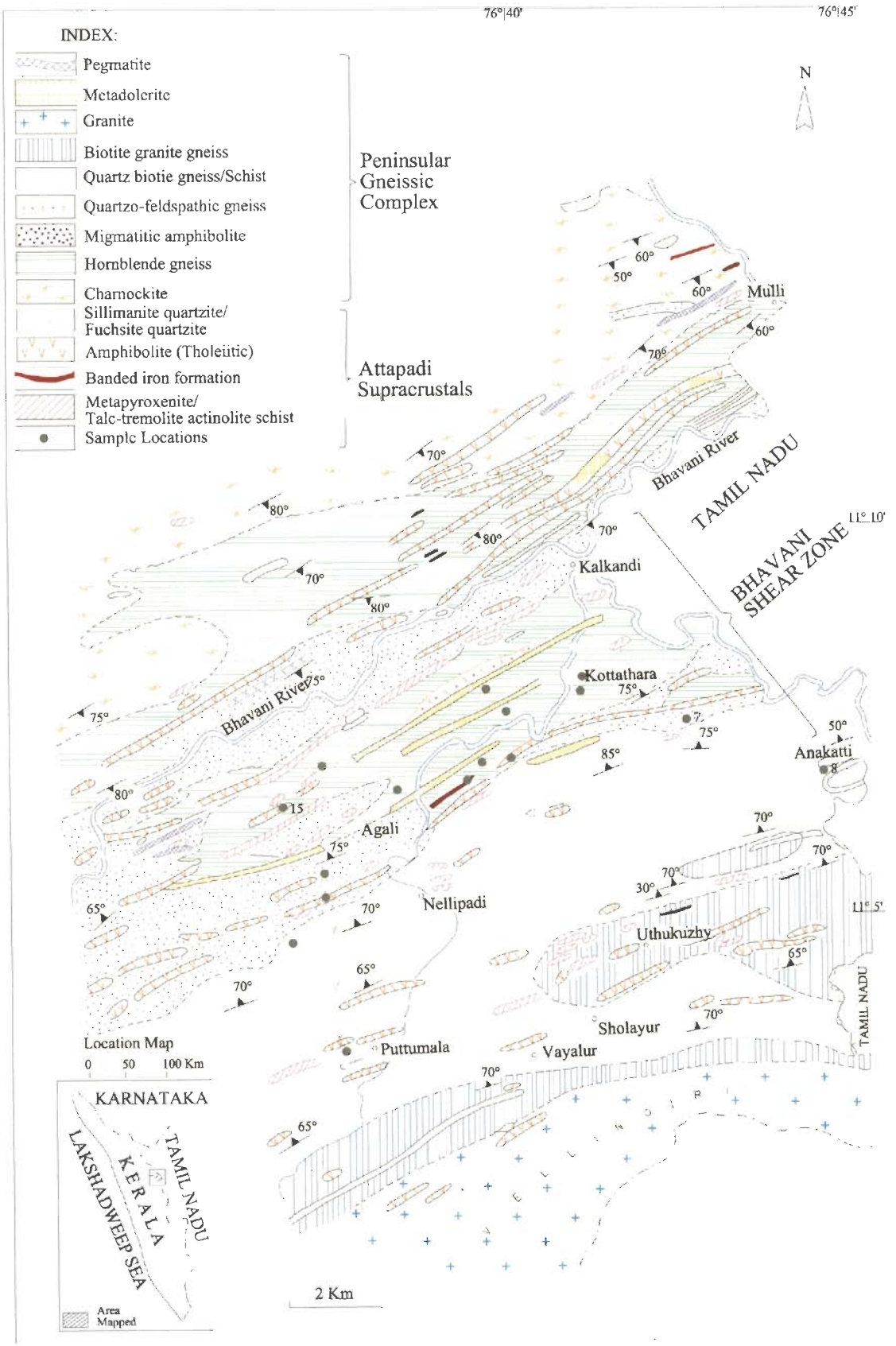

Figure 4.2 Geological map of Attappadi showing sampling locations

Enclosing gneisses include hornblende gneiss, migmaititic-ambhibolite, quartz-biotite gneiss, quartz-feldspathic gneiss, biotite-granite gneiss.

4.2.1a Metaultramafic/talc-tremolite-actinolite schist

Metaultramafic/talc-tremolite-actinolite schist bands and lenses are commonly observed in gneissic rocks of Attappadi Figure 4.3.

Figure 4.3 Metaultramafic bands in hornblende gneiss at Nakkupathi

The alteration of metaultramafic to talc-tremolite- actinolite schist is very common (Fig4 .4), the talc-tremolite - actinolite schist in the Attappadi represents the alteration product of metaultramafic rock. Out crops of metaultramafic/talc-tremolite-actinolite schist rocks are present in the Anaikatti-Sholayur road, Nakkupathi, Narasimukku, Vannathorai, Kattuvalavu, Bhuthavazhi and Puttumala areas. The best exposures are observed in the central part of the study area within biotite gneiss. However, primary volcanic structures and relict textures in metaultramafic rocks described by previous workers were not observed during our study. The mode of emplacement of this metaultramafic rock is not clear. These are white and green,

inequigranular, fine to coarse grained, poorly foliated rock in which tremolite and actinolite occur as radiating needles in a fine grained matrix.

Figure 4.4 The alteration of metaultramafic to talc-tremolite- actinolite schist

4.2.1b Amphibolite

Amphibolite occurs as discontinuous layers and lenses throughout the migmatiitic amphibolite, hornblende gneiss and quartz-biotite gneiss units. The amphibolites range in width from few centimeters to even hundreds of meters. These enclosed amphibolites are parallel to the foliation of the gneisses. They are dark–green to greenish black, equigranular, fine to coarse grained, foliated/massive with hornblende and plagioclase dominated rock. In most of the places, amphibolites are interlayered with BIF (Figure 4.5) and are juxtaposed with BIF with a sharp lithological boundary. Narasimukku, Anaikatti, Vannathorai, Karaiyur, Kattuvalavu are the important locations where good outcrops of both the amphibolite and BIF are present.

Figure 4.5 Amphibolite is juxtaposed with BIF exhibiting sharp lithological boundary in Anakatti

Detailed sampling of different metavolcanics was done for petrogenetic studies. Samples were collected only from those rocks where the effects of syn- or post metamorphic effects are appeared to be minimal.

4.2.2 Banded Iron Formation

The distribution of the BIF in the study area has been shown in Figure 4.6 where the iron formations are found to be typically banded magnetite quartzite associated with metamorphosed volcanic sequences. The BIF occur as layers up to 20m width which persist for only about ten or a few tens of metres along strike. They occur as ridges, and have a general trend of NE-SW direction. These BIF shows millimeter to centimeter scale banding with alternate silica and iron rich layers, which are often less than a few millimeters thick. In Narasimukku area two parallel bands of BIF' that are having variable width (2 to 5 meters) are traceable discontinuously over a cumulative strike length of 3 km (Figure 4.7).

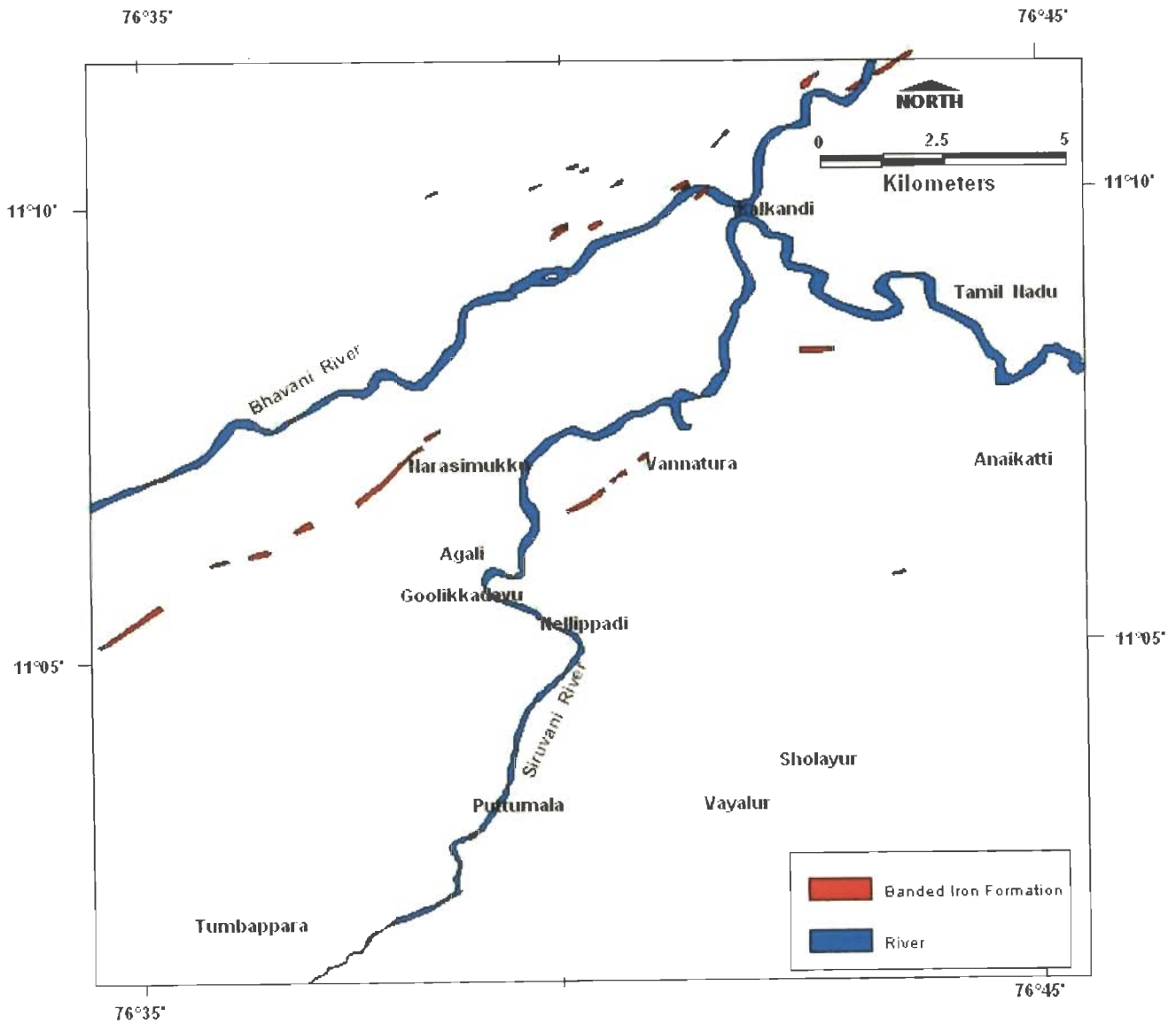

Figure 4.6 Distribution of BIF in Attappadi

These bands have NE-SW trend and steep dips. Exposures of BIF occur in many parts of the study area such as Anaikatti, Vannanthorai, Karaiyur area where, BIF is found to be interlayered with metavolcanics. It is difficult to trace the continuity of these bands due to thick soil cover. Generally in Archaean age greenstone belts BIF occur as few kilometers long and wide and BIF in Attappadi can be classified as Algoma type BIF.

Figure 4.7 BIF in Narasimukku Area

4.2.3 Gneisses

Gneisses are the predominant rock type in the study area with a regional trend of NE-SW which is parallel to the BSZ. These are hornblende gneiss, migmatitic amphibolite, quartz- biotite gneiss, quartz-feldspathic gneiss and biotite granite gneiss which host AS.

Hornblende gneisses are well foliated and are dark gray, medium to coarse grained and consist of hornblende, plagioclase feldspar, quartz and biotite (Figure 4.8).

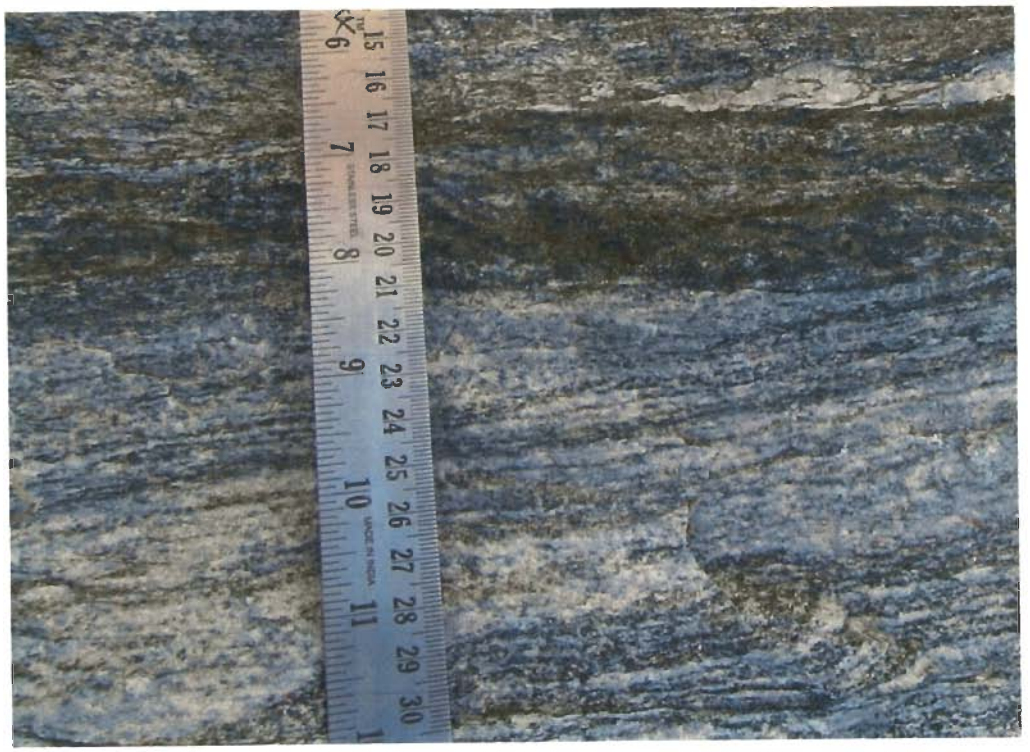

Figure 4.8 Hornblende gneiss in Kottathara

Hornblende gneiss is mainly exposed in the northern part of the area and contains abundant enclaves of meta- sedimentary and ultramafic rocks. They also occur as lenses in the central part, but are less abundant. In the previous studies, it was shown that there is a gradational contact with charnockite in the northern part of the study area, but during the present study such a contact relation has not been observed.

The migmatitic amphibolite is a heterogeneous lithounit of the study area. It is well exposed for about half a kilometer in the Karaiyur, the central part of the study area (Figure 4.9). The migmatitic amphibolites consist of layered mafic and felspathic bands of thickness ranging from few centimeters to several meters. Amphibolite occurs as discontinuous layers and lenses throughout the migmatititic anmphibolite.

Quartz-biotite gneiss/ quartz-feldspathic gneiss/ biotite granite gneiss are exposed in the central part of the study area and are showing high degree of shearing/ deformation. (Figure 4.10). Quartz biotite gneiss occurs in the central part of the study area showing a gradational contact with the hornblende gneiss.

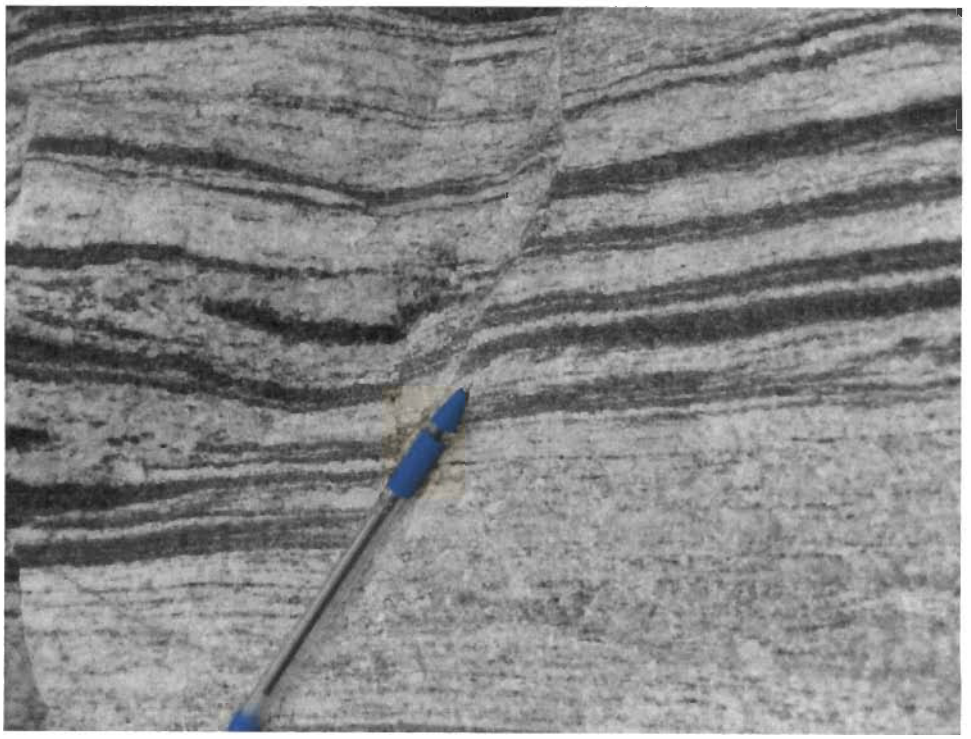

Figure 4.9 Migmatitic amphibolites with layers of mafic and felsic bands in Karaiur

Fig. 4.10 Quartz biotite gneiss in Vattulakki area

It is a fissile rock with the fissility marked by clusters of biotite along shear planes. Granite gneiss is medium to coarse grained, weakly foiliated, leucocratic rock

dominantly composed of quartz, feldspars and biotite which are observed in the Puttumala area of Attappadi. Other lithological units such as sillimamite/kyanite bearing quartzite and fuchsite-quartzite, granite, metadolerite, pegmatite are not dealt in this work.

4.2.4 Gold-quartz veins

Gold bearing quartz veins in Attappadi are present within occurring within different lithounits developed proximal to the contact zone of metavolcanics rocks. Abundant veins are present in the central and the southern parts of the study area. The abundance of veins decreases rapidly to the north of the Attappadi, and gold bearing quartz veins are unknown from this part of the region. Most of the gold quartz veins are within ductile shear zone and thus show characteristic style of sheared veins, such as strongly folded (Figure 4.11), fractured and boudinaged patterns (Figure 4.12).

Figure 4.11 Folded mineralized vein in Naikerpadi

On the basis of structural style and field relations, quartz veins are classified as foliation parallel type (Figure 4.13).

Figure 4.12 Multiple fractures in mineralized vein of Kallakkara

Fig. 4.13 Foliation parallel mineralized vein in Kottathara

The field evidence shows that these pre-existing gold- quartz vein systems are characteristically controlled by foliation and shear zones. The veins occur as a series of sub parallel, moderate to steeply dipping reefs, trending NNE-SSW to NE-SW, with widths varying from a few tens of centimeters to a few meters (Figure 4.14). The vertical extent of individual veins is unknown; laterally the veins are generally tens to a maximum of few hundreds of meters in length and usually pinch out quite rapidly. The quartz veins are mainly comprise of milky translucent quartz and sulfide minerals, but often they appear 'dirty' due to the weathering of sulfide minerals in consequence of extreme tropical weathering conditions in this terrain (Figure 4.15).

Figure 4.14 Massive quartz vein in Kattuvalavu area

The quartz veins consist of pyrite as the major sulfide mineral with chalcopyrite (Figure 4.16), galena and covellite as minor mineral constituents. Visible specks of gold were noticed in the samples collected from the veins, particularly

where associated sulfides have been subjected to weathering and leaching (Figure 4.17) resulting in the formation of limonite.

Figure 4.15 Limonotized Quartz vein in Vannathorai

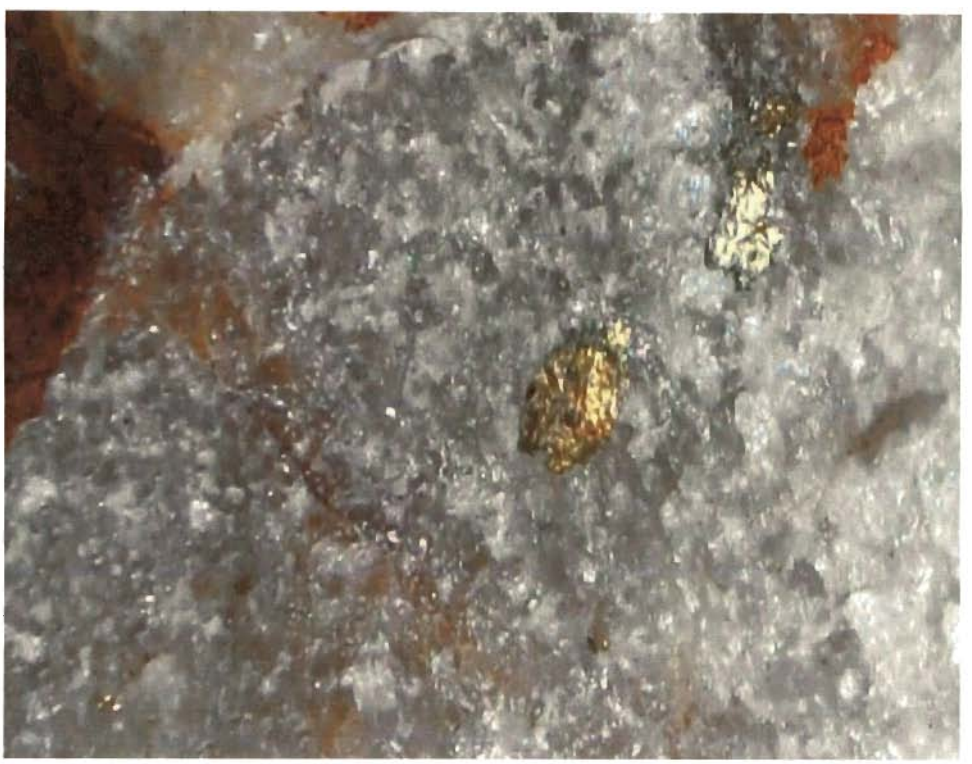

Figure 4.16 Chalcopyrite and Pyrite in quartz veins

Figure 4.17 Leached pyrite in quartz vein

4.3 Petrography

Detailed petrographic study is a necessary step in the classification of rock types and a prerequisite for geochemical studies. As a first step, the constituent minerals and modal proportions were estimated for further nomenclature. Texture, mineralogy and microstructures were also identified. The mineral chemistry of selected samples were analyzed using EPMA and the results were given in Table 4.1

4.3.1 Metaultramafics/ Talc –Tremolite Schist

Several metaultramafic layers and its alteration product- talc-tremolite schist occur within different gneissic rock in the study area. Mafic rocks with relict pyroxenes, mineral are not wide spread in the studied samples. Relict pyroxenes in the medium to coarse grained rocks are invariably partly altered to various hydrous phases (Figure 4.18) and in fine grained rocks the pyroxene are completely pseudomorphosed by actinolite and chlorite.

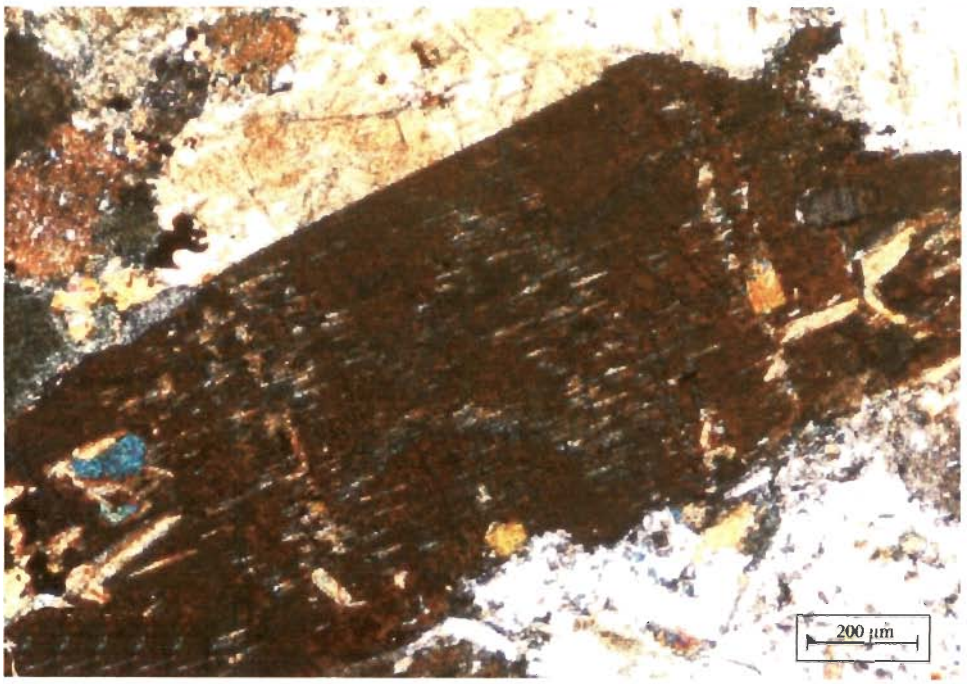

Figure 4.18 Relict pyroxene in metavolcanis of Anaikatti area of Attappadi

Tremolite and actinolite occur as needles in a talcose matrix (Figure 4.19). These rocks have greenshist facies mineral assemblage (actinolite+tremolite +chlorite) The modal mineralogy (in vol %) is: 50-55% Talc 15-20% and tremolite, 10-20 % actinolite.

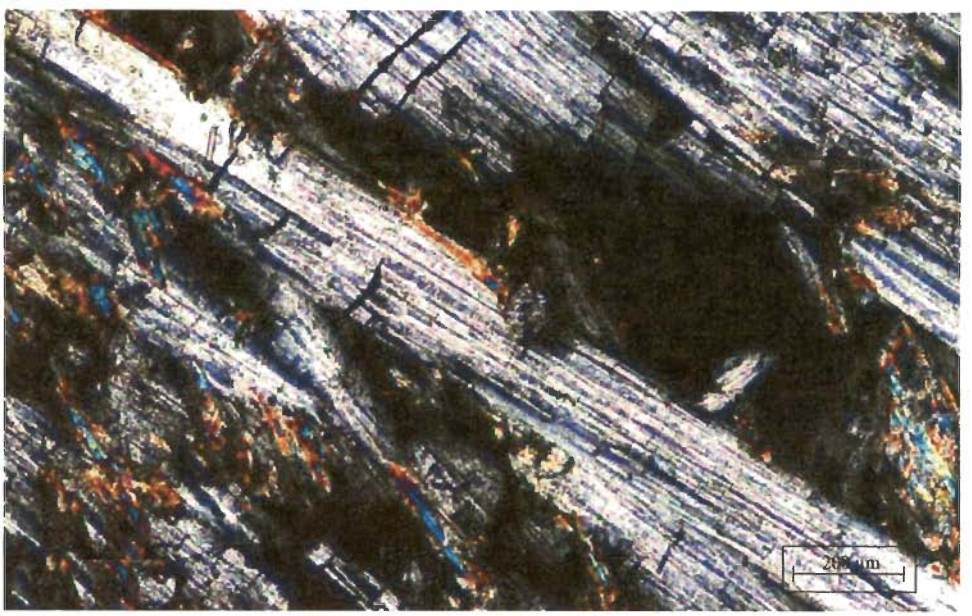

Figure 4.19 Tremolite and actinolite in metavolnanics of Anaikatti area of Attappadi

4.3.2 Amphibolites

These amphibolites are coarse grained rocks showing equigranular texture (Figure 4.20) and are dominantly composed of hornblende and plagioclase (Figure 4.21). In thin section, subordinate amount of fine grained chlorite, quartz, and opaque minerals are present. Most of the hornblende grains have been partly converted into chlorite probably due to hydrothermal fluid alteration. Plagioclase is the second main constituent of these rocks. Mineral assemblage indicates that the rocks could have undergone lower to middle amphibolite facies metamorphism. The average model mineralogy is 45-50% hornblende, 20-25 % plagioclase feldspar, 5-8% biotite and chlorite, and rest of the mode is constituted by the accessory minerals namely epidote, orthoclase, microcline and opaque.

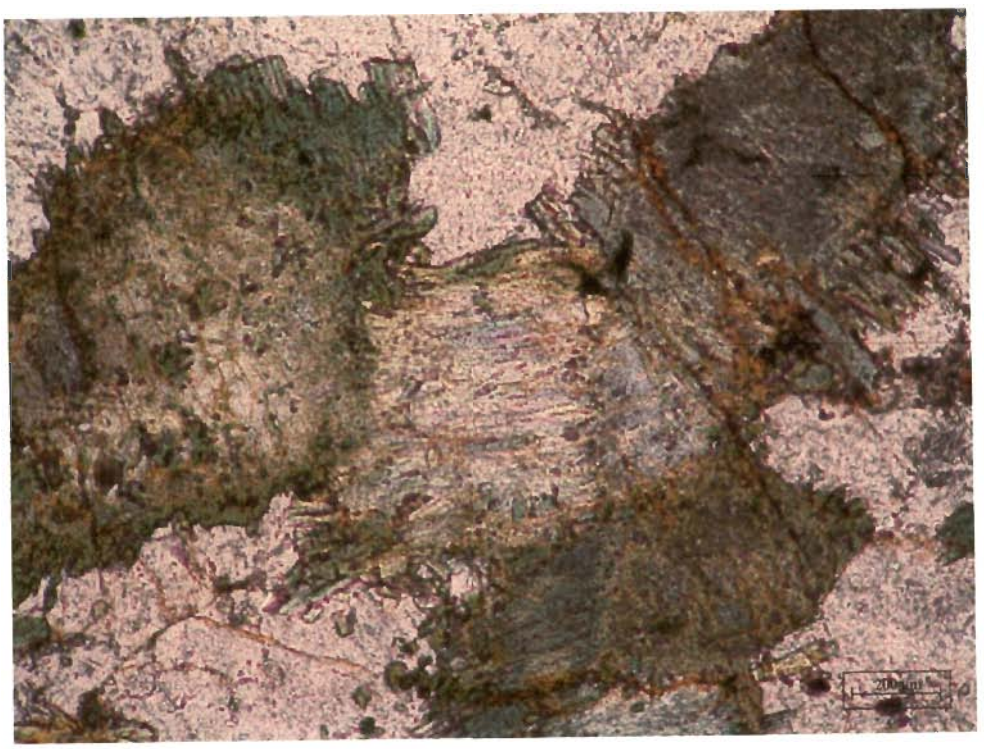

Figure 4.20 Amphibolite showing equigranular texture Vannathorai area

Figure 4.21 Hornblende and plagioclase in Amphibolite

4.3.3 Hornblende Gneiss

Hornblende gneisses are foliated and exhibit medium to coarse grained texture. The dark coloured band composed of hornblende and light coloured bands are made up of felsic minerals. Biotite represents an alteration product of hornblende, at places chlorite is seen developed within biotite (Figure 4.22). The average modal mineralogy is 45-50% hornblende, 20-25 % quartz, 10-20 % plagioclase feldspar, and rest of the mode is constituted by the accessory minerals namely epidote, zoisite, chlorite, apatite, zircon and opaque.

4.3.4 Quartz-Biotite Gneiss

Strongly sheared quartz-biotite gneiss has well developed mylonitic fabric and composed chiefly of quartz, biotite, feldspars and sulfide minerals. Foliation and lineation in the quartz-biotite gneiss are defined by recrystallized quartz and biotite ribbons (Figure 4.23).

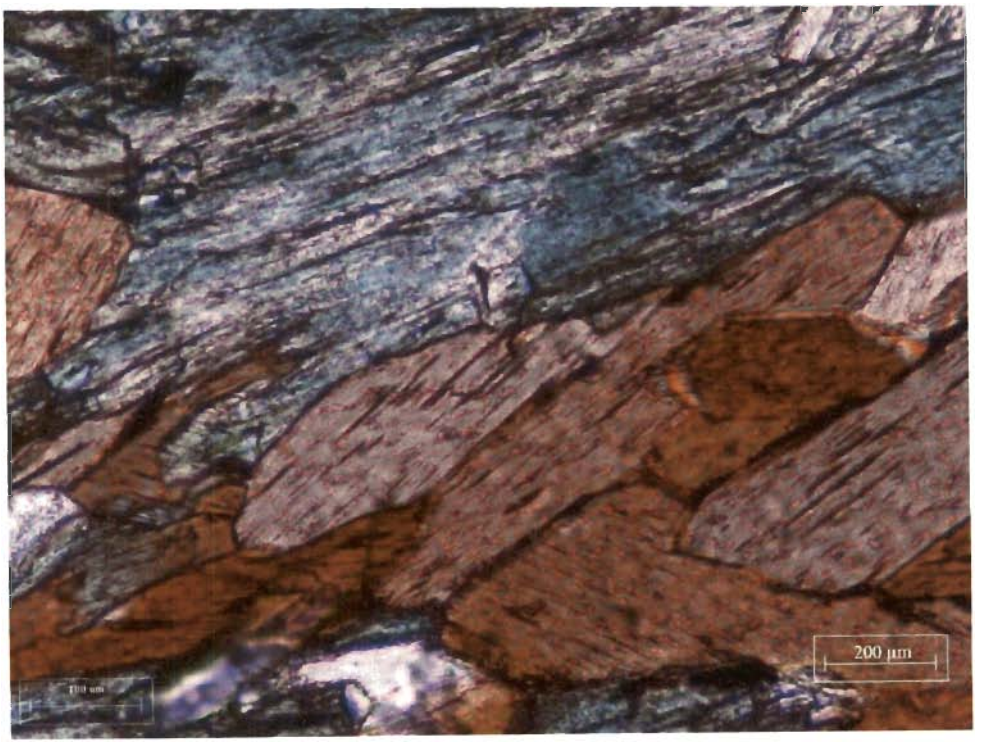

Figure 4.22 Hornblende and biotite in Hornblende gneiss

Figure 4.23 Recrystallized quartz and biotite in quartz biotite geniess

Deformation fabric in the rocks is exhibited by dynamically recrystallized quartz and bent twin lamellae of plagioclase (Figure 4.24). Quartz aggregates are seen surrounded by the biotite to develop an augen structure (Figure 4.25). The modal mineralogy is: quartz 50-55 % Biotite 30%, plagioclase 10 % rest of the mode is constituted by the accessory minerals such as muscovite and opaque

4.3.5 Migmatitic-Amphibolite

Migmatitic amphibolites are medium to coarse grained rock with prominent bandings developed. The gneissic band is defined by amphiboles and felsic minerals. Hornblende, quartz and plagioclase are the major minerals. Biotite, apatite and opaque are accessory minerals.

Figure 4.24 Bent twin lamellae of plagioclase in quarz biotite gniess

Table 4.1 Microprobe analysis of amphiboles. Calculations based on 24 oxygen atoms

	Amphibolite									
SiO_2	55.07	51.05	40.88	42.4	49.49	47.85	49.19	52.53	48.16	47.98
TiO_2	0.08	0	0.43	0.48	0.19	0.34	0.27	0.08	0.35	0.25
$Al2O_3$	0.05	0	13.53	12.52	5.84	7.62	6.53	3.17	6.9	7.21
FeO	0.77	0.12	17.66	17.76	14.38	15.23	14.12	15.68	14.98	14.52
MnO	0.03	0.54	0.22	0.38	0.29	0.29	0.35	0.48	0.29	0.28
MgO	17.95	0.03	8.11	8.86	12.86	11.95	12.79	14.83	12.12	12.17
CaO	24.73	46.86	11.06	11.18	11.51	11.27	11.55	8.84	11.6	11.42
Na_2O	0.09	0.02	1.8	1.61	0.78	1.04	0.82	0.57	0.95	0.93
K_2O	0.02	0	0.44	0.24	0.13	0.18	0.19	0.06	0.22	0.18
P_2O_5	0	0.03	0.06	0.08	0	0	0.02	0	0	0.01
Total	98.79	98.65	94.19	95.51	95.47	95.77	95.83	96.24	95.57	94.95
Si	8.04	8.01	6.66	6.79	7.70	7.47	7.62	8.06	7.54	7.53
Ti	0.01	0.00	0.05	0.06	0.02	0.04	0.03	0.01	0.04	0.03
Al	0.01	0.00	2.60	2.36	1.07	1.40	1.19	0.57	1.27	1.33
Fe	0.09	0.02	2.41	2.38	1.87	1.99	1.83	2.01	1.96	1.91
Mn	0.00	0.07	0.03	0.05	0.04	0.04	0.05	0.06	0.04	0.04
Mg	3.91	0.01	1.97	2.12	2.98	2.78	2.96	3.39	2.83	2.85
Ca	3.87	7.88	1.93	1.92	1.92	1.89	1.92	1.45	1.94	1.92
Na	0.03	0.01	0.57	0.50	0.24	0.31	0.25	0.17	0.29	0.28
K	0.00	0.00	0.09	0.05	0.03	0.04	0.04	0.01	0.04	0.04
P	0.00	0.00	0.01	0.01	0.00	0.00	0.00	0.00	0.00	0.00

	Migmatitic Amphibolite									
SiO_2	38.1	48.23	43.63	43.16	50.97	43.76	37.86	37.84	45.7	47.95
TiO_2	0	0.23	0.33	0.3	0.08	0.33	0.13	0.09	0.32	0.2
Al_2O_3	25.97	7.21	10.93	11.57	4.8	11.34	24.13	23.06	9.04	7.23
FeO	8.11	14.38	16.82	17.2	13.31	16.56	9.92	11.64	16.24	14.37
MnO	0.15	0.31	0.27	0.3	0.3	0.31	0.15	0.01	0.38	0.24
MgO	0.03	12.62	10.15	9.7	14.76	9.8	0.04	0	11.19	12.96
CaO	23.49	12.12	11.75	11.76	12.07	11.89	23.23	23.25	12.05	12
Na_2O	0	0.71	1.24	1.26	0.45	1.21	0.01	0.01	0.95	0.63
K_2O	0	0.2	0.47	0.39	0.15	0.52	0.02	0	0.4	0.2
P_2O_5	0.03	0.04	0.01	0	0.01	0.04	0.04	0.02	0.02	0.05
Total	95.88	96.05	95.6	95.64	96.9	95.76	95.53	95.92	96.29	95.83
Si	5.93	7.49	6.95	6.89	7.77	6.95	5.98	6.00	7.19	7.46
Ti	0.00	0.03	0.04	0.04	0.01	0.04	0.02	0.01	0.04	0.02
Al	4.76	1.32	2.05	2.18	0.86	2.12	4.49	4.31	1.68	1.33
Fe	1.05	1.87	2.24	2.30	1.70	2.20	1.31	1.54	2.14	1.87
Mn	0.02	0.04	0.04	0.04	0.04	0.04	0.02	0.00	0.05	0.03
Mg	0.01	2.92	2.41	2.31	3.36	2.32	0.01	0.00	2.62	3.01
Ca	3.91	2.02	2.01	2.01	1.97	2.02	3.93	3.95	2.03	2.00
Na	0.00	0.21	0.38	0.39	0.13	0.37	0.00	0.00	0.29	0.19
K	0.00	0.04	0.10	0.08	0.03	0.11	0.00	0.00	0.08	0.04
P	0.00	0.01	0.00	0.00	0.00	0.01	0.01	0.00	0.00	0.01

	Hornblende Gneiss				
SiO_2	44.05	43.91	44.04	43.67	44.91
TiO_2	0.12	0.29	0.31	0.19	0.22
Al_2O_3	12.33	11.92	11.67	12.92	10.85
FeO	14.66	14.69	14.27	14.77	14.12
MnO	0.27	0.30	0.27	0.21	0.35
MgO	11.13	11.21	11.28	10.91	11.85
CaO	11.52	11.64	11.69	11.36	11.35
Na_2O	1.68	1.60	1.53	1.56	1.36
K_2O	0.18	0.23	0.29	0.23	0.19
P_2O5	0.00	0.02	0.00	0.05	0
Total	95.94	95.81	95.35	95.87	95.20
Si	6.90	6.90	6.94	6.84	7.06
Ti	0.01	0.03	0.04	0.02	0.03
Al	2.28	2.21	2.17	2.39	2.01
Fe	1.92	1.93	1.88	1.94	1.86
Mn	0.04	0.04	0.04	0.03	0.05
Mg	2.60	2.63	2.65	2.55	2.78
Ca	1.93	1.96	1.97	1.91	1.91
Na	0.51	0.49	0.47	0.47	0.41
K	0.04	0.05	0.06	0.05	0.04
P	0.00	0.00	0.00	0.01	0.00

Table 4.2 Microprobe analysis of Plagioclase. Calculations based on 8 oxygen atoms

	Migmatitic amphobolite				Hornblende Gneiss				Amphibolite	
SiO_2	61.76	61.99	60.94	62.15	61.04	60.24	61.83	62.11	59.28	63.09
TiO_2	0	0	0	0	0	0.05	0	0.03	0	0
Al_2O_3	23.05	23.5	23.07	23.33	23.76	23.97	23.3	23.4	24.62	23.12
FeO	0.12	0.11	0.01	0.2	0.06	0.04	0.15	0.01	0.05	0.21
MnO	0	0.04	0	0.02	0	0	0	0.02	0	0.03
MgO	0.02	0.01	0	0.01	0.02	0	0	0.01	0.09	0
CaO	5.11	5.53	5.62	5.56	5.81	6.46	5.31	5.45	0.12	4.86
Na_2O	8.74	8.37	8.57	8.84	8.4	8.04	8.86	8.66	15.14	8.98
K_2O	0.1	0.08	0.09	0.05	0.15	0.07	0.09	0.08	0.01	0.05
P_2O5	0	0	0	0.02	0	0.01	0.04	0.01	0.02	0
Total	98.9	99.63	98.3	100.18	99.24	98.88	99.58	99.78	99.33	100.34
Si	2.77	2.76	2.75	2.76	2.73	2.71	2.76	2.76	2.68	2.79
Ti	0.00	0.00	0.00	0.00	0.00	0.00	0.00	0.00	0.00	0.00
Al	1.22	1.23	1.23	1.22	1.25	1.27	1.22	1.23	1.31	1.20
Fe	0.00	0.00	0.00	0.01	0.00	0.00	0.01	0.00	0.00	0.01
Mn	0.00	0.00	0.00	0.00	0.00	0.00	0.00	0.00	0.00	0.00
Mg	0.00	0.00	0.00	0.00	0.00	0.00	0.00	0.00	0.01	0.00
Ca	0.25	0.26	0.27	0.26	0.28	0.31	0.25	0.26	0.01	0.23
Na	0.76	0.72	0.75	0.76	0.73	0.70	0.77	0.75	1.33	0.77
K	0.01	0.00	0.01	0.00	0.01	0.00	0.01	0.00	0.00	0.00
P	0.00	0.00	0.00	0.00	0.00	0.00	0.00	0.00	0.00	0.00

Table 4.3 Microprobe analysis of Biotite and Chlorite. Calculations based on 20 oxygen atoms

	Biotite In Amphibolite				Chlorite in Hornblende gneiss				
SiO_2	64.56	36.39	35.6	36.15	99.52	26.63	26.68	25.98	26.94
TiO_2	0.02	2.06	2.1	2	0	0.14	0.06	0.09	0
Al_2O_3	17.6	14.52	14.77	14.26	0.01	20.56	20.37	20.35	20.7
FeO	0.04	17.73	17.85	17.63	0.15	16.23	16.93	16.16	16.21
MnO	0	0.07	0.12	0	0	0.14	0.1	0.23	0.15
MgO	0	12.11	12.29	12.22	0	20.75	20.6	19.7	21.17
CaO	0.01	0.08	0.02	0.13	0.05	0.02	0.05	0.16	0.05
Na_2O	1.46	0.22	0.24	0.21	0.07	0.02	0.02	0.1	0.03
K_2O	15.28	9.27	9.11	8.95	0	0.03	0.02	0.06	0
P_2O5	0	0.06	0	0	0	0	0	0.09	0
Total	98.97	92.51	92.1	91.55	99.80	84.52	84.83	82.92	85.25
Si	9.04	6.20	6.11	6.22	1.00	3.96	3.97	3.95	3.97
Ti	0.00	0.26	0.27	0.26	0.00	0.02	0.01	0.01	0.00
Al	2.90	2.92	2.99	2.89	0.00	3.60	3.57	3.64	3.59
Fe	0.00	2.53	2.56	2.54	0.00	2.02	2.11	2.05	2.00
Mn	0.00	0.01	0.02	0.00	0.00	0.02	0.01	0.03	0.02
Mg	0.00	3.08	3.14	3.13	0.00	4.60	4.57	4.46	4.65
Ca	0.00	0.01	0.00	0.02	0.00	0.00	0.01	0.03	0.01
Na	0.40	0.07	0.08	0.07	0.00	0.01	0.01	0.03	0.01
K	2.73	2.02	1.99	1.96	0.00	0.01	0.00	0.01	0.00
P	0.00	0.01	0.00	0.00	0.00	0.00	0.00	0.01	0.00

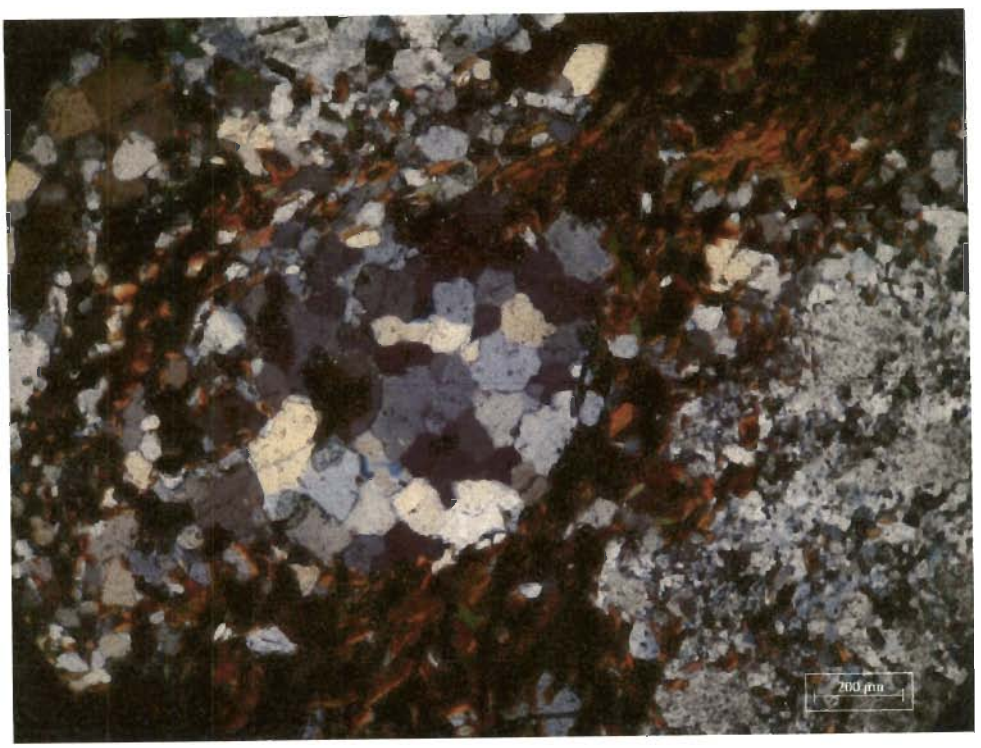

Figure 4.25 Biotite is surrounding the quartz aggregate to give augen

4.3.6 Petrography of mineralized vein

Quartz veins have undergone several modifications because of metamorphism and deformations. These veins are characterized by recrystallized quartz and are consistently seen in all studied samples Figure 4.26 and 4.27

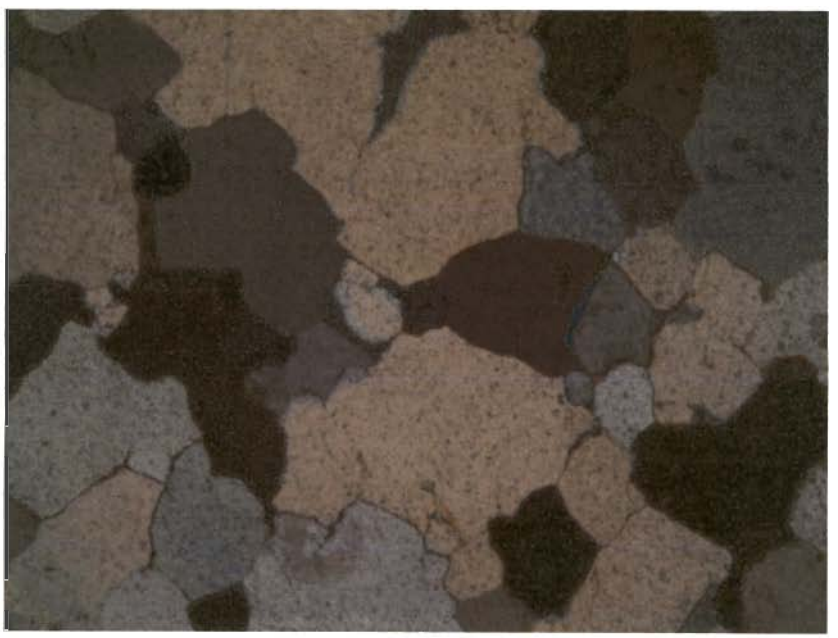

Figure 4.26 Grain boundary migration recrystallization in quartz vein

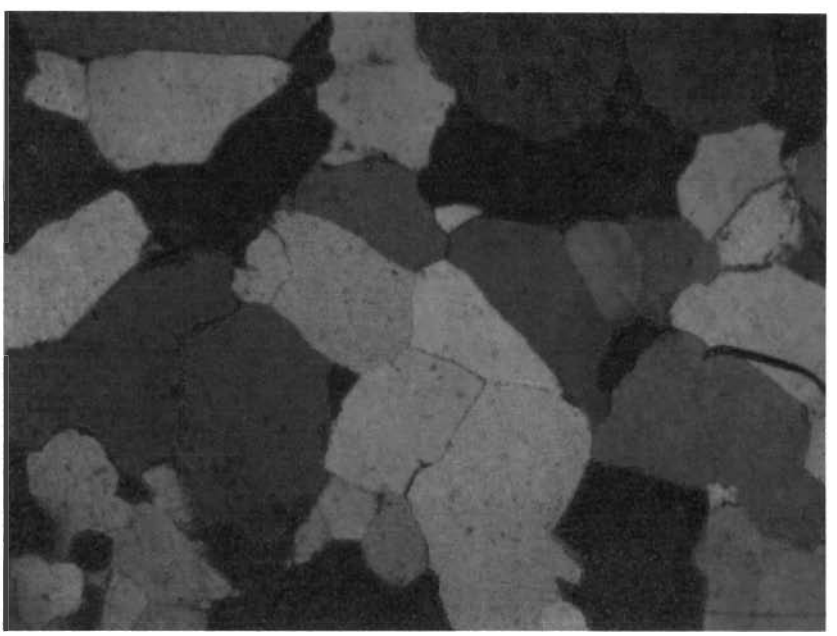

Figure 4.27 Recrystallization in mineralized quartz vein

4.3.7 Banded Iron Formation (BIF)

Banded iron formations are fine to medium grained, laminated and consist mainly of quartz rich and iron rich layers (Figure 4.28).

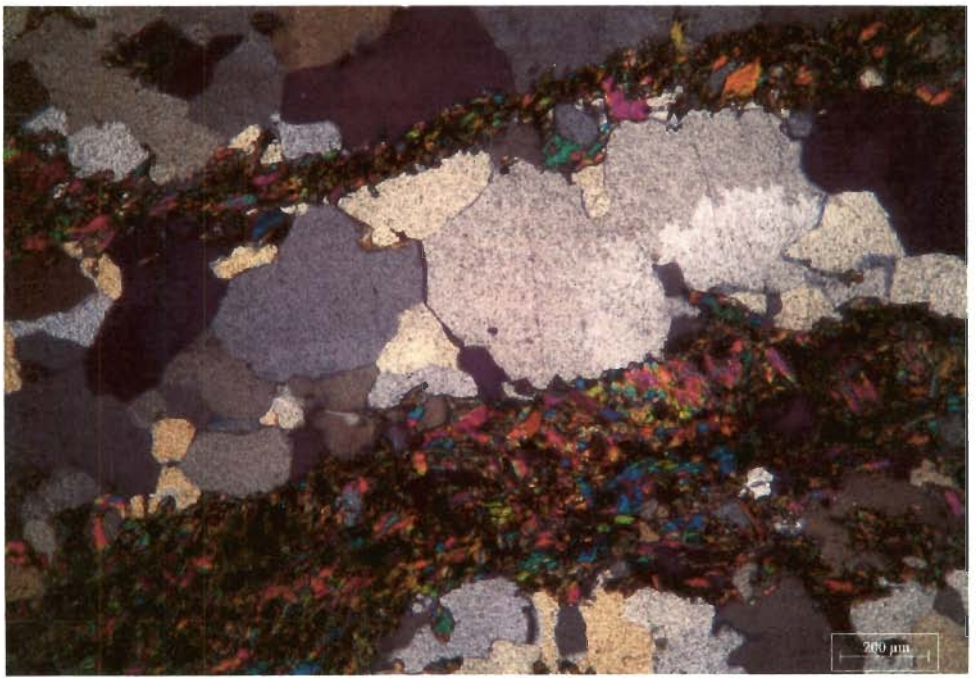

Figure 4.28 quartz rich and iron silicate rich layers in BIF

Few samples of BIF are characterized by the presence of grunerite as a major component in the iron rich layers. Quartz and abundant opaque minerals also present in the BIF. The details of ore microscopic study of these opaques are given in next section

4.4 Ore Mineralogical Study

Mineralized veins, quartz biotite gneiss and banded iron formation samples collected from the Attappadi area were studied under reflected light microscope. The quartz veins had been sheared and subsequently recrystallized. It has been observed that the abundance of opaque minerals is significantly more in quartz biotite gneiss among the different litho-units in the study area. Hence, these opaque minerals were also studied under reflected light microscopic to identify sulfide minerals and their relationships to associated silicate and other phases.

Ore microscopic studies were mainly limited to surface samples collected from different prospects since there is no working mine/old workings or sub- surface exploration activity in this terrain. The sulfide minerals present in mineralized zones have been found to be altered.

4.4.1 Quartz veins

Microscopic observation of the polished specimens of quartz vein samples indicate the presence of pyrite, pyrrhotite, chalcopyrite and galena are present. Other minor opaque phases include covellite and malachite. Few gold grains were separated (by panning) from the weathered samples collected in the field and were confirmed through SEM-EDAX in the laboratory. The results have been given in Figure 4.29 and Figure 4.30.

4.4.1a Pyrite

Pyrite is the dominant sulfides mineral present in the samples and occurs as euhedral grains, fracture filling and also small disseminated grains. At least two generations of pyrite could be recognized in all the samples. The early generation is represented by the massive aggregates of euhedral to subhedral cubic crystals.

Most of the euhedral pyrite has been leached due to surface alteration evidenced by relict cubic shapes in the sample. So, during ore microscopic studies pyrite of this generation not identified. Pyrite of second generation occurs as stringers and fracture fillings (Figure 4.31) which appear to be fresh and not affected much surface alteration. Abundant small disseminated euhedral pyrite also identified during the study (Figure 4.32).

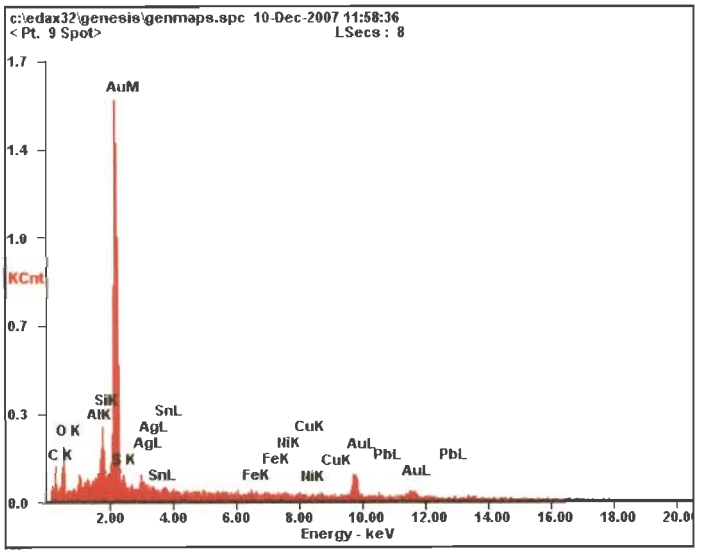

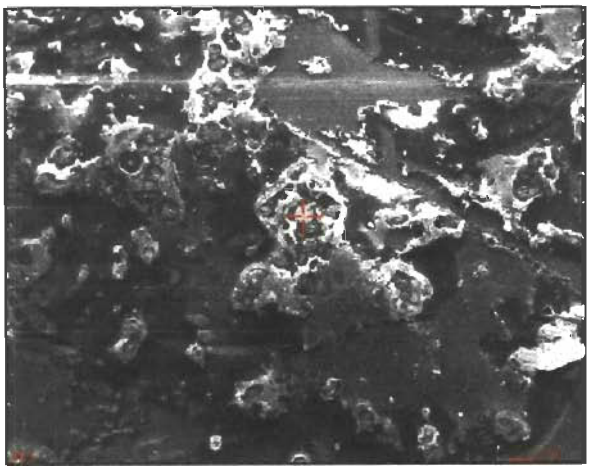

Element	Wt%	At%
CK	14.20	50.70
OK	09.97	26.74
AlK	00.14	00.23
SiK	02.97	04.53
SK	00.00	00.00
AgL	03.91	01.55
SnL	00.54	00.20
FeK	00.97	00.74
NiK	00.89	00.65
CuK	00.57	00.38
AuL	58.91	12.83
PbL	06.93	01.43
Matrix	Correction	ZAF

Figure 4.29 EDAX results for separated gold grains from veins

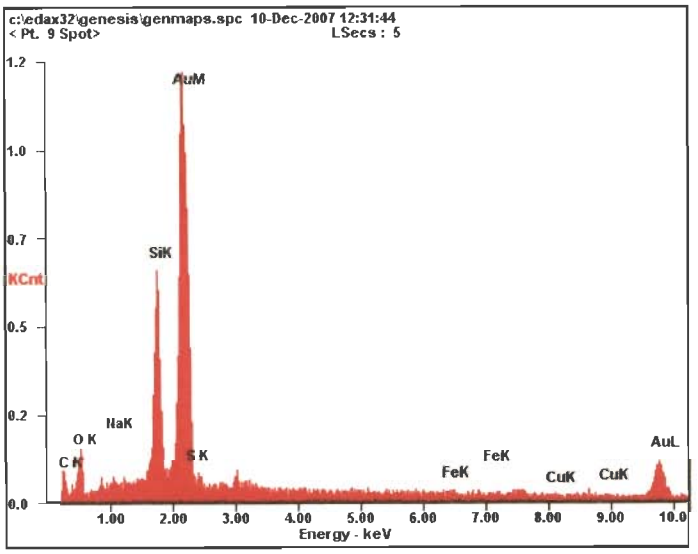

Element	*Wt%*	*At%*
CK	10.80	40.79
OK	09.04	25.63
NaK	00.45	00.90
SiK	09.62	15.53
SK	00.00	00.00
FeK	00.86	00.70
CuK	01.04	00.74
AuL	68.19	15.71
Matrix	Correction	ZAF

Figure 4.30 EDAX results for separated gold grains from veins

4.4.1b Chalcopyrite

Chalcopyrite is another dominant sulfide phase within quartz lodes and is distributed as disseminations and also as fracture filling. Chalcopyrite is associated with pyrite and all other sulfide minerals. It shows golden yellow colour and feeble anisotropism with colour changes from yellow to grey. Chalcopyrite occurs in close association with covellite, and this covellite appears to be an alteration product of chalcopyrite (Figure 4.33) exhibiting marginal alteration.

4.4.1c Galena

Galena is commonly found to occur as fracture filling in the lode. It has been identified by its characteristic triangular pits and bright white colour. Marginal replacement of galena by anglesite is very common (Figure 4.34).

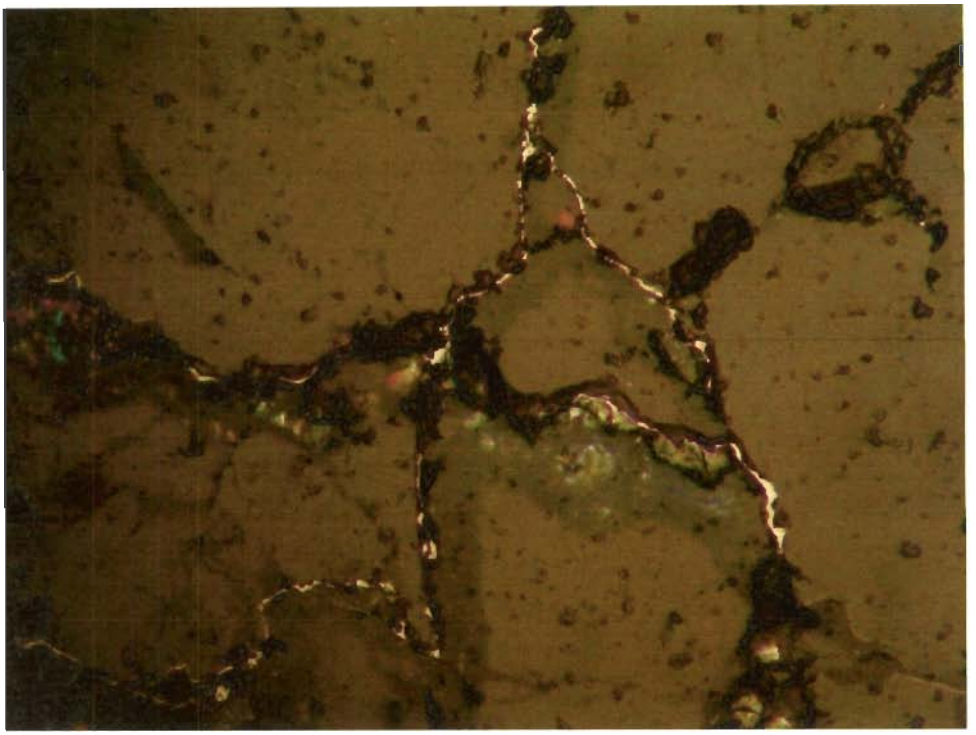

Figure 4.31 Pyrite of second generation occurs as stringers and fracture fillings

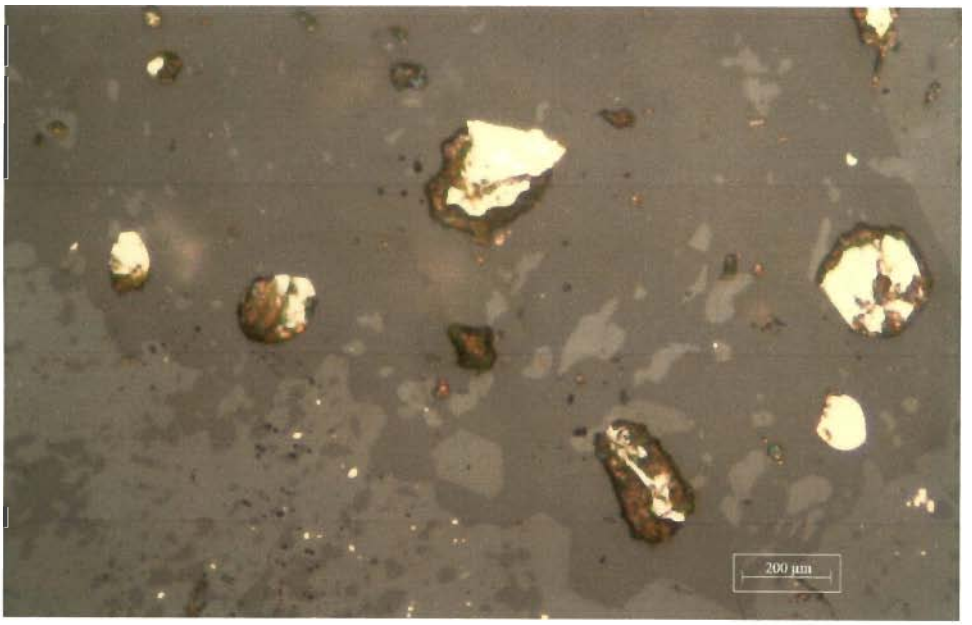

Figure 4.32 Disseminated pyrite

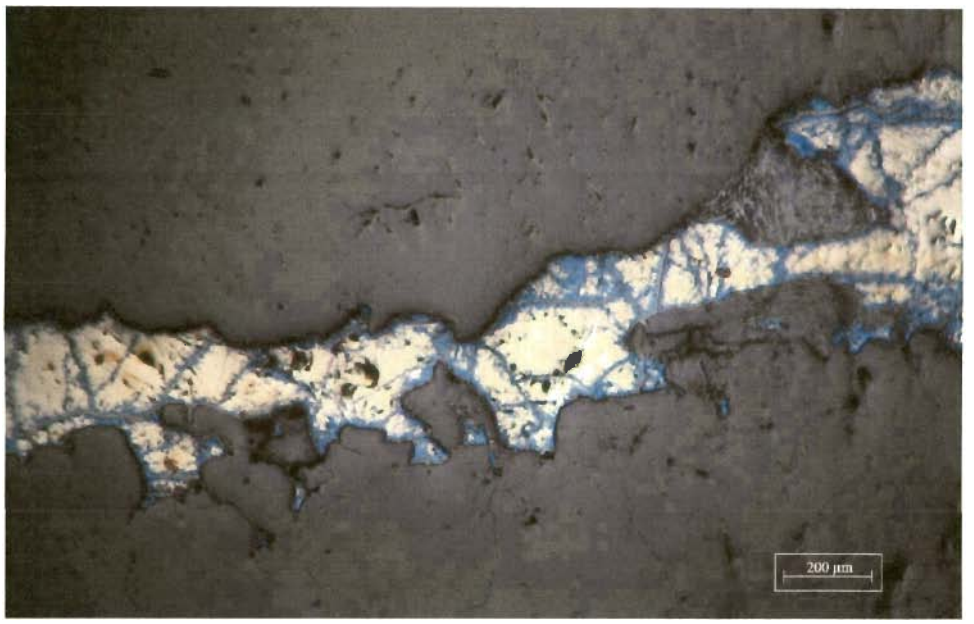

Figure 4.33 Chalcopyrite being replaced by covellite

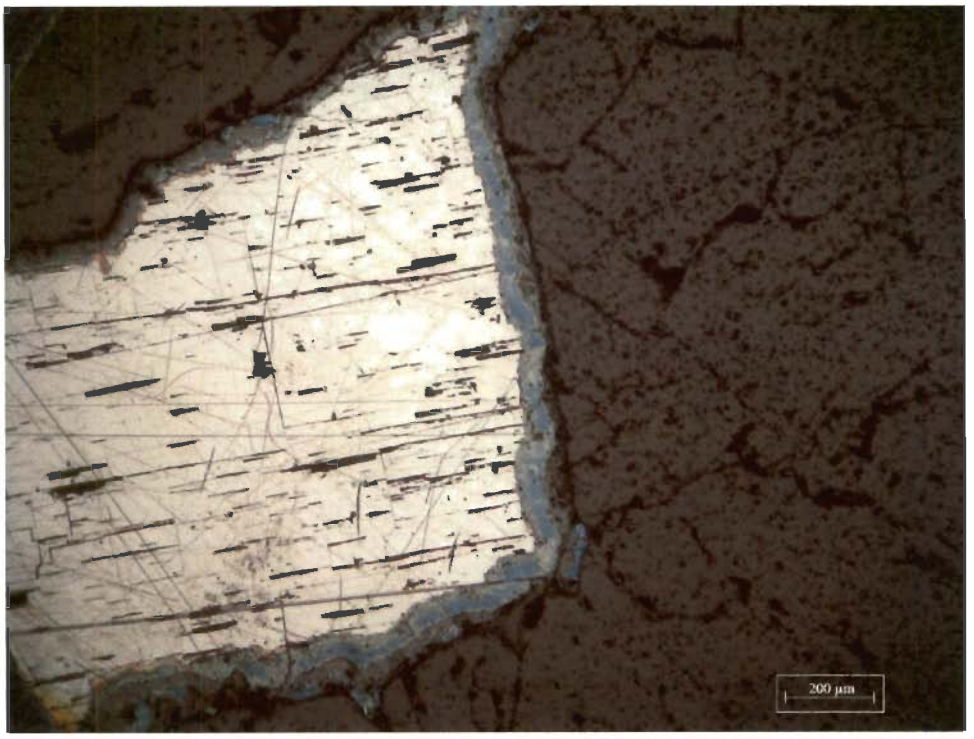

Figure 4.34 Galena is being replaced by anglesite

4.4.2 Quartz biotite gneiss.

Abundant sulfide minerals have been observed in quartz biotite gneiss. Major ore minerals present in quartz biotite gneiss are pyrrotite, chalcopyrite and pyrite. The grains of pyrrhotite show creamy brown colour. It is strongly anisotropic with colour changes from grayish yellow to grayish blue. It has medium polishing hardness which is higher than chalcopyrite. Pyrrohtite exhibit as irregular grains and laths and commonly associated with chalcopyrite. Pyrrhotite and chalcopyrite exhibit sharp boundary in this rock indicating their co- genetic origin. Figure 4.35 Pyrrhotite also occurs as elongated crystals along the shear plane may be due to the post deformation of the earlier formed minerals (Figure 4.36). In these rocks pyrite occur interstially between quartz and feldspar crystals or along veinlets crosscutting these minerals suggesting that the pyrite is hydrothermal in origin.

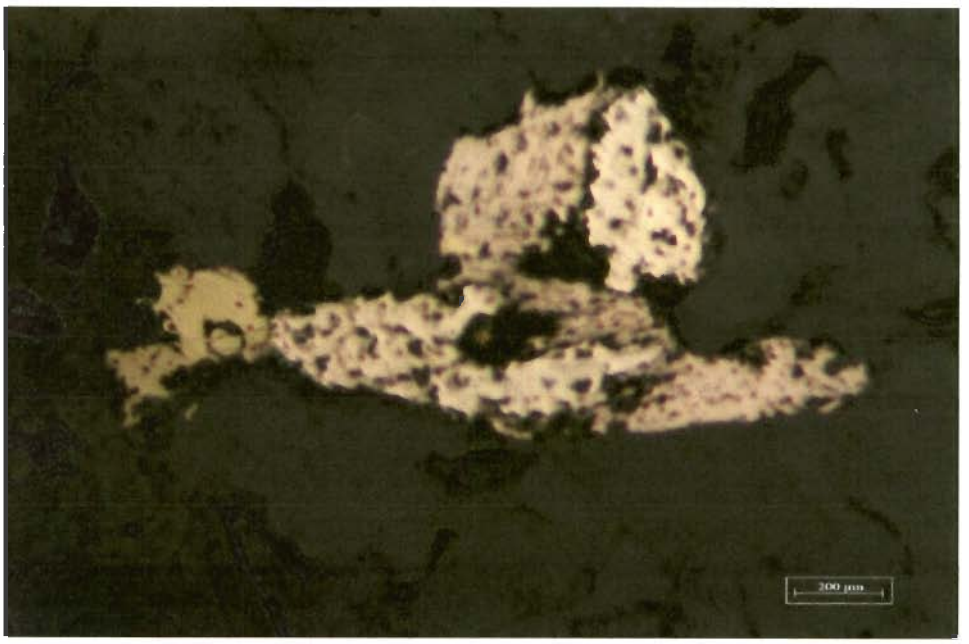

Figure 4.35 Pyrrhotite and chalcopyrite exhibit sharp boundary

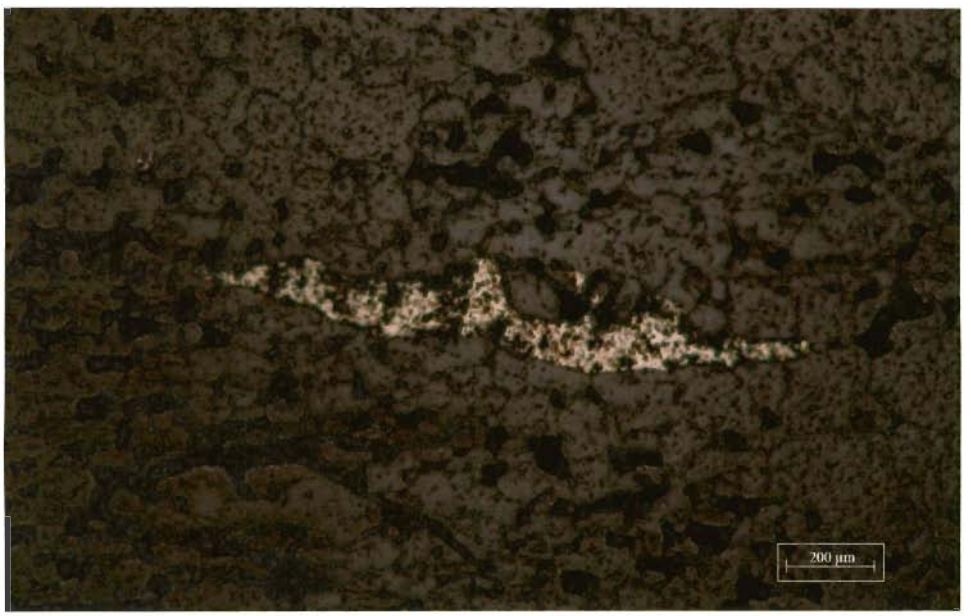

Figure 4.36 Pyrrhotite occurs as elongated crystals along the shear plane

4.4.3 Banded Iron Formation (BIF)

BIF's are characterized by the predominance of minerals such as hematite-magnetite. Magnetite is the dominant oxide mineral in the samples from Narasimukku and Vannanthura (Figure 4.37). It was distinguished by its greyish

white colour with brownish tint, isotropism, moderate reflectivity and high scratch hardness. Most of the grains are anhedral and pitted and occurring in an individual layer.

Hematite is the another dominant oxide mineral in the samples from Karaiyur.(Fig 4.38) Hematite is distinguished by its grey-white with bluish tint, high reflectivity, anisotropism, showing deep red internal reflection and high scratch hardness. It is observed that the hematite present in the specimens is mostly altered products of magnetite.

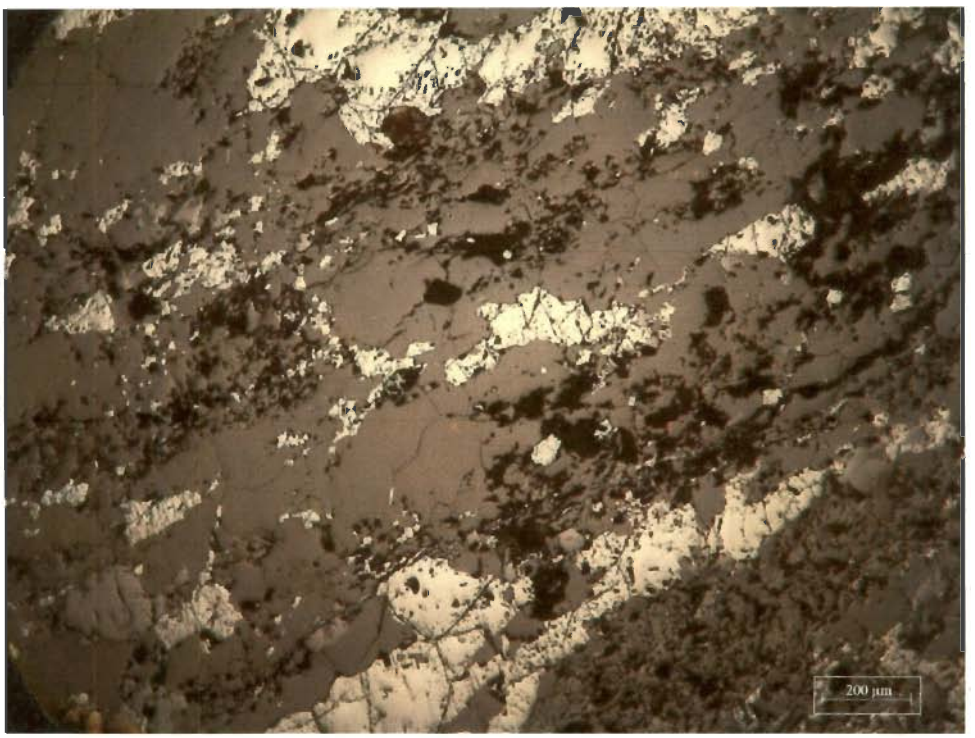

Figure 4.37 Alternating layers of silica and Fe-oxide minerals (hematite and magnetite)

Pyrite is also observed in the samples from Anaikatti, Narasimukku (Figure 4.39). The pyrite is mostly leached and they are mostly confined to silitcate layers. Association of pyrite and magnetite is also seen in Narasimukku BIF. Pyrrhotite, found as tiny specks in the specimens. It is distinguished by its light yellow to creamy

pinkish brown colour, low scratch hardness and strong anisotropism showing yellow grey to grayish blue. Chalcopyrite is found as tiny specks in the specimens.

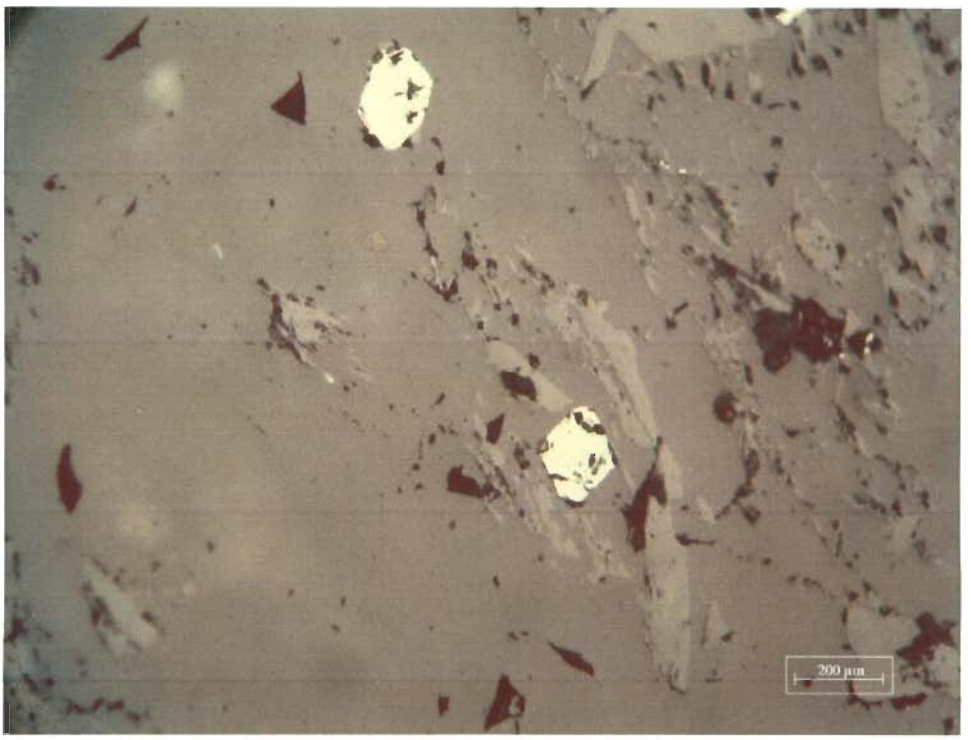

Figure 4.38 Euhedral magnetite in BIF

Figure 4.39 Sulfides in BIF

CHAPTER 5

Geochemistry

GEOCHEMISTRY

5.1 Introduction

The Attappadi Supracrustals and associated gneisses are spatially related to mineralization, they may represent potential source of gold and other metals. Based on preliminary geochemical study of metavolcanics and BIF Nair and Nair (2004) proposed that the metavolcanics in Attappadi are of komatiitic/tholeiitic composition, and the banded iron formation belongs to the Precambrian age. Association of tholeiites and BIF is a characteristic feature of Archaean greenstone belts. Lode gold deposit are one of the striking features of Archaean greenstone belts in many parts of the world and these deposits show a marked volcanic host rock control (Phillips et al., 1984; Giritharan and Rajamani, 1999). The main objective of this chapter is to discuss the geochemical nature of metavolcanics and associated gneisses belonging to Attappadi greenstone belt and to evaluate the importance of these rock suits in gold metallogeny in BSZ.

5.2 Analytical Procedures

5.2.1 Sample processing

Approximately 3 kg of the fresh samples were taken for processing. The samples were washed with double distilled water to remove dust and other impurities. After drying the samples they were broken into small chips of about 0.5 to 1.0 cm size. About 500 gm of the chipped samples were taken after coning and quartering for crushing. The steel mortar and pestle were used for crushing the rocks to-60 to -80 meshes and then again coning and quartering is done to select 250 gm of the crushed sample for powdering using a mechanical steel mortar followed by an agate mortar to -200 mesh size. Geochemical analysis involves many steps from powdering to

dissolution and finally analysis. For the purpose of geochemical modeling one needs to determine the concentration of elements with great accuracy and precision. To fulfill this requirement utmost care was taken at every step to avoid any kind of cross contamination.

5.2.2 Major and Trace Element Analysis

X-ray Fluorescence Sequential Spectrometer (XRF- Siemens SRS -3000 Sequential X-ray Spectrometer) available at Wadia Institute of Himalayan Geology, Dehradun was used for the determination of major and selected trace elements. The major element analysis using pressed powder pellets made from -200 mesh homogenized rock samples, the analytical procedure used has been discussed in detail by Saini et al. (1998).

5.2.3 Open Vessel Acid Digestion for REE Determination

For REE determination, about 0.04 g of -200 mesh sample was taken in a Teflon crucible and moistured with double distilled water. 10 ml of acid mixture (HF and HNO_3 in the ratio 2:1) was added to it and kept on a hot plate for three hours, and evaporated at 200°C until a crystalline paste results. 10 ml acid mixture (HF and HNO_3 in the ratio 2:1) was added again and evaporated to incipient dryness. About 5 ml of HF was added and contents were evaporated to dryness. 10 ml of HNO_3 was added, warmed gently to get a clear solution. It is then made up to 100 ml volume with double distilled water. The solution was used for the determination of the REE concentration .using. The rare earth elements were determined at Wadia Institute using ICP-MS (Perkin Elmer, ELAN DRC-e). Precision and accuracy for ICP-MS technique is given in Ahmad et al. (2005) and Rao and Rai (2006).

5.3 Results

Major and trace element geochemistry were analyzed for selected samples to provide additional data to characterize the evolution of rocks and related gold mineralization in Attappadi. The results of the sample analyses are given in Table 5.1 to Table 5.4. Hand specimen analysis and petrography were used to select samples for major element geochemistry. Twenty samples (thirteen metavolcanics, five gneissic rocks, two banded iron formation) were analyzed out of 60 samples collected from the Attappadi. Samples were chosen for major element analysis based on the following criteria a) the sample is a part of a set that represents a complete spectrum of lithologic variation, b) they are closely associated with auriferous veins. In addition to the above criteria, major element geochemistry aided in selecting sample for rare-earth and additional traces elements determination.

5.3.1 Major element distribution

The silica content of the Attappadi metavolcanic is about 48.8 wt% on an average and the maximum concentration obtained is 54.76 wt%. These metavolcanics have high iron content of 5 wt% minimum and a maximum of 15.4 wt%. The TiO_2 concentration is about 0.64 wt% on an average. The Mg number (MgO/MgO+FeO) of the metavolcanics ranges between 32 and 79. The alumina content is varying from 2.9 to 17.23 wt% showing large variation. Na and K do not show much variation. CaO/Al_2O_3 ratio is less than 0.9. The $A1_203/Ti0_2$ ratio of amphibolites is 18.35. The gneisses (sample number AG1, AG2, AG3, AG4, and AG5) are showing uniform geochemical characteristics. The silica content of gneissic rocks vary from 52 .92wt % to 57.63 wt% and there is not much difference in TiO_2, Al_2O_3, MgO, FeO content.

5.3.2 Geochemical Classification

It is found that the best way of classifying the volcanic rocks is by using chemical data involving total alkali, Na_2O+K_2O and SiO_2 variation diagram (TAS diagram) on Le Bas and Striekisen (1991), recommended by IUGS .In this plot metavolcanics of the Attappadi falls on the sub alkaline or tholeiite series as shown in Figure 5.1, field after (Irvin and Baragar, 1971).

Table 5.1 Major element data of Metavolcanics and gneisses around Attappadi

Major element oxide data in weight percentage									
Samples	AM1	AM2	AM3	AM4	AM5	AA1	AA2	AA3	AA4
SiO_2	50.21	46.72	51.81	54.76	42.58	49.49	52.26	52.79	48.91
TiO_2	0.45	0.19	0.44	0.23	0.06	0.65	0.75	0.45	0.88
Al_2O_3	7.16	6.67	5.32	2.9	3.63	12.92	15.53	17.23	12.63
Fe_2O_3	1.76	1.76	1.44	0.76	1.07	1.94	1.38	1.09	2.23
FeO	10.03	10.05	8.22	4.34	6.13	11.06	7.84	6.25	12.68
MgO	13.94	28.22	19.36	19.75	11.38	7.43	5.61	6.27	7.05
MnO	0.34	0.2	0.19	0.14	0.39	0.2	0.12	0.11	0.2
CaO	10.5	0.81	12.43	16.9	24.13	10.1	10.24	8.92	10.5
Na_2O	0.67	0.53	0.39	0.32	0.21	2.54	3.95	3.61	1
K_2O	0.09	0.01	0.2	0.06	0.14	0.25	0.19	0.12	0.28
P_2O_5	0.02	0.03	0.07	0.05	0.08	0.08	0.47	0.15	0.12
LOI	1.91	6.24	1.11	0.65	9.18	0.86	0.87	0.62	0.96
Sum	97.08	101.44	100.98	100.86	98.99	97.52	99.21	97.62	97.44
Samples	AA5	AA6	AA7	AA8	AG1	AG2	AG3	AG4	AG5
SiO_2	46.49	47.87	48.18	42.7	52.92	54.90	56.75	56.22	57.63
TiO_2	1.26	0.55	1.1	1.41	0.84	0.77	0.67	0.84	0.76
Al_2O_3	11.15	11.81	11.41	9.25	12.26	14.67	14.96	15.21	14.80
Fe_2O_3	1.83	1.25	2.34	2.29	1.23	1.14	0.96	1.00	1.01
FeO	3.82	7.13	13.32	13.01	7.02	6.50	5.51	5.70	5.76
MgO	8.49	9.68	7.51	13.16	9.81	6.95	6.66	5.34	4.63
MnO	0.22	0.32	0.22	0.21	0.12	0.10	0.09	0.07	0.09
CaO	10.16	16.88	10.12	10.35	6.34	5.46	6.77	3.05	5.74
Na_2O	1.24	1.22	1.34	0.75	2.22	2.98	3.32	3.14	3.56
K_2O	0.6	0.46	0.32	1.86	2.63	2.43	1.04	3.40	1.74
P_2O_5	0.27	0.13	0.15	0.8	0.38	0.12	0.36	0.19	0.13
LOI	0.84	0.37	1.32	1.44	1.89	0.94	0.72	0.69	1.08
Sum	86.37	97.67	97.33	97.23	97.66	96.96	97.81	94.85	96.93

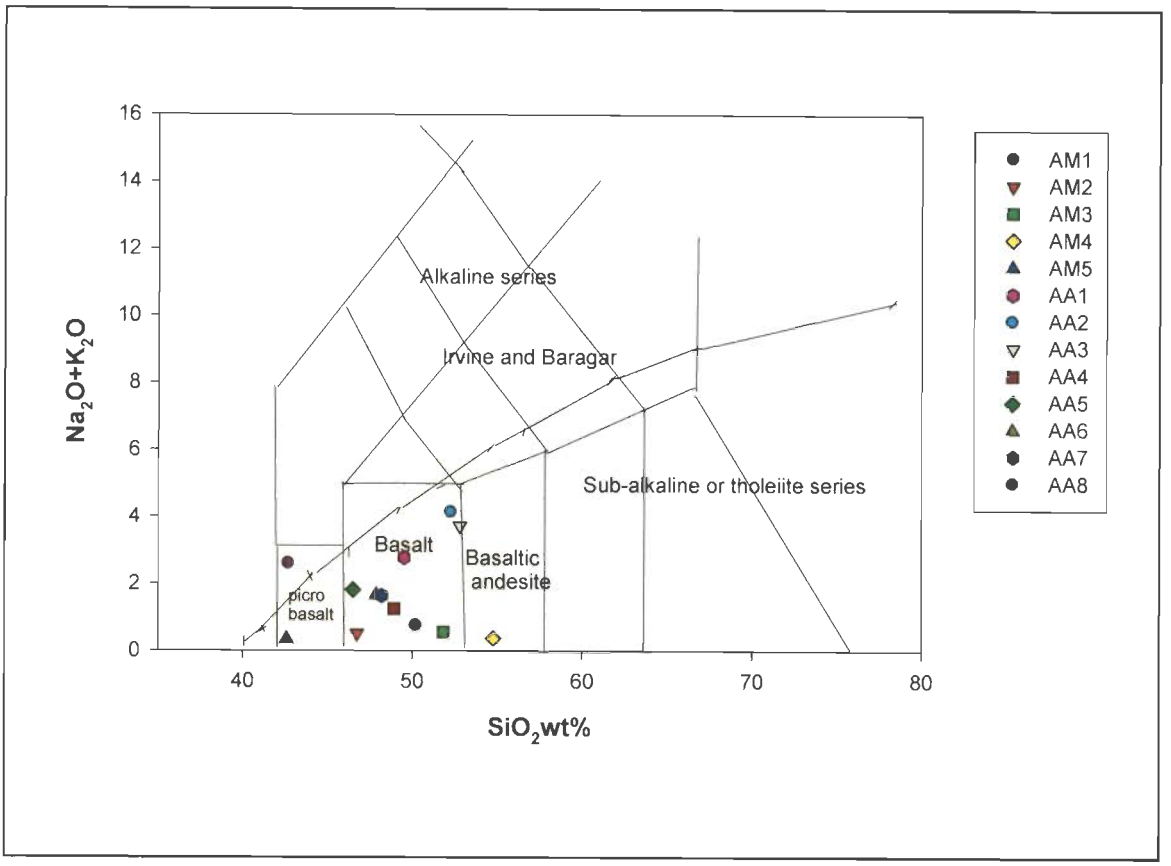

Fig 5.1 Chemical classification and nomenclature of metavolcanics using the total alkali versus silica TAS diagram (after Le Bas and Streckeisen 1991).

From this figure 5.1, metavolcanics of Attappadi could be considered as tholeiite. CaO/Al_2O_3 ratio is less than 0.9 and absence of spinifex textures in the mafic metavolcanics would suggest á tholeiitic character. The low Al_2O_3 (<16%) and high FeO content (>8.9%) also support the tholeiitic character. They are characteristically poor in K_2O (< 1%), TiO_2 (<1%), and are enriched in FeO(t), and could be classified as low-K Fe-rich tholeiites (Figure 5.2) The tholeiitic nature of these rocks is also evident from the Na_2O+K_2O- FeO(t)- MgO ternary AFM diagram (Figure 5.3). Since, felsic units are comparatively more enriched in FeO(t)/MgO ratios and depleted in MgO, some of these samples may not fall in the tholeiitic field. In A-F-M diagram (Figure 5.3), the metavolcanics exhibit a typical tholeiitic differentiation trend. Two samples follow a calc-alkaline trend, though not in the perfect order.

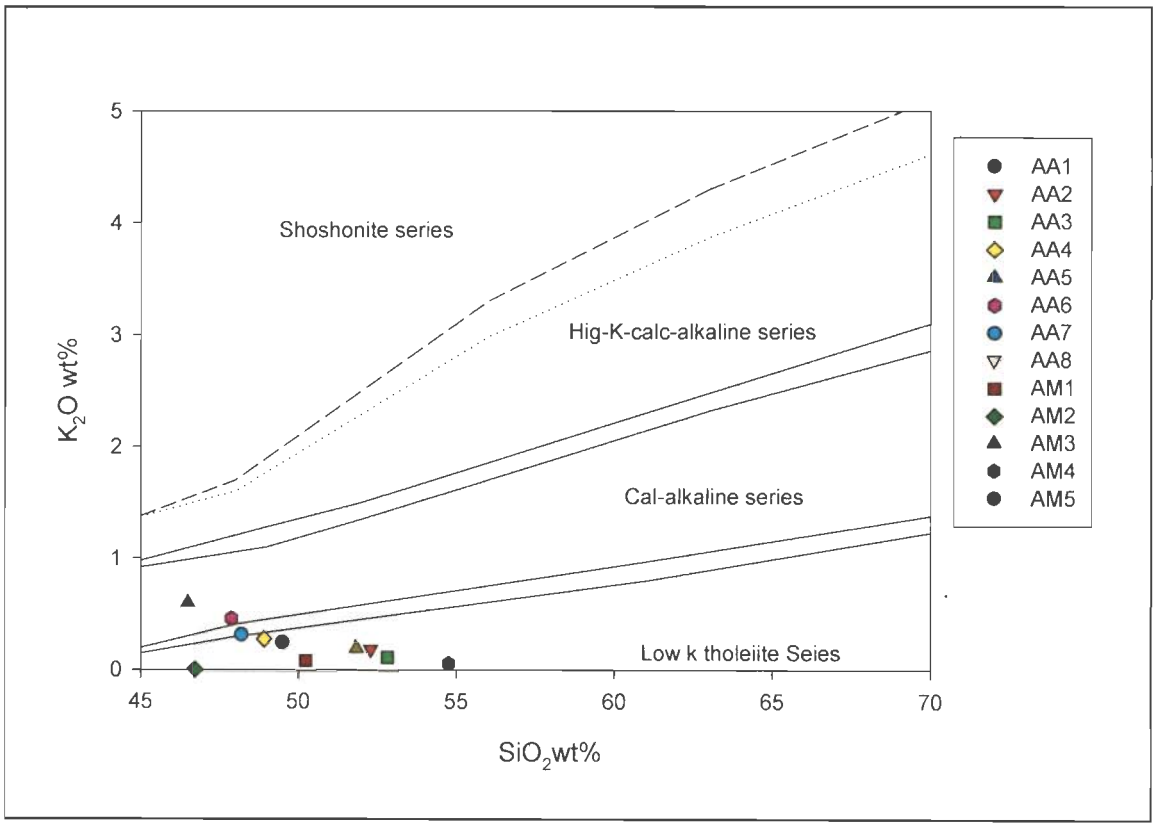

Figure 5.2 The subdivision of sub-alkaline rocks using K_2O versus SiO_2 diagram

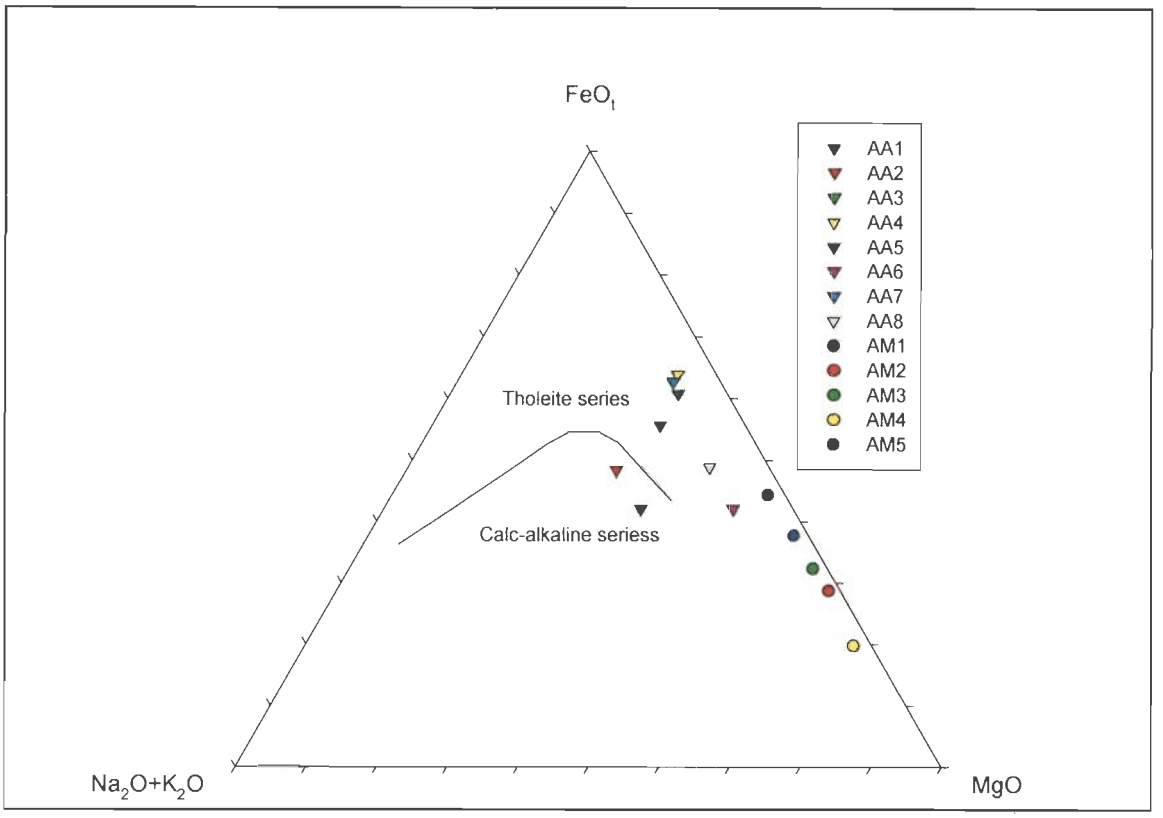

Fig 5.3 AFM diagram metavolcanics exhibit a tholeiite differentiation trend

An attempt has been made to classify the gneisses surrounding the Attappadi supracrustals using the QAP diagram. For this the geochemical data has been reconstituted in to CIPW normative mineralogy. The amounts of quartz and feldspar have been plotted in QAP to assign the name of the rock. In QAP plot the gneisses in the Attappadi fall in the monzodiorite field (Figure 5.4).

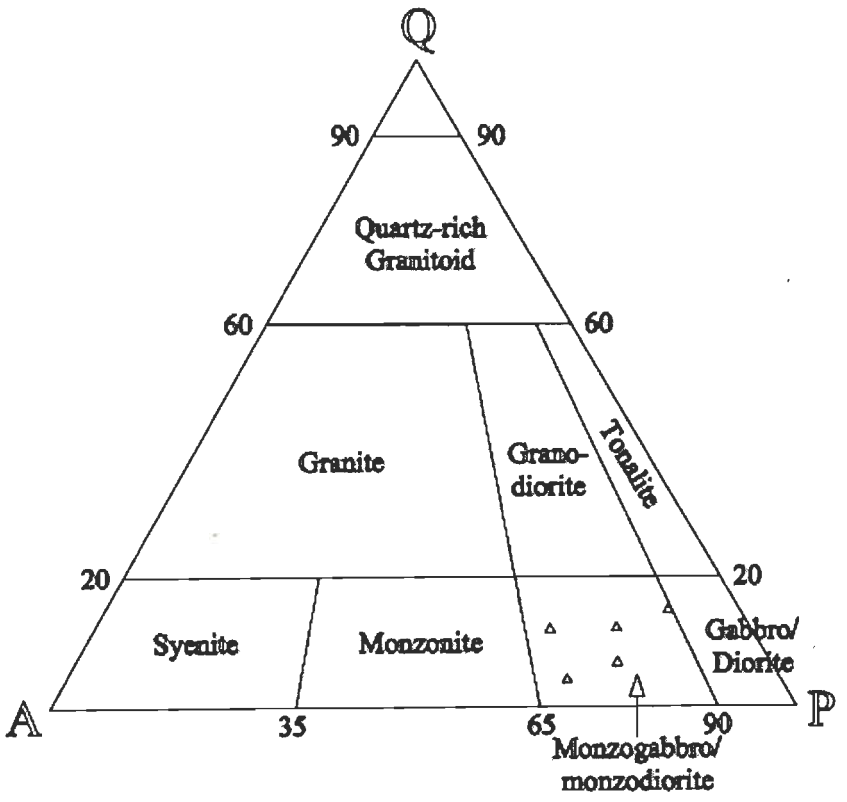

Fig 5.4 The normative data of gneisses rocks in the Attappadi as plotted in QAP modal diagram. The gneisses lie in the field of monzodiorite (the field after, Streckeisen, 1976).

A subset of samples analyzed for major elements contain alteration as they are apparently affected their geochemistry (AM1, AM2, and AM5). These samples were excluded from other trace element analysis. Seventeen samples were selected for XRF trace and ICPMS rare earth element analysis. The results of trace element analysis including REE has been given in the Table 5.2 and Table 5.3

Table 5.2 Trace element including REE data of metavolcanics around Attappadi

Sample	AA1	AA2	AA3	AA4	AA5	AA6	AA7	AA8	AM4	AM5
Sc	40	23	23	54	49	35	53	40	48	18
Co	65	40	31	48	63	35	46	78	40	26
Ni	70	86	51	63	102	67	66	228	152	24
Cu	23	174	19	55	107	41	133	20	28	20
Zn	117	91	84	183	134	90	121	178	81	94
Ga	17.7	19.1	15	22.2	16.7	10.8	14	23.2	1.7	3.1
Pb	11.4	5.6	4.3	13.2	13.4	53.7	12.2	15.5	8	16.9
Th	5.8	7.6	0.3	0.7	3.2	0.9	0.2	4.6	0.7	2.7
Rb	4	3.1	4.1	2.5	6.1	3.3	3.3	24.5	3.3	2.9
U	0.1	0.9	1.8	0.2	0.5	1.1	0.1	0	1.2	0.8
Sr	331	998	604	131	100	143	91	131	112	84
Y	17.1	19.8	10.5	34	30.6	31.6	25.7	38.9	9.2	24.3
Zr	50	112	65	50	81	55	56	175	20	23
Nb	4.4	4.3	5.9	11.2	5.6	5.4	7.5	7.9	3.5	4.4
La	8.69	69.2	9.86	16.6	50.6	5.74	4.78	4.63	5.43	16.47
Ce	20.17	147.31	21.78	51.35	120.04	14.17	8.96	8.67	17.6	30.5
Pr	2.65	19.26	3.1	8.82	17.38	1.94	1.74	1.66	3.06	3.6
Nd	10.25	73.66	12.35	38.44	70.95	8.86	8.57	8.22	15.3	13.25
Sm	2.28	10.21	2.49	9.82	14.15	2.19	2.03	2.53	3.68	2.05
Eu	0.65	2.31	0.86	1.4	3.29	0.56	0.51	0.9	0.79	0.05
Gd	2.89	10.9	2.09	7.01	15.26	2.71	2.56	2.76	2.75	2.73
Tb	0.43	1.17	0.35	1.15	1.69	0.59	0.6	0.59	0.41	0.5
Dy	2.65	4.22	1.84	5.63	7.47	4.22	3.95	4.05	1.94	2.99
Ho	0.58	0.68	0.36	1.1	1.26	0.95	0.89	0.91	0.32	0.65
Er	1.54	2.24	0.92	2.89	3.54	2.43	2.4	2.39	0.68	1.71
Tm	0.25	0.24	0.14	0.45	0.44	0.39	0.39	0.4	0.08	0.28
Yb	1.58	1.6	0.88	2.94	2.8	2.47	2.54	2.57	0.49	1.87
Lu	0.24	0.24	0.13	0.44	0.41	0.38	0.4	0.4	0.07	0.3
∑REE	54.85	343.24	57.15	148.04	309.28	47.6	40.32	40.68	52.6	76.95
Zr/Y	2.92	5.66	6.19	1.47	2.65	1.74	2.18	4.50	2.17	0.95
Zr/Nb	11.36	26.05	11.02	4.46	14.46	10.19	7.47	22.15	5.71	5.23
La/Nb	1.98	16.09	1.67	1.48	9.04	1.06	0.64	0.59	1.55	3.74
Th/La	0.67	0.11	0.03	0.04	0.06	0.16	0.04	0.99	0.13	0.16
Th/Yb	3.67	4.75	0.34	0.24	1.14	0.36	0.08	1.79	1.43	1.44
Nb/Yb	2.78	2.69	6.70	3.81	2.00	2.19	2.95	3.07	7.14	2.35
LaCN	26.41	210.33	29.97	50.46	153.80	17.45	14.53	14.07	16.50	50.06
(La/Sm)CN	2.35	4.18	2.44	1.04	2.21	1.62	1.45	1.13	0.91	4.96
(La/Ce)CN	1.13	1.24	1.19	0.85	1.11	1.07	1.40	1.40	0.81	1.42
(La/Yb)CN	3.68	28.92	7.49	3.78	12.08	1.55	1.26	1.20	7.41	5.89
(Dy/Yb)CN	1.08	1.69	1.34	1.23	1.71	1.10	1.00	1.01	2.54	1.03

Table 5.3 Trace element including REE data of gneisses around Attappadi

Element	AG1	AG2	AG3	AG4	AG5
Sc	17	20	18	16	18
Co	32	31	24	30	43
Ni	112	85	29	49	91
Cu	43	41	13	21	80
Zn	132	109	90	77	105
Ga	14.9	18.1	15.8	20	21.2
Pb	6.6	5.7	4.5	24.6	6.6
Th	0.2	1.1	0.8	21.8	6.7
Rb	33.7	20.1	5	79.5	16.2
U	1.6	1.4	2.5	1.3	1.5
Sr	602	354	762	503	396
Y	20.2	25.7	20.6	19.6	21.6
Zr	145	125	172	193	188
Nb	7.1	8.3	6.5	9.9	7.6
La	28.31	19.38	21.65	37.27	19.38
Ce	63.3	44.49	55.1	68.07	37.38
Pr	8.84	6.41	8.39	7.99	4.63
Nd	34.71	25.57	35.07	28.94	18.39
Sm	7.15	5.14	7.18	6.34	4.53
Eu	2.08	0.9	1.9	1.96	1.19
Gd	5.09	4.33	5.16	5.3	4.85
Tb	0.74	0.73	0.77	0.63	0.6
Dy	3.55	3.98	3.58	2.94	3.44
Ho	0.64	0.81	0.66	0.59	0.73
Er	1.7	2027	1.66	1.92	2.11
Tm	0.24	0.33	0.23	0.31	0.34
Yb	1.51	2.16	1.42	2.13	2.38
Lu	0.22	0.32	0.2	0.33	0.38
∑REE	158.08	2141.55	142.97	164.72	100.33
Zr/Y	7.18	4.86	8.35	9.85	8.70
Zr/Nb	20.42	15.06	26.46	19.49	24.74
La/Nb	3.99	2.33	3.33	3.76	2.55
Th/La	0.01	0.06	0.04	0.58	0.35
Th/Yb	0.13	0.51	0.56	10.23	2.82
Nb/Yb	4.70	3.84	4.58	4.65	3.19
LaCN	86.05	58.91	65.81	113.28	58.91
(La/Sm)CN	2.44	2.33	1.86	3.63	2.64
(La/Ce)CN	1.18	1.15	1.03	1.44	1.36
(La/Yb)CN	12.54	6.00	10.20	11.70	5.45
(Dy/Yb)CN	1.51	1.18	1.62	0.89	0.93

5.3.3 Trace element distribution

The average Ni content of the metavolcanics are 91ppm which is significantly less than the Ni range reported for primary magmas (Ni 250-50 ppm). The Zr content of metavolcanics are generally low and ranges from 20-81ppm, two samples (AA2 and AA8) had shown relatively higher Zr values 112 and 175 ppm respectively. The metavolcanics of Attappadi greenstone belt have $(La/Yb)_N$ ratios average 3.22 indicating fractionated mantle sources for their derivation. The chondrite normalized REE patterns of metavolcanics are characterized by a marked overall enrichment of all REE (Figure 5.5). They are showing negative Eu anomalies indicating subordinate fractionation of plagioclase prior to the eruption of the basaltic melt.

Gneisses are showing uniform trace element distribution. The relative enrichment of Rb and Zr (150 ppm), La (25 ppm), Ce (53ppm), and Nb (7 ppm) high $(La/Yb)_N$ gneisses indicate that these were crustal derived. All the above evidences suggest that the role of crustal contamination was involved in the formation of felsic rocks. The gneisses have shown LREE enriched chondrite normalized REE pattern (Figure 5.6).

Major and trace element (including REE) data of BIF of Attappadi area are given in Table 5.4. During this investigation two representatives BIF samples were analyzed and the data is compared with the average geochemical data already reported from Attappadi (Nair and Nair, 2004). The Al_2O_3-Fe_2O_3-SiO_2 ternary diagram (Govett, 1966) was used to classify the BIF. The BIF of Attappadi plot within the field of Precambrian iron formation (Figure 5.7). Al_2O_3/TiO_2 ratio of BIF (19.61) is comparable to the mean value of metavolcanics (18.35). The BIF show a light REE enrichment with a striking positive Eu anomaly (Figure 5.8)

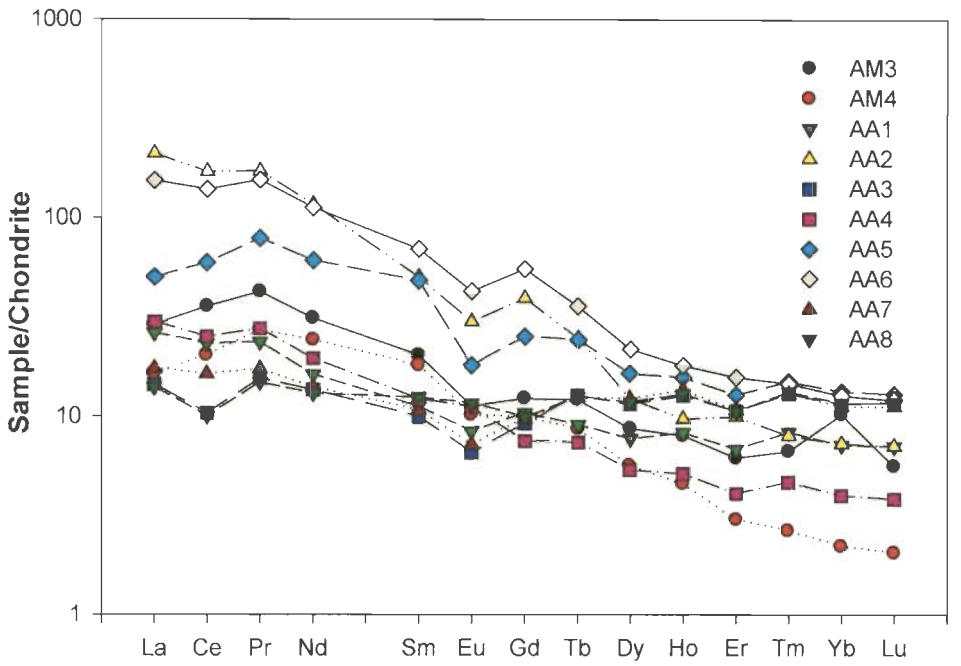

Fig 5.5 The chondrite normalized REE patterns of metavolcanics.

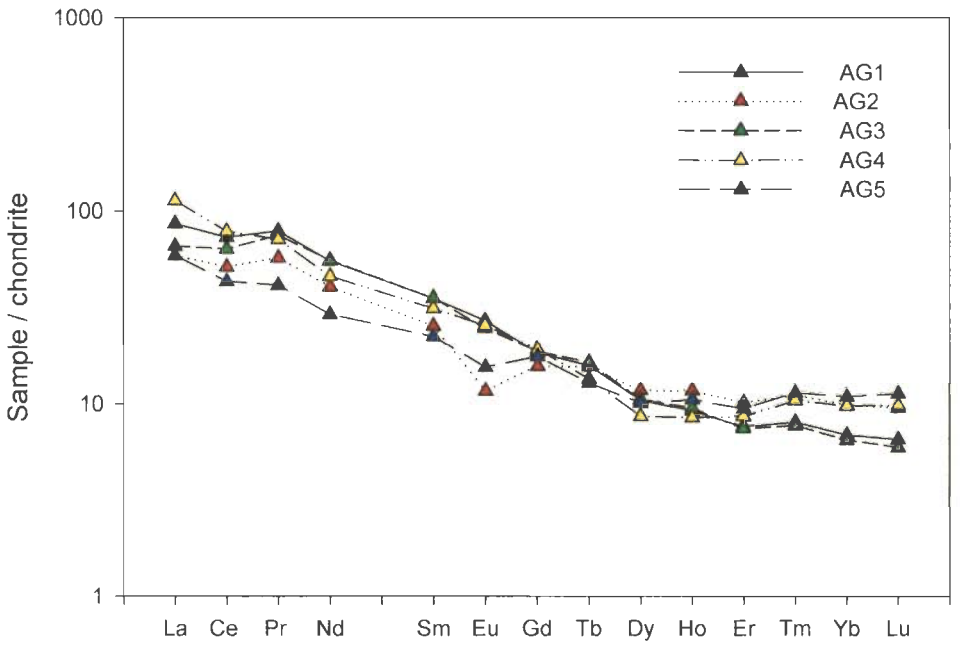

Fig 5.6 The Chondrite normalized REE pattern of gneisses

Table 5.4 Major and trace element including REE data of BIF around Attappadi

Major Element Oxides Data in Wt%		
Sample	AB1	AB2
SiO_2	60.35	70.47
Al_2O_3	4.61	4.36
Fe_2O_3	26.64	20.75
Na_2O	0.31	0.33
K_2O	0.01	0.01
MgO	2.13	1.82
CaO	0.59	0.81
MnO	0.62	0.26
TiO_2	0	0.01
P_2O_5	0.07	0.11
LOI	0.59	0.57
SUM	95.92	99.5
Trace element data in ppm		
Sc	1	3
Co	28	44
Ni	23	13
Cu	165	135
Zn	91	68
Ga	2.2	2.2
Pb	1.7	1.3
Th	0.8	2.4
Rb	1.5	3.1
U	0.4	0.1
Sr	9	15
Y	4.1	2.7
Zr	3	2
Nb	1.7	1.8
REE data in ppm		
La	4.14	1.96
Ce	4.11	3.24
Pr	0.76	0.41
Nd	2.66	1.76
Sm	0.72	0.44
Eu	0.3	0.17
Gd	0.68	0.32
Tb	0.09	0.057
Dy	0.53	0.33
Ho	0.11	0.08
Er	0.34	0.266
Tm	0.06	0.039
Yb	0.36	0.25
Lu	0.06	0.04

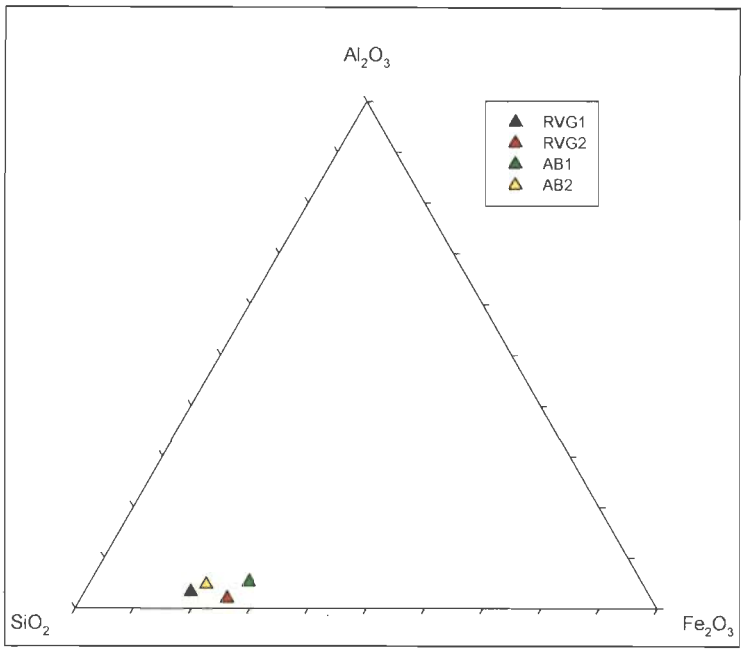

Figure 5.7 Al_2O_3-Fe_2O_3-SiO_2 plots of BIF of Attappadi (after Govett, 1966) of Attappadi. Along with the analyzed data reported values of two BIF sample (Nair and Nair, 2004) were also plotted.

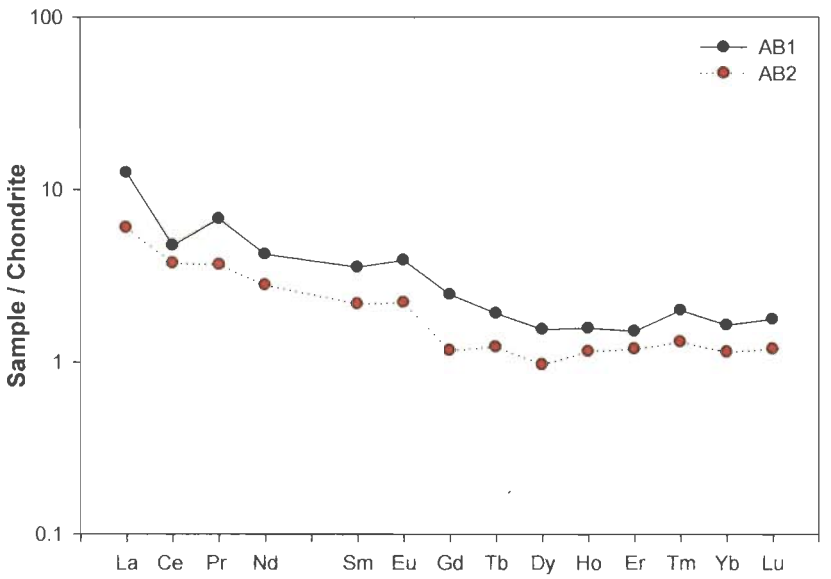

Figure 5.8 Chondrite normalized REE pattern of BIF showing light REE enrichment with a striking positive Eu anomaly

5.4 Tectonic Discrimination Diagrams

Plate tectonics are accepted as the principal mechanism for Archaean greenstone formation and deformation (De Wit, 1998). During the last two decades, correlation between geochemistry and palaeotectonic setting environments has been extrapolated back in time to Archaean in an attempt to identify their ancient analogues. However, it is questionable whether the discriminations based merely on the geochemical data for present day volcanics from different tectonic settings, can be used with confidence for determining Archaean volcanic tectonic provinces. The geochemical correlations and discriminant diagrams alone must not be claimed to be singular evidence for establishing the tectonic setting. For this reason, it is also taken into consideration the geologic setting, lithologic assemblages and their structures for interpretations along with the volcano-geochemical parameters, to suggest the most appropriate plate tectonic settings for rocks of Attappadi greenstone belt. In Nb/Yb-Th/Yb, Ti/Y-Nb/Y (Figure 5.9) and Zr/Y-Ti/Y diagrams (Figure 5.10.) the metavolcanics of Attappadi plot within MORB (Mid Oceanic Ridge Basalt) fields.

Geochemically there are two types of MORB basalts found in oceanic environment, each of them having a unique set of trace element characteristics. The parental magmas to these types of basalts are generally considered to be product of partial melting of mantle sources to varying extents under different physical conditions.

MORB are considered to be generated by relatively large extents of melting about 20-25% of convectively upwelling oceanic upper mantle (White and Mackenzie, 1989). They are associated with divergent tectonic margins and are geochemically characterized by LREE depleted patterns.

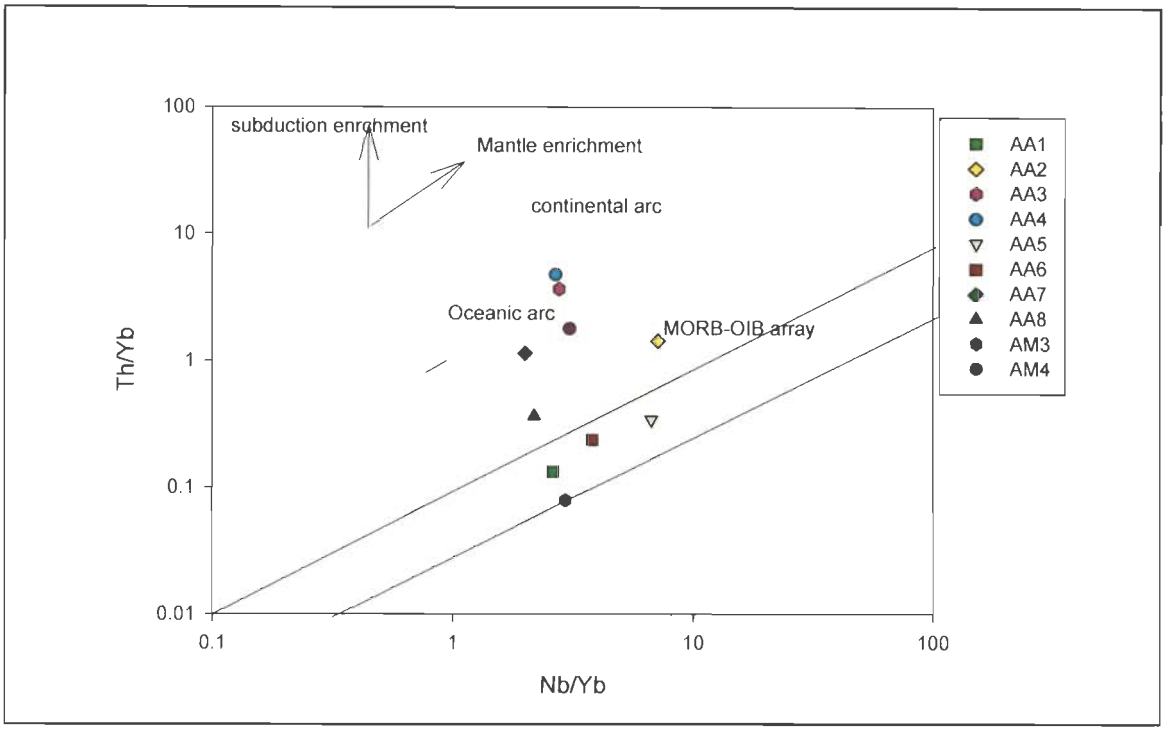

Figure 5.9 Nb/Yb-Th/Yb, Ti/Y-Nb/Y discrimination diagram for basalts

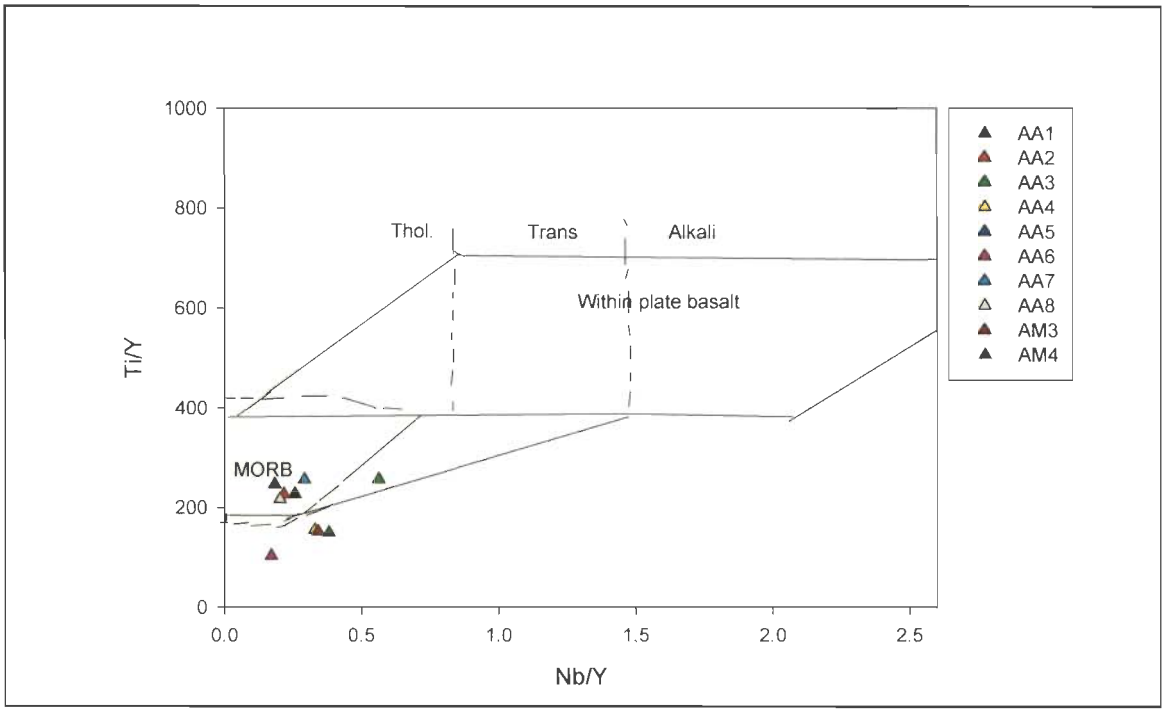

Figure 5.10 Zr/Y-Ti/Y discrimination diagram for basalts showing of within plate basalts, MORB and volcanic-arc basalts (after Pearce, 1982)

This type of MORB is also known as normal MORB or N-MORB. Another type of MORB is known as enriched MORB or E-MORB which is characterized by LREE and LILE enrichment compared to N-MORB and they also show smooth multi element patterns. The difference between E-MORB and N-MORB is due to the enriched /depleted nature of their mantle sources although pressure temperature conditions of melting are thought to be similar globally (Anderson, 1989).

The N-Type source is supposed to have undergone a previous episode of melt removal, thereby depleting the source in incompatible elements whereas the E-type source is a relatively undepleted mantle (Sun and McDonough, 1989). The chondrite normalized REE patterns of Attappadi metavolcanics are characterized by a marked overall enrichment of all REE.

E-MORB show 10-fold enrichments of highly incompatible elements compared to N-MORB despite similar extent as compared to N-MORB. In order to achieve this level of enrichment, the element must be derived from a volume of normal mantle at least 10 times larger than the mixed source that gives rise to E-MORB. If the enrichment step takes place at depth in subduction zones, this volume constraint is easily accommodated. The incompatible trace elements are first concentrated in the oceanic crust at ocean ridges, and subsequent low-degree melting of subducted oceanic crust at subduction zones forms the enriched reservoir by metasomatising the mantle wedge (Donnelly et al., 2004; Hofmann and Hemond, 2006).

The basaltic rock of the Attappadi is particularly enriched in large ion lithophile elements (LILE) and light rare earth elements (LREE). A likely source for the volcanics of this study could have been an enriched mid-ocean ridge basalt

(EMORB)-type mantle that underwent higher degrees of partial melting than regions involved in MORB generation or a previously depleted source.

Tectonic discrimination diagram for gneiss in the Attappadi has been shown in Figure 5.11 and 5.12. In this diagram gneisses are of volcanic arc granite. Primitive mantle normalized multi-element diagram for monozodiorite is given in Figure 5.13

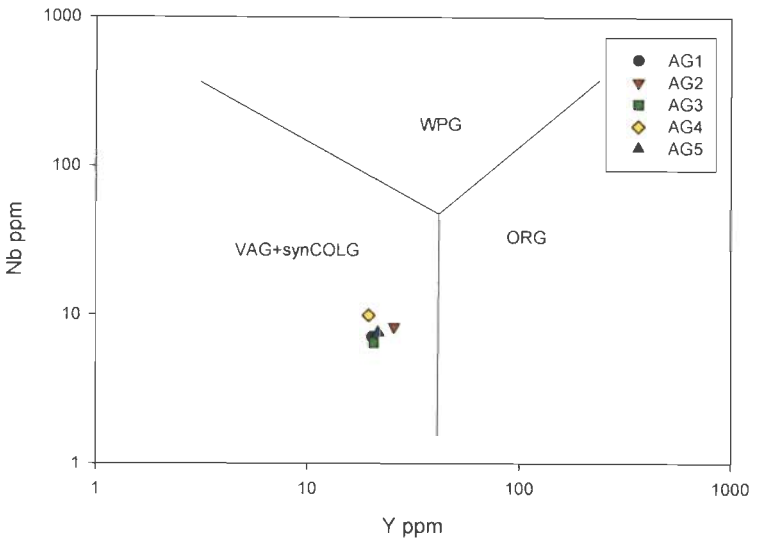

Figure 5.11 The Nb-Y discrimination diagram for granites (after Pearce et al., 1984)

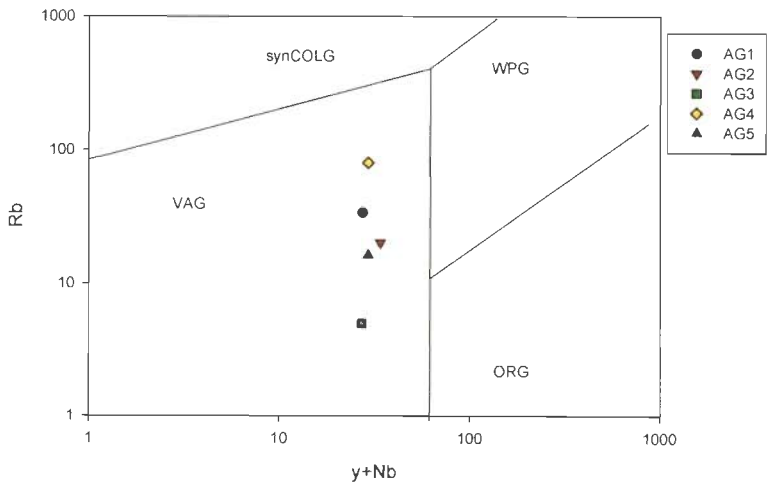

Figure 5.12 The Rb-(Y+Nb) discrimination diagram for granites (after Pearce et al., 1984)

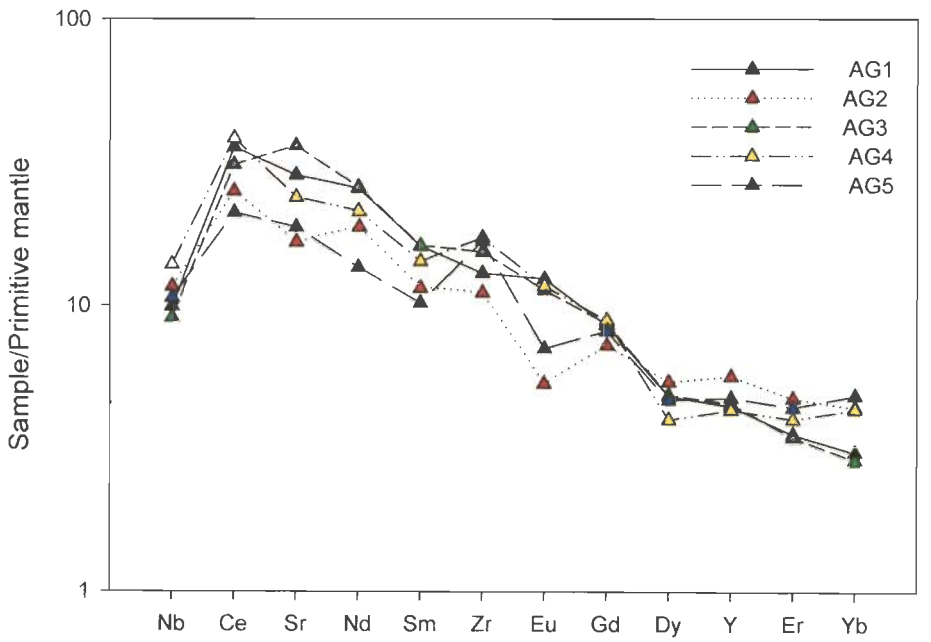

Figure 5.13 Multi-element primitive mantle normalized diagram for monozodiorite. Normalizing factors from Sun and McDonough, 1989

CHAPTER 6

Fluid inclusion studies

FLUID INCLUSION STUDIES

6.1 Introduction

This chapter discusses one of the important aspects of the environment of formation of gold-quartz veins, fluid inclusion studies. Data from the fluid inclusion studies provide important information to estimate the temperature-pressure of formation, and fluid composition. The following sections will describe types of fluid inclusions, their distribution, relative fluid inclusion chronology, composition of inclusions and microthermometric studies. Fluid inclusion studies were carried out on samples of auriferous vein quartz, barren quartz veins, quartz biotite gneiss and hornblende gneiss representing different prospects.

6.2 Sample Selection and Preparation

During field work, variations of the different lithologies within one outcrop have been documented and the position of the sample in the rock sequence has been specified. Even within the same lithology, fluid inclusions may also show considerable variation in composition and densities therefore; at least two or three samples from the same outcrop were taken in order to assess the variation in the fluid characteristics related to gold mineralization.

A total of 20 samples were selected from different parts of Attappadi to investigate the geochemical characteristics of fluid inclusions. The sample locations are given in Figure 4.2. The details of the samples used for fluid inclusion studies are as follows.

1) Mineralized vein, usually parallel to the foliation of the host rocks and they are closely associated with all the rock types and have strike length of more than 5 meters long and are more than 5 cm wide.

2) Barren quartz veins, usually cutting across the foliation / rock types

3) Quartz biotite gneiss, which is one of the dominant and more sheared rocks

4) Hornblende gneiss, the host rock for Attappadi supracrustals

Doubly polished thin wafers for 20 samples were prepared after preliminary study of thin sections. Doubly polished 300-350μm thick wafers were prepared to characterize the fluid inclusions and used for microthermometric investigations. These sections were soaked in solutions of methyl chloride (CH_2Cl_2) or acetone ($C_6OH_{12}O_{22}$) to remove Canada balsam.

6.3 Fluid Inclusion Petrography

Over 200 fluid inclusions ubiquitously present in host quartz grains of all the samples were studied. Abundant inclusions were observed in samples of mineralized veins and quartz biotite gneiss. These fluid inclusions are either present as isolated or occur extensively along trails. Their trails are limited to the single grain or transgranular. However, fluid inclusions trapped within quartz of hornblende gneiss and barren quartz are usually less than 5μm, therefore inclusions from these samples could not be used for microthermometry.

Fluid inclusions petrography was carried out to understand size, shape, phases present at room temperature and mode of distribution. Abundant inclusions have been observed in samples of mineralized veins and quartz-biotite gneiss. The fluid inclusions in mineralized veins and quartz-biotite gneiss are present as isolated or occur extensively along the shear planes.

It has been observed that quartz grains were plastically deformed. They are showing grain boundary migration recrystallization, deformation lamellae and deformation bands. Hence, the inclusions preserved in these samples might have resulted from metamorphism of pre-existing rocks and quartz veins or from the

different degrees of reworking of primary inclusions during or after the peak metamorphic condition.

Rodder (1984) suggested standard criteria to distinguish primary secondary and pseudosecondary inclusions. In studied samples of Attappadi, abundant inclusions along healed micro shear planes and some times isolated inclusions are also observed. Growth planes in quartz crystals are not present hence, the primary nature of inclusions along the growth planes were difficult to establish. Quartz grain boundaries are generally irregular because these veins have been deformed due to later deformational events.

6.4 Fluid Inclusion Types

A variety of fluid inclusions are present in quartz grains of mineralized veins and quartz in quartz biotite gneiss. Five different types of fluid inclusions have been identified at room temperature. This classification of these inclusion types are based on the number of phases / phase ratio observed at room temperature and mode of occurrence of the inclusions. i) aqueous carbonic (type-1), ii) aqueous carbonic (type-2), iii) pure carbonic (type-3), iv) inclusions with daughter mineral (type-4) and v) aqueous inclusions (type-5). Fluid inclusions to each compositional type can be early or late with respect to the host mineral depending on the relative entrapment time.

Among the five different types of fluid inclusions, type-1, type-2 and type-3 are the most common in studied samples. The linear arrangement of type-2 and type-3 inclusions along healed fracture surfaces and their crosscutting relationship with respect to grain boundaries are clearly indicating their secondary origin. The type-4 inclusions are restricted to samples of vein quartz from only one area.

6.4.1 Type-1 inclusions

Type-1 inclusions occur as isolated inclusions and being considered as the earliest inclusions, size varies from 10 to15μm. These are bi-phase and primary with respect to the quartz vein formation and are distributed in mineralized veins and also in quartz-biotite gneiss. These inclusions are of various shapes from negative crystals to irregular and oval shape. The proportions of the aqueous-carbonic phase are 6:4 to 7:3. CO_2 occurs in the form of liquid and liquid meniscus was not been observed at room temperature (Figure 6.1 and Figure 6.2).

Figure 6.1 Type-1 Inclusion in mineralized vein

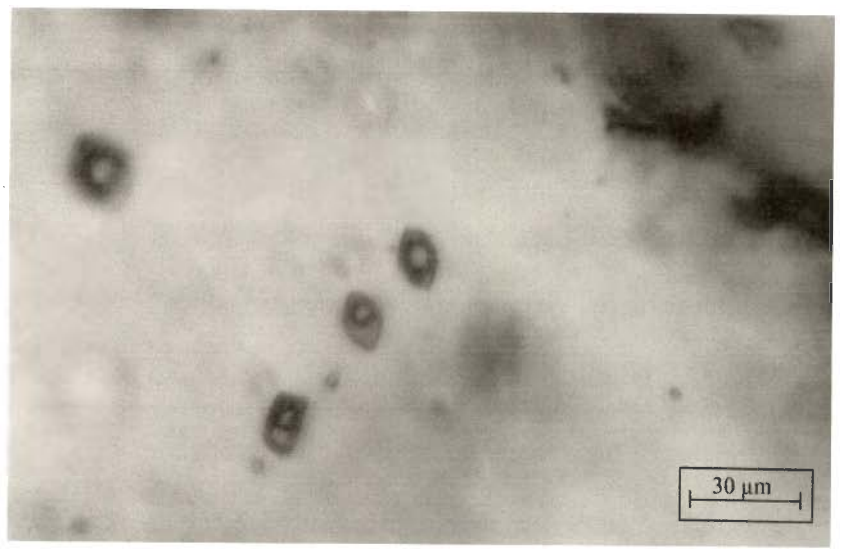

Figure 6.2 Type-1 Inclusion in quartz-biotite gneiss

6.4.2 Type-2 inclusions

Two phase liquid rich, H_2O + CO_2 inclusions occur extensively along the shear planes. These inclusions range in diameter from 5to15μm. They are often of similar size and uniformly spaced along the trails. They are occurring in mineralized quartz vein as well as in quartz biotite gneiss (Figure 6.3 and Figure 6.4).

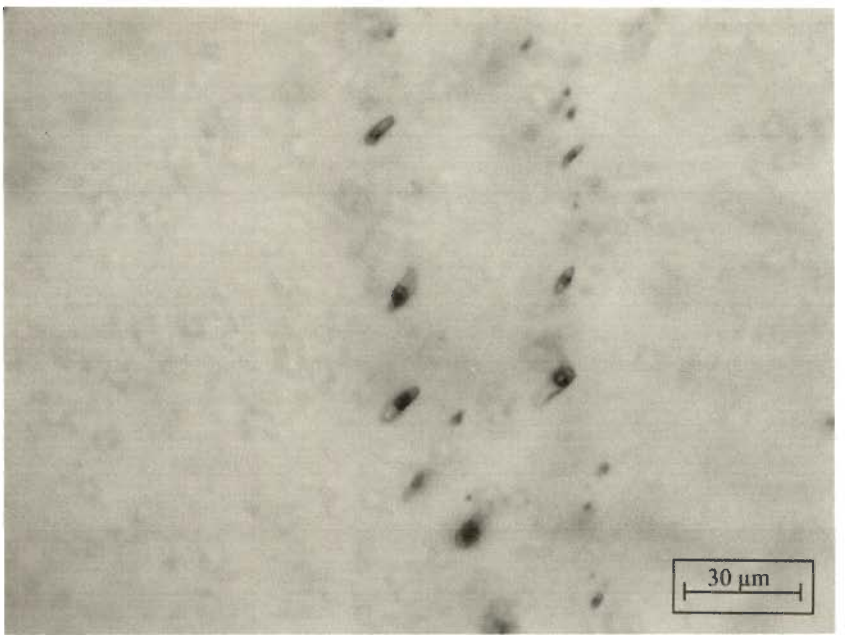

Figure 6.3 Type-2 inclusion in mineralized vein

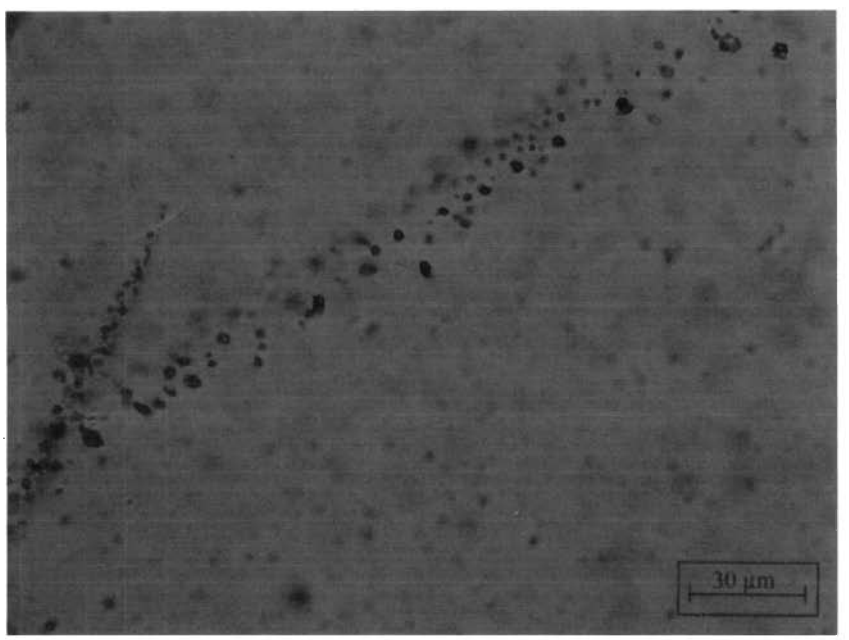

Figure 6.4 Type-2 Inclusion in quartz-biotite gneiss

6.4.3 Type-3 inclusions

Type-3 inclusions are carbonic inclusions filled with near pure liquid CO_2. Some times gas CO_2 also present, wherein the inclusions appear to consist of two phase (liquid CO_2+ gaseous CO_2) at room temperature. They are often rounded, anhedral or negative-crystal shape and are found to be aligned along micro shears(Figure 6.5 and Figure 6.6)

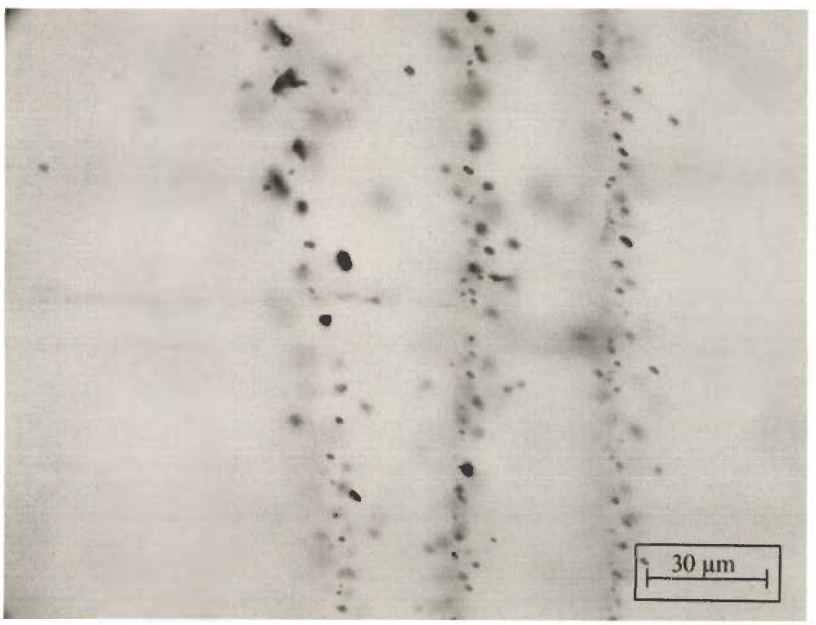

Figure 6.5 Type-3 inclusions in mineralized vein

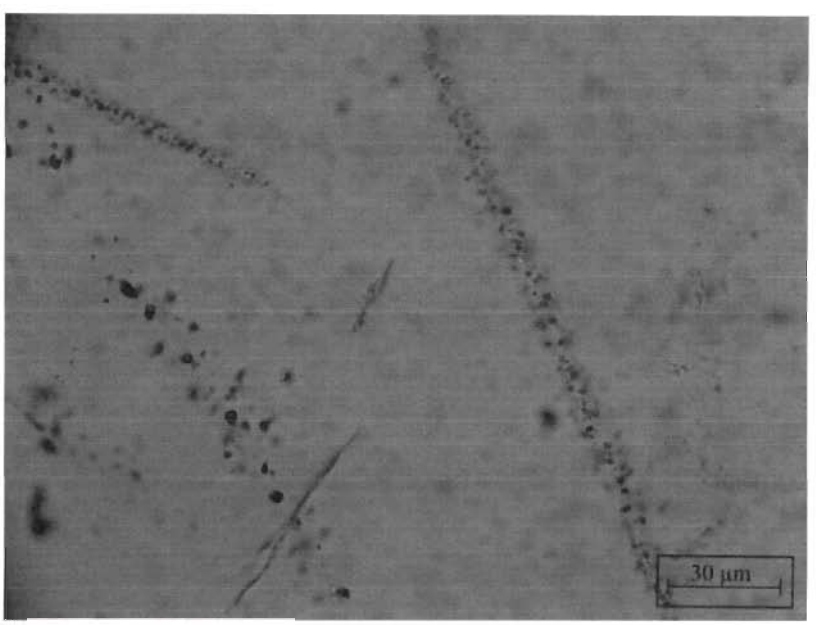

Figure 6.6 Type-3 inclusions in quartz-biotite gneiss

6.4.4 Type-4 inclusions

There are some multiphase inclusions observed in the quartz veins and are restricted to Kottathara area of Attappadi, vary in size from 10 to 30μm. These are three phase inclusions consisting of liquid, vapor phase and daughter mineral. The daughter crystals are identified as halite on the basis of morphology and refractive index. These inclusions are present as isolated and as well as in trails. Some times they are confined to a single grain. These multiphase inclusions have not been observed in other part of the study area (Figure 6.7).

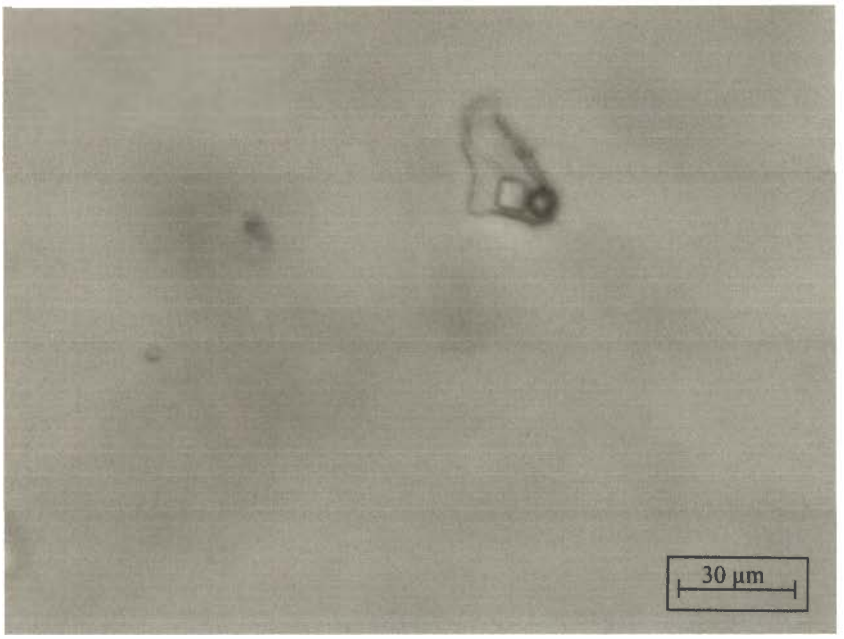

Figure 6.7 Type-4 inclusions in mineralized vein

6.4.5 Typ-5 inclusions

Type 5 inclusions are aqueous biphase inclusions, present in quartz veins, size varying from 5 to20μm. They are occurring in trails /clusters and appeared to be a later fluid.

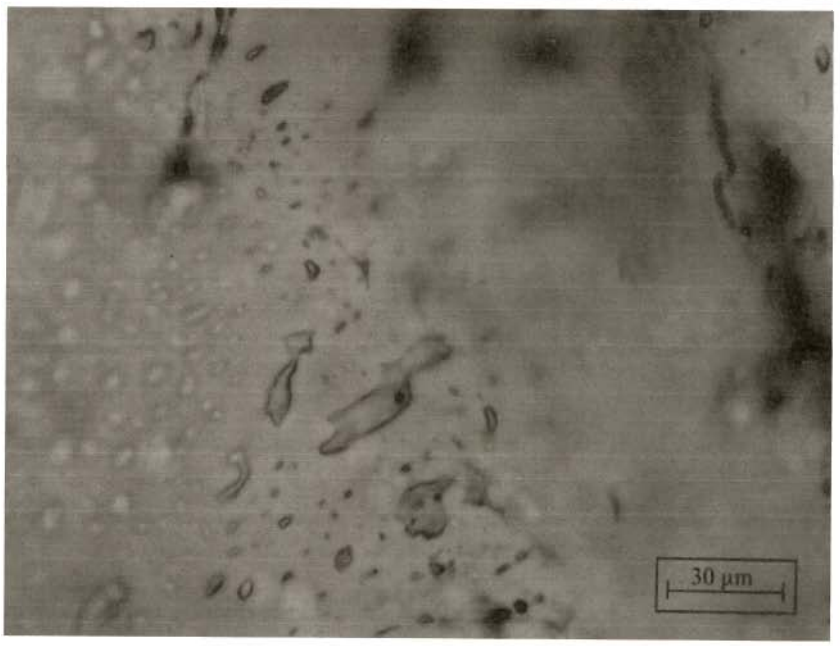

Figure 6.8 Type-5 inclusions in mineralized vein

6.5 Chronology of Fluid Inclusions

The relative time of entrapment of fluid in various inclusions in the studied samples has been determined considering the occurrence and distribution of inclusions in the host rocks/mineralized veins. The following criteria were considered while establishing the chronology of the inclusions: a) Fluid inclusion occurrence as isolated distribution in quartz biotite gneiss , b) fluid inclusion occurrence as isolated inclusions in mineralized vein, c) fluid inclusions in the micro-shears generated during metamorphism , d) occurrence of pegmatite in an area close to Kottathara prospect and the vein quartz of this area is characterized by the presence of type-4 inclusions in addition to other types of inclusions , f) similarities in nature of fluid in type 1 and type 2 inclusions, g) the co-existence of type-2 and type-3 inclusions in a single trail and h) the occurrence of type 2 and type 3 inclusions both in transgranular trails and in limited arrays.

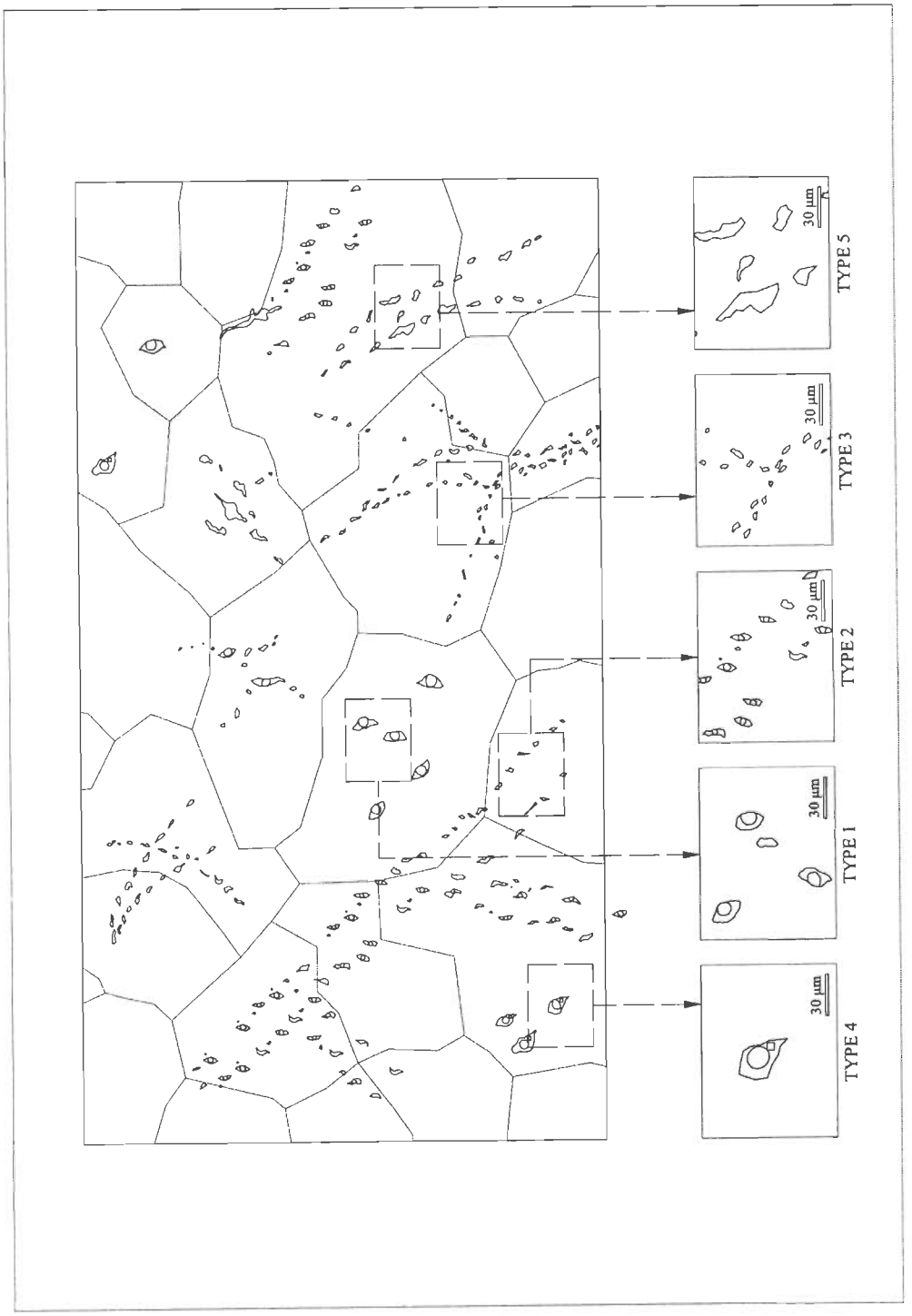

Figure 6.9 A hand-drawn sketch, based on microscopic observations, shows the distribution of fluid inclusion types in the auriferous quartz veins of Attappadi

Type-1 inclusions appear to be earliest because of their isolated occurrence in mineralized vein quartz/quartz-biotite gneiss. Type-2 and type-3 inclusions occur along the transgranular trails probably representing shear planes and entrapment of fluids subsequent to regional Bhavani shearing. They show similar characteristics in both mineralized vein and also in quartz biotite gneiss. The most prominent planar structure observed in the study area is the mylonitic foliation (S_2), attributed to the regional NE-SW trending Bhavani shear. Mylonitic development, micro-granulation, biotitization and chloritization are found to be associated with these surfaces. Development of multiple shear and recrystallization of early formed quartz vein representing this deformational event and linked retrogression of metamorphic rocks.

Type-4 multiphase inclusions are restricted to the vein quartz of Kottathara prospect. It has been observed that the pegmatites are occurring quite closer to the mineralized quartz veins. Hence, type-4 inclusions are likely to be related to the fluid released from pegmatite (high saline fluid) and not at a regional scale. Type -5 inclusions probably represent the last stage of fluid event as evidenced by the samples and contains the solutions of shallow fluid circulation after dehydration or meteoric ingress.

6.6 Microthermometry

Microthermometric data of inclusions have been obtained in this study from host rocks and vein quartz samples of Attappadi Valley. For each sample, microthermometric analyses were carried out on a small chip taken out from the double-polished plates. Heating-freezing runs were conducted on a Linkam THMSG600 heating-freezing system fitted on to a Nikon E600 microscope at the Wadia Institute of Himalayan Geology, Dehradun. The unit operates in the temperature range of -196°C to + 600 °C. The stage was periodically calibrated by

synthetic pure CO_2 inclusions (triple point = -56.6°C) in quartz. The samples containing suitable inclusions were marked before attempting microthermometry.

In general a normal rate of a 5°C/minute was maintained during thermometric runs, the melting of CO_2 and ice was checked repeatedly, doubtful inclusions showing necking or leakage were not used while presenting and interpreting the data. The freezing temperature found to be correct in the order of 0.2° C and heating runs were correct to 2°-3° C. The result of heating and freezing studies of fluid inclusions has been summarized in tabular form (Table 6.1).

6.6.1 Freezing Data

Parameters that were measured in freezing include first melting temperature of aqueous phase (Te), the first melting temperature of ice (Tfm), temperature of CO_2 melting (Tm CO_2), temperature of homogenization of CO_2 (Th CO_2). Several freezing runs were made up to – 180°C to check the presence of methane in the carbonic liquid.

6.6.2 First Melting Points of CO_2 ($TmCO_2$)

CO_2 bearing inclusions were frozen to -110°C , then the inclusions were slowly heated to note the first melting points of CO_2 (Tm CO_2). The first melting temperature of CO_2 can be detected from observation of sudden phase changes of solid CO_2 in to liquid. The first melting point for pure CO_2 is known to be -56.6 °C. Most inclusions show Tm CO_2 between -57° to-58° C and have been shown in Figure 6.10 ,11&12 The ranges below -56.6 °C imply that the trapped fluids consists minor amount of other gases and contaminants mostly of CH_4 in CO_2 and N_2.

6.6.3 Homogenization Temperature of CO_2 (Th CO_2)

After measuring the melting temperature of CO_2, further heating causes homogenization of liquid and gaseous CO_2 in to a single phase (Th CO_2). During the

Table 6.1 Results of fluid inclusion studies

	TYPE2				TYPE1				TYPE3		Type4		Type5		
Sample	TmCO2	Tm Ice	ThCO2	Th Total	TmCO2	Tm Ice	ThCO2	Th Total	Tm CO2	ThCO2	TdS	Th (l+v=l)	T Fir melt	T Fin melt	ThTotal
P27	-55.7	-3.1	18.2	234.1		4.5		231.5	-60.1	19.8					168
	-55.7	-1.8	25.4	242		4.7		231.6	-62.1	20.2					165
	-57.7	-6.9	29	275		5.3		231.5	-61	20.1					167
	-54.3	-4.8	29.7	214		6		231.2	-60.2	18.6					166
	-55	-4.6	22.2	277		5.7		231.2	-60.1	20.1					
	-57.8		33.7					233.2	-62.1	20.2					
P12	-55.8	-4.8	26.6	192	-57.2		24	235	-61	21			-23.1	-7.8	182
	-55.2	-5.5	28	198	-57.4	5.5	24.2	232.4	-58.3	22			-21.2	-6.8	193
	-55.2	-4.3	28	198	-57.1	4.8	23.9	235.3	-58.2	22.8			-25.8	-9.3	189
	-57.2	-5.5	29	197	-56.4	4.6	24.1	234	-62.3	21.7					
	-55.8	-5.6	28.2	198.1		4.9	22.3	232.7	-62.2	21.7					
	-56.9	-6.3	26.9	197.8		5.8	22.6	232.5							
P24	-55.9	-6.2	26.8	199.1	-56.5		23.8	236	-61	20.1					
	-57.1	-7	27.2	195.5	-57.1		23.8	235.1	-60.2	20.2					
	-56.8	-7	33	194.3			22.5	232	-60.1	21.2					
	-57.3		33.7	195.8				232.1	-60.1	20.8					
	-57.5		15.8					232.6	-60	22.3					
	-57.3		15.5					233.1							
	-57.6		21.4					234							
	-58		21.3												
	-58.1		24.8												
	-58.3		24.4												
	-59.1		23.4												
	-59.1		22												
			31.8												
			31.5												

		Vein											
P33	-58.1	-4.9	18.9	219	-57.2	-3.9	23	231.8	-61.3	9.9			
	-56.9	-4.2	22.2	231	-57.1	-3.8	23.8	233.1	-61.2	9.8			
	-57.7	-5.1	22.8	229	-57.4		24.7	231	-61.1	9.7			
	-57.8	-4.9	23.8	233				234.7	-61.3	9.7			
	-59.4	-0.8	17.9	221.3				235.4					
P32	-57.8	-4.9	22.8	233.2	-57.5		23.5	231.4	-61.3	9.3			
	-57.9	-0.9	24.9	238	-57.5		24.4	231.6	-61.4	9.3			
	-56	-0.8	28.2	298.5	-57.3		24.2	232.5	-61.2	9.9			
	-54.9	-0.4	28	198.6	-56.3			232.8	-61.2	10.1			
	-55.1	-4.3	27.9	225	-56.2			232.9	-60.9	11.2			
	-55.9	-4.8	28	226.2				232.5					
	-55.7	-5.3	26.9	227				235.6					
	-56.6		27.4	289.4				235.6					
KR8	-57.4	-4.9	26.5	223					-57.2	14.8	-17	-4	127.1
	-57.8	-4.7	26.7	223.8					-57.4	15.8	-17.3	-7.8	127.2
	-57.8	-4.8	26.9	221.6					-57.3	15.9	-17.8	-4.3	107.9
	-57.6	-4.7	24.5	224.8					-57.3	22.8	-17.9	-4.9	126.9
	-57.5		23.9	223.9					-57.2	15.5	-19.3	-4.1	126.9
	-57.4		23	223.4					-57.3	16.7	-19.3	-4.1	126.5
	-57.4		24.1	228.1					-56.9	5	-21.1	-4.1	126.8
										1.8	-16.3	-6.1	139
KR2	-58.1	-2.3	22.3	223.8									
	-58.3		8.9	238.3									
	-57.9		8.7	239.7									
	-57.3		9.1	232.2									
KR3	-57.2		8.9	237.1					-57.4	14.6			
	-57.7	-1.2	14	221.2					-58.8	29.7			

	-57.9	-3.9	23	223.8				-57.8	29.3					
	-56.8	-3.8	23.8	231.8				-57.3	28.8					
	-57.9	-4.2	23.1	233.1				-57.1	23.7					
KR4	-57.1	-4.8	23.9	223.7				-58.2	17					
	-57.2	-4.3	23.8	221.8				-57.2	14					
	-57.6			274				-57.4	22					
	-57.8	4.9	24.8					-58.7	28.8					
	-58.1	5.7	25.7	283				-57.4	5.8					
								-58.1	10					
P37	-55.2		26.2	192				-61.2	9.8					
	-57.1		25.1	198				-61.1	10.3					
	-57.8		27	196				-61.1	11.2					
	-55.4		27.1	196.1				-61.1						
								-61.1	11.3					
P38	-55.4		25.4	193.3				-60.3	11.3					
			29.1	196.2				-61.2	9.9					
	-55.4		29.1	196.1				-61.2	9.8					
	-57.2		27	197.2				-61.1	9.8					
			22.9	171.1				-61.3	28.2					
								-53.5	26					
RVG1	-55.2		26.2		-57.5	22.9	234.9			121.5	193.4	-26.4	-4.4	185.7
	-57.1		25.1		-55.1	22.8	233.9			208.1	175.2	-31.6		189
	-57		13.8	281	-55.3	23.7	232.6			213.6	237.6	-23.5	-12.5	194
	-53		13	224	-55.2	23.5	232.4			248.3	207	-29.3	-9.8	192.3
	-56		11	221	-55.3	23.7	232.4			360	254.1			
		-58.5		12						189.1	157.2			
RVG2	-57.8		13	231				-58.3	27	178.1	154.1	-40	-2	180
	-57.1		31	220				-53.5	25	217.2	189.2		-2	180
	-57.2		30.9	249						198	173		-3	182
			30.9	258						194	238.9			

		31.5	287			194	208				
						190	203				
RVG3			295	-58.4	27.3	193	237.1				
			298	-58.4	27	197	239.3				
			254	-57.3	24.4	194.6	213.2				
	-55.8	30	291	-58.1	23.2	222	204.2				
	-58.1	30	290	-57.4	26.1	207	237				
						250.1	324.1				
						198.1	228.7				
						196.3	241.2				
						241.2	292.5				
RVG5	-57.4	31		-61.9	18.1	212		-23	-8	189.7	
	-57.9	29	288.2	-61.4	18.1	217		-34	-8.8	173	
	-57.4	28.9	279.1	-61.4	18.3	233.1		-33	-6.8	189	
		24.5		-61.5	18.9	182.1	145				
		24		-61.3	18.6	192.1					
				-61.3	24.8	230					
				-61	9.8	206					
				-60.9	9.7	193.5	168				
				-61.1	-9.7	249.8	237.2				
				-61.3	9.7	237.2					
				-58.1	23.2	251.1					
				-58	29.7	223.3	181.3				
				-58.3	27	323					
				-58.4	27.3	241	189				
				-57.4	29						
				-57.9	31						
				-58.4	27.4						

present study, most of the inclusions homogenized into liquid phase. The distribution of the temperature of the recorded range is given in the histogram (Figure13, 14&15). The presence CO_2 has been confirmed by laser Raman spectroscopic studies. Figure 16&17.

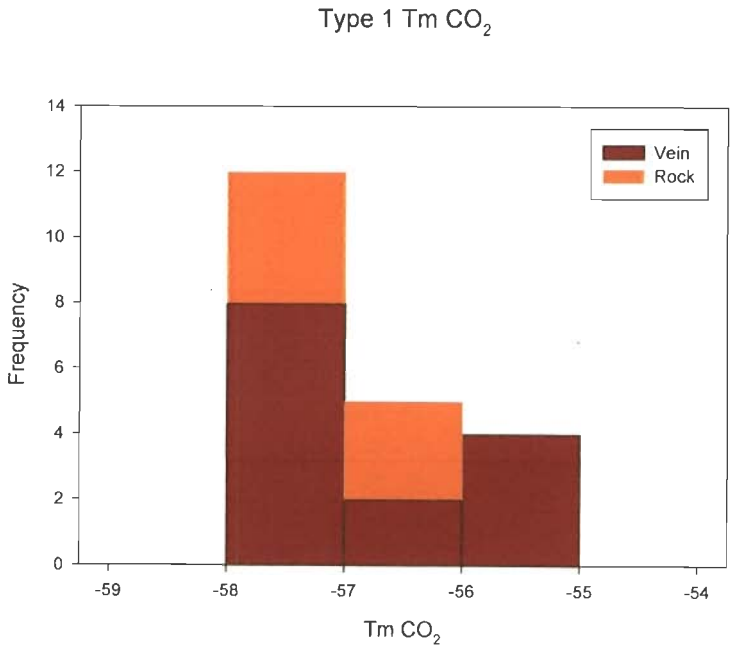

Figure 6.10 Histogram showing melting temperature (°C) of CO_2 in type-1 inclusions

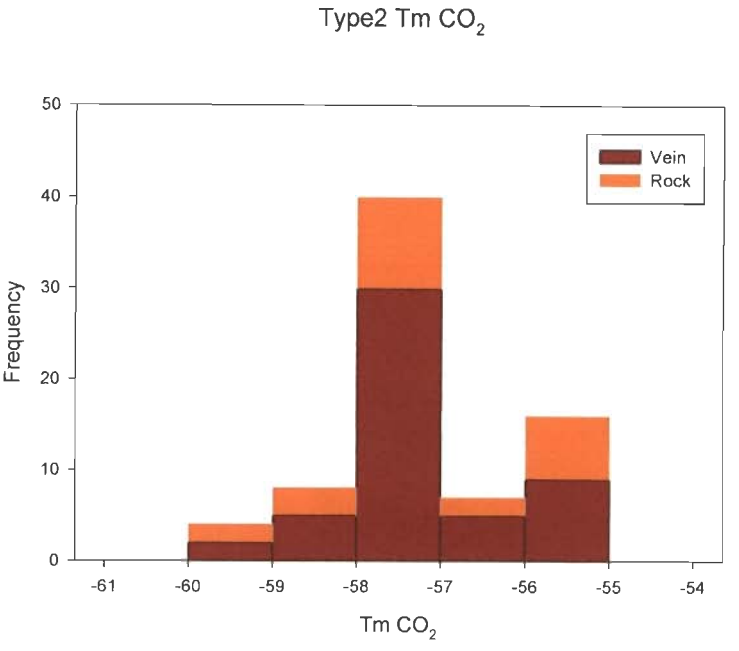

Figure 6.11 Histogram showing melting temperature (°C) of CO_2 in type-2 inclusions

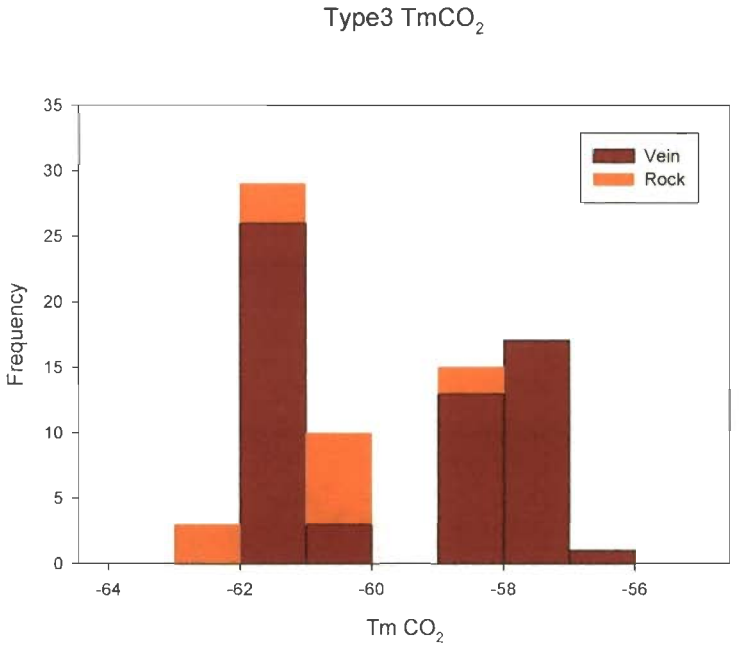

Figure 6.12 Histogram showing melting temperature (°C) of CO_2 in type-3 inclusions

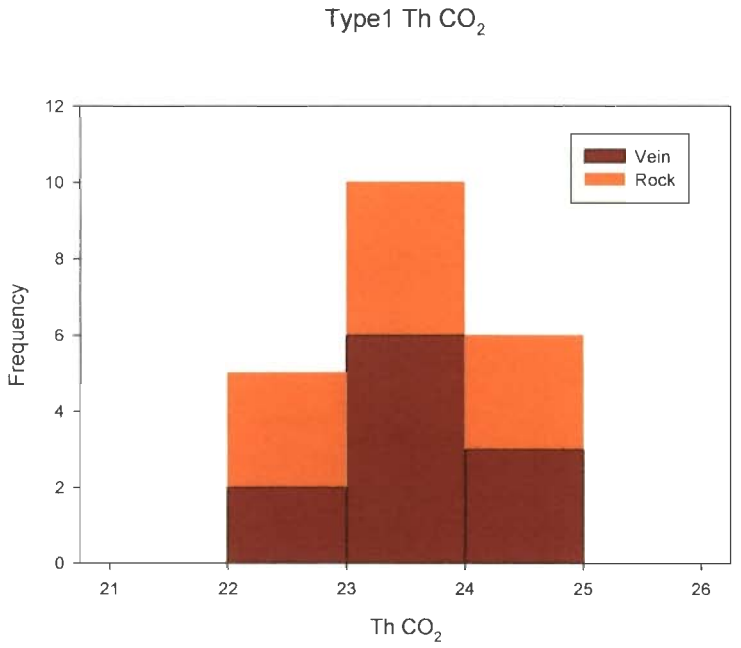

Figure 6.13 Histogram showing homogenization temperatures (°C) of CO_2 in type-1 inclusions

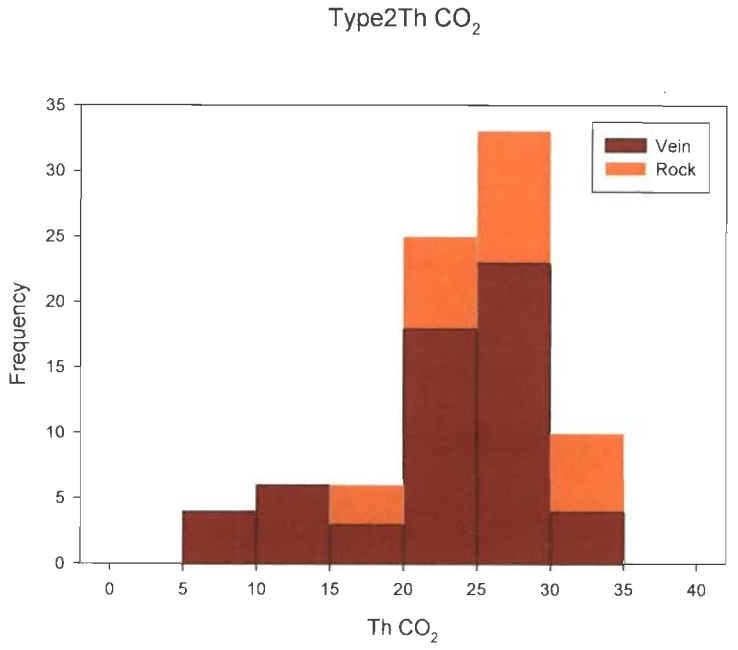

Figure 6.14Histogram showing homogenization temperature (°C) of CO_2 in type-2 inclusions

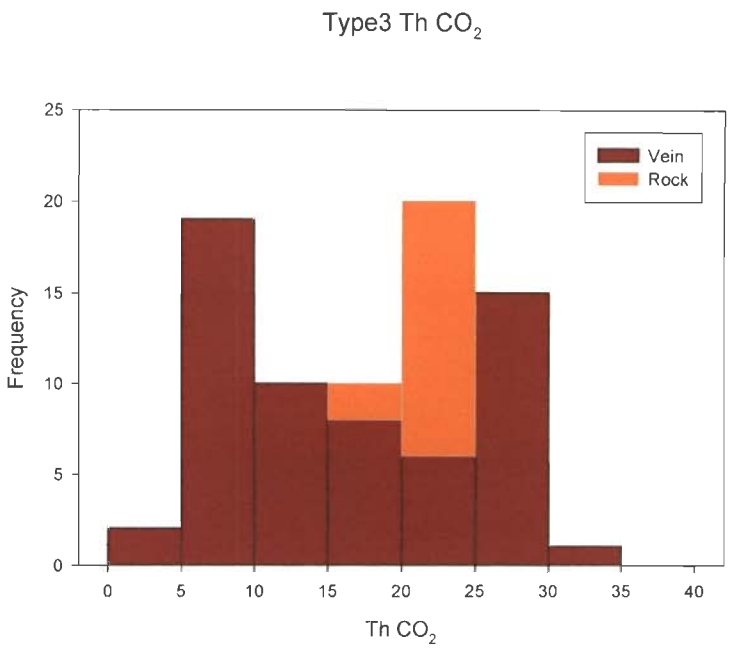

Figure 6.15 Histogram showing homogenization temperatures (°C) of CO_2 in type-3 inclusions

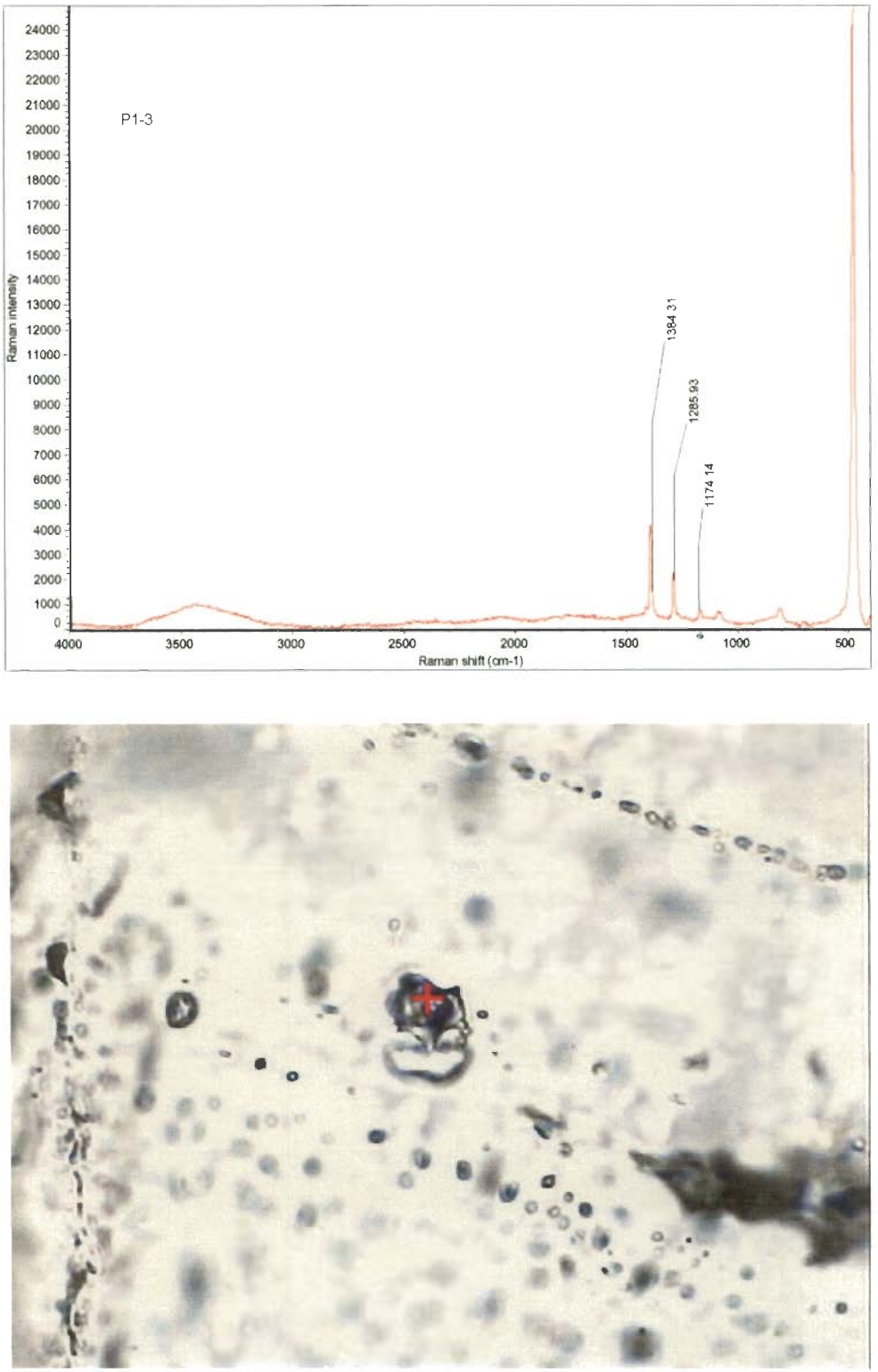

Figure 6.16 Laser Raman spectrographs for CO2-rich inclusion

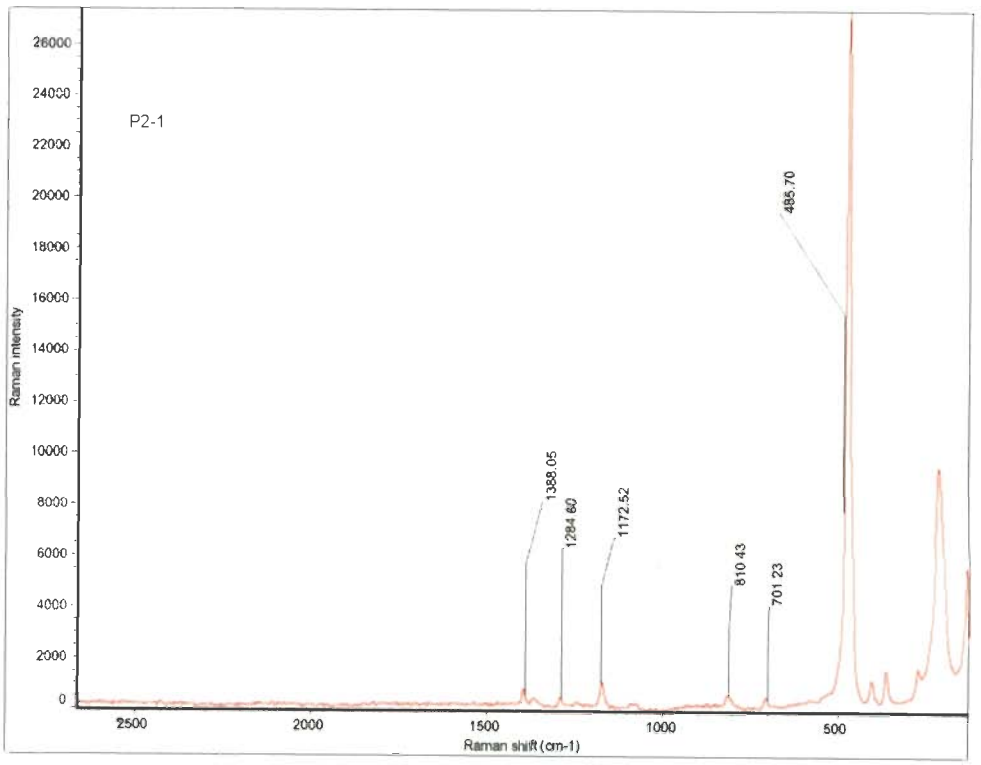

Figure 6.17 Laser Raman spectrographs for CO2-rich inclusion

6.6.4 Heating Data

Heating data include total homogenization temperatures (T_h total) of type-1 type- 2, type- 4 and type-5 fluid inclusions. The data obtained from microthermometric study of different inclusion types have been plotted (Figure 6.12). The temperature of disappearance of gas phase or the dissolution of the last daughter mineral was considered as temperature of homogenization for the type-4 inclusions because in few samples daughter mineral dissolve before gas phase, in other samples dissolution of daughter mineral has been observed after the disappearance of gas phase. For bi-phase inclusions, a temperature of disappearance of gas bubble was designated as Th. It is observed that all fluid inclusions homogenized to the liquid phase. The temperatures of homogenization are reported without pressure corrections due to the lack of any independent geothermometer.

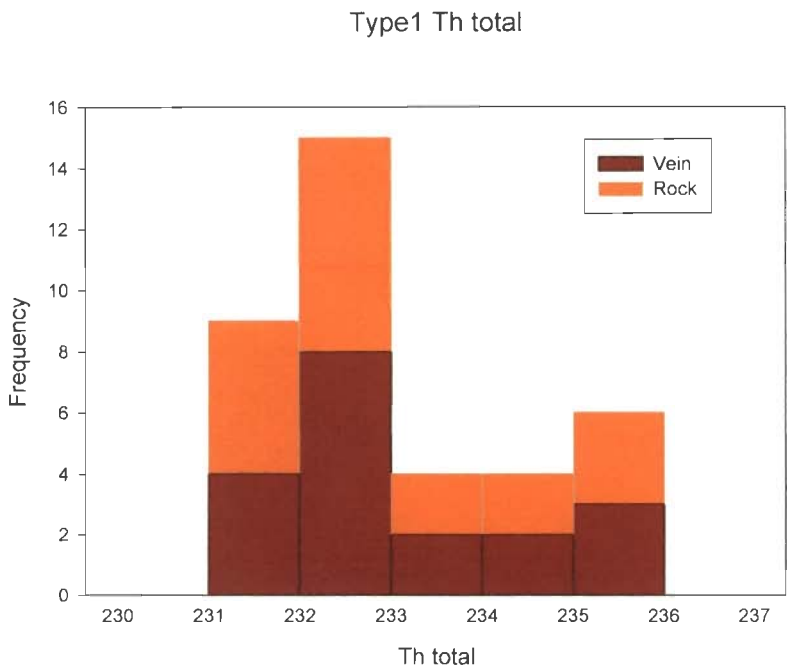

Figure 6.18 Histogram showing homogenization temperature (°C) of Type-1 inclusion

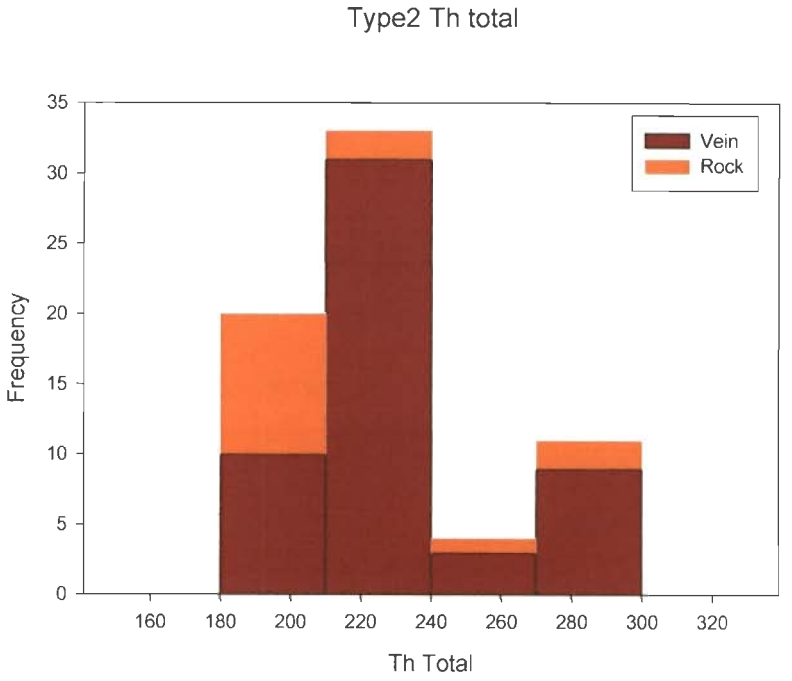

Figure 6.19 Histogram showing homogenization temperature (°C) of Type-2 inclusion

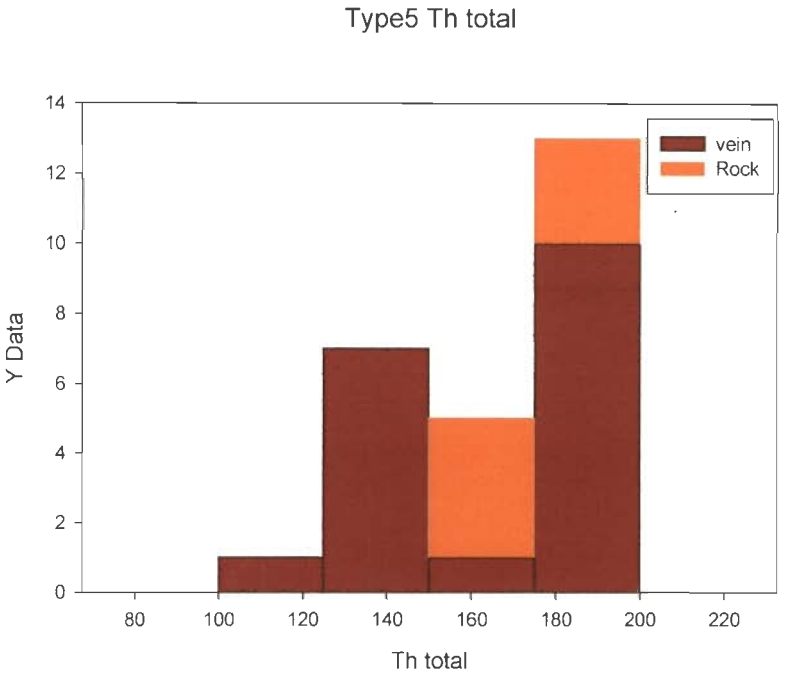

Figure 6.20 Histogram showing homogenization temperature (°C) of Type-5 inclusion

6.6.5 Salinity

Salinity of fluid is expressed as equivalent weight percent NaCl (wt % NaCl eq.). Final melting point of Clathrate (TmCl) indicates salinity (wt% NaCl equivalent) of type-1 and type-2 fluid inclusions. For type-4 inclusions salinities were calculated from equation given by Zhang & Frantz (1989). Final ice melting temperatures were used to determine the for salinity of type-5 fluids. The multiphase inclusions (type-4) have salinities ranging from 28.63 wt % to 43.34 wt % NaCl and these salinities are higher than those of other samples. Eutectic melting points of the H_2O inclusions associated with CO_2 phase was difficult to observe, probably because of their low salinities. However, in two to three cases, first melting was noticed at -19°C. The final melting temperatures of these inclusions were obscured by the formation of clathrate. The salinity calculations from clathrate melting temperatures have been used to calculate the salinity of type-1 and type-2 inclusions. The melting temperature of clathrate found to be between 2 to 5.5°C.

6.6.6 Density of CO_2

Equations given by Kerrick and Jacobs (1981) were applied to estimate CO_2 density based on H_2O-CO_2-CH_4 ternary system. The density calculation using the equation of state of Kerrick and Jacobs (1981) takes into account several other parameters (like the fraction of CO_2 present) than the homogenization temperatures of fluids, to determine the bulk density of the fluid. On the basis of these data fluid densities were estimated 0.66g/ cm^3 for type-1, .67g/cm^3 for type-2, 0.7 /cm^3 for type-3 (Table 6.2). However, the fluid density estimated from different types of inclusions does not show significant difference between clusters throughout the Attappadi area.

Table6.2 Summary of classification, properties and microthermometric data for fluid inclusions in Attappadi

Fluid InclusionTypes	Type-1	Type-2	Type-3	Type-4	Type-5
Samples	In quartz vein Quartz biotite geiss	Quartz vein Quartz biotite geiss	Quartz vein Quartz biotite geiss	In quartz vein	In quartz vein
Size (μm)	10-20 μm	5-15 μm	5-15 μm	5-30 μm	5-30 μm
Melting temperature of solid CO_2 Tm CO_2 °C	-55 to -58	-55 to -60	-56 to-62		
Homogenization temperature of CO_2 Th CO_2 °C	22 to 25	5 to 31	5 to 32		
Temperature of final ice melt Tm Ice °C	-3 to -4	-1 to -7			-2 to -13
Temperature of dissolution of solid Tds °C				121 to 360	
Th total °C	233 to 236	170 to 300		145 to 324	100-195
Density	0.66	0.66	0.70		
Salinity Wt% Nacl.eqv.	2 to 6°C	2 to 6°C		28-43	

CHAPTER 7

Discussion and Conclusions

DISCUSSION AND CONCLUSIONS

Late Archaean greenstone-granite terrains, all over the world, typically host lode-gold deposits, an amazingly efficient product of crustal-chemical processes. Genetic considerations of these deposits must address some key components such as, evolution of greenstone belt, deposit-scale structural style/ shearing, evolution of quartz veins, metamorphism of host (and associated rocks), vein mineralogy, source of metallic minerals, fluid characteristics with emphasis on transport and deposition of gold. The observations and results recorded in the earlier chapters have been considered in a collective manner and the correlations are used to evolve a comprehensive picture of various processes responsible for gold mineralization in Attappadi.

7.1 Evolution of Attappadi Greenstone Belt

Metavolcanis and metasedimentary rocks designated as 'Attappadi supracrustals' occur as enclaves and remnants within the gneisses exposed in the crustal scale BSZ. The assemblage of rock types such as metapyroxinite, talc-tremolite-actinolite schist, amphibolites, BIF, sillimanite/kyanite bearing quartzite and fuchsite quartzite in Attappadi represents a greenstone belt setup. Geochemical study of exposed and sampled metavolcanis show that the Attappadi greenstone belt consists of Fe-rich tholeiites. This metavolcanics (tholeiitic composition) intercalated with BIF and surrounded by granite gneisses of monozodiorite composition. Field relations, geochemical characteristics, mineral assemblage (oxides and sulfides) of BIF indicate these are Algoma type BIF. Thus Attappadi belongs to Thurston and Chiver's (1990) classification of greenstone belt "deep-water oceanic sequences consisting largely of tholeiitic basalt with minor felsic pyroclastic rocks, chert, and

iron formation". The Al_2O_3/TiO_2 ratio of BIF is similar to the mean value of tholeiite indicating that there is a genetic relation between BIFs and amphibolite (e.g. Kato et al. 1996). The chondrite-normalized REE patterns (Figure 5.5) of low K- tholeiite of Attappdi exhibit enrichments in LREE with respect to HREE. As this pattern is different from normal basalts, the possible reasons for overall enrichment of LREE can be: (1) reflects the composition of an enriched source EMORB or (2) related to metasomatic enrichment in a hydrothermal system. The BIFs show LREE enrichment with a striking positive Eu anomaly. Possible source materials of positive Eu anomaly of BIFs have been attributed to a hydrothermal activity in oceanic environment (Michard and Albarede, 1986; Campbell et al., 1988) caused by redox state of Europium. Many others have shown that deposition of extensive BIFs in the Archaean is often considered as evidence for intense seafloor hydrothermal activity in the oceanic crust (Jacobsen and Pimentel-Klose, 1988; Derry and Jacobsen, 1990; Shimizu et al., 1990; Morris, 1993; Chown et al., 2000). All BIFs deposited in the Archaean and Proterozoic show REE patterns with pronounced positive Eu and negative Ce anomalies (Fryer, 1977; Appel, 1983; Jacobsen and Pimentel-Klose, 1988; Alibert and McCulloch, 1993). These patterns have been attributed to chemical precipitation from solutions that were mixtures of seawater and hydrothermal input (Fe) from the spreading centres in the oceanic crust (Jacobsen and Pimentel-Klose, 1988; Derry and Jacobsen, 1990; Isley, 1995; Isley and Abbott, 1999). Considering various criteria like lithological assemblages geological setting, and geochemistry it is proposed that at least a major part of the volcanism of the Attappadi supracrustal sequence must have evolved in a spreading center tectonic setting. Since no radiometric age data on the Attappadi greenstone belt are presently available, definite time constraints between magamtism and tectonism cannot be readily placed. But the

high-grade rocks of the Sathyamangalam Group, regarded as equivalents of the Sargur Group (Ramakrishnan, 1993), form the northeastern extension of Attappadi supracrustals. Thus the age of the Attappadi supracrustals can be correlated to the Sargur Group of rocks (3100-3330 Ma)

The Attappadi supracrustals are surrounded/intruded by the gneisses .The gneisses are showing mineralogical variation but geochemical studies indicate that the protoliths of this igneous rocks are monozodiorite and the tectonic discrimination diagrams (Figure 5.2 and 5.13) show that they are volcanic arc granite formed at convergent tectonic setting. Monozodiorite showing uniform trace element distribution with relative enrichment of Rb and Zr (150 ppm), La (25 ppm), Ce (53ppm), and Nb (7 ppm) high $(La/Yb)_N$ indicate that these were lower crustal derived. Eu-anomalies in the chondrite-normalized REE diagrams (Figure 5.6) also indicate a plagioclase-depleted crustal source. Thus one likely scenario for the protoliths of gneisses in Attappadi greenstone belt is that they had intruded into the Attappadi supracrustals during the melting of lower crust in a convergent tectonic setting and crustal thickening possibly associated with a subduction related processes. Granulite blocks north of the CSZ (NGB, Figure 2.1) are largely composed of late Archaean rock units. Peucat et al. (1989 and 1993) proposed that much of this region is composed of "syn- accretion" charnockite formed by the metamorphism of juvenile calc-alkalic granitoid plutons emplaced at 2500 Ma. Their generation is ascribed to the late Archaean subduction related crustal thickening (Drury et al. 1984). Many types of granite in Archaean terrains appear to be associated with crustal thickening and anatexis during late stages of collision (Kusky and Polat, 1999). In general the Attappadi greenstone belt represents an association of different lithounits of various tectonic environments juxtaposed together. According to Sylvester et al. (1997)

Archaean greenstone belts are typically combinations of rocks that formed in different tectonic environments which later became juxtaposed during tectonic thrusting and imbrications

The different lithological assemblage that make up the Attappadi greenstone belt occur as narrow strips that extend for several kilometers parallel to the strike of the BSZ (Figure 3.2). The contacts between these rock units are generally linear, even though the rocks themselves are deformed. For this reason, contacts between different lithological assemblages in the Attappadi greenstone belt have been treated as structural. The rocks in Attappadi have experienced polyphase deformation and metamorphism (Figure 3.3). The area was isoclinally folded twice (F_1 and F_2; F_1 being refolded coaxially by F_2 folds). Available published geochronological data have been used for reconstructing these deformational events. The oldest event reported here D1 affected the entire belt and produces NE-SW trending F_1 fold deformational zones and F_1 axial planar penetrative foliation S_1.(Figure 3.3) The D1 and M1 temporally related to the regional metamorphism of SGT 2500 Ma (Raith et al., 1999) According to Kerrich and Cassidy (1994), Goldfarb et al.(2001) and Groves et al. (2003), the orogenic lode gold deposits were formed typically during the late stages of the deformational–metamorphic–magmatic history of an evolving orogen, synchronously with at least one main penetrative deformation stage of the host rocks. Thus the early mineralizing event in Attappadi can be correlated to the regional metamorphism and shearing of Attappadi greenstone belt. M2 metamorphism and D2 event attribute the most prominent planar structure mylonitic foliation S_2 in BSZ. This metamorphic and deformational can be correlated to Neo-Proterozoic reactivation of BSZ (Ghosh et al., 2004).

The petrography and mineral chemistry of different lithounits belonging to greenstone belts of Attappadi are characterized by the assemblage of chlorite-tremolite-actinolite-hornblende + plagioclase +quartz indicate metamorphism of protoliths under greenshist to lower-amphibolites facies conditions. The pressure-temperature conditions of this metamorphism and deformational history suggest that metamorphism occurred in collisional setting. Thus, the rocks of this study are most likely representing an exhumed mid-crustal terrain.

7.2 Gold-Quartz Vein

The gold-quartz veins in Attappadi are hosted by strongly deformed, metamorphosed rocks of different lithologies, The veins occur as a series of sub parallel, moderate to steeply dipping reefs, trending NNE-SSW to NE-SW direction. This regional distribution of the gold-quartz veins defines a broad linear, NE-SW trending zone in Attappadi greenstone belt and acted as a large scale shear zone and become the foci of fluid flow and vein emplacement. The textural and microstructural characteristics (undulose extinction, the development of deformation lamellae, bands and grain boundary migration recrystallization) of the quartz veins imply that they formed in brittle- ductile regimes. Under these environments, the stresses are compressive in all directions, which imply that the rocks are stable. However, the presence of pore fluid at depth allows rocks to be unstable and causes rock failure by lowering the confining pressure. Such hydraulic fracturing is one of the major causes of rock failure that leads to precipitation of vein material at depth, and may be facilitated in the presence of mechanical anisotropies in rocks, such as cleavage. Therefore, abundant veining of consistent orientation, parallel to foliation can be explained in terms of hydraulic fracturing as one of the possible mechanisms to cause rock failure in Attappadi greenstone belt.

Mineralogical studies of the polished specimens of quartz vein samples exhibit an assemblage of pyrite + pyrrhotite + chalcopyrite + galena. Covellite, anglesite and malachite are often associated with chalcopyrite and galena formed due to the supergene alteration. Quartz is the predominant gangue mineral showing evidences of deformation and recrystallization. The mineralogical studies of ore minerals indicate a paragenetic sequence with early pyrite and gold followed by chalcopyrite and galena. The first stage gave rise to a mineral assemblage consisting of simultaneous pyrite and gold deposition (Nair et al. 2005) presumably from a hydrothermal fluid source. The first stage was followed by a late stage deposition of chalcopyrite and galena filling micro-fractures in quartz. This stage also resulted in the remobilization of gold from earlier formed pyrite and resulted in the formation of discrete gold in recrystallized quartz. The occurrence of pyrrhotite as elongated crystals along the shear plane of quartz biotite gneiss also suggests the post deformation of the early formed minerals. Nair et al. (2005) also reported closely spaced shear planes in gold present in quartz veins with striations indicating the effects of brittle to ductile shearing of earlier formed minerals.

7.3 Source of Gold

The metavolcanics of Attappadi greenstone belt represent high Fe-thoeliitic basalt. On a worldwide and craton scale, many have stressed the significance of Fe-rich tholeiities of Archaean greenstone belts as the most important host rocks for gold mineralization (Groves and Foster, 1993). Petrogenetic processes involved in the generation of high-Fe tholeiitic magmas require mantle sources had undergo melt metasomatism to a large extent to significantly increase the Fe/Mg ratio of the source (Giritharan and Rajamani, 2001). Such melt addition processes enriched gold and sulphur content of the generated magma. Thus the sulfur required for the

hydrothermal transport of gold would also be available in the high-Fe tholeiitic protoliths. Based on this fact it is possible that same Fe-rich tholeiitic protoliths possibly under different physical conditions, (perhaps deep seated) must have provided required sulfur and gold in Attappadi greenstone belt. Further Fe-rich tholeiites became more competent lithology at amphibolite grade metamorphism for brittle ductile fracturing so that focused fluid flow was possible for vein formation (Giritharan and Rajamani, 1998).

7.4 Ore forming fluids

The results of fluid inclusion studies from gold-quartz vein and quartz-biotite gneiss in Attappadi greenstone belt show five different types of inclusions. Type-1 and type-2 fluid inclusions in Attappadi greenstone belt are characterized by 1) low salinity, 2) presence of liquid CO_2 and 3) relatively consistent density of CO_2 phase (0.6-0.7 g/cc). The consistent fluid chemistry and inclusion characteristics indicate that the fluids were relatively homogenous, derived from single source. CO_2 bearing fluid inclusions in auriferous quartz veins from Attappadi suggest that carbonic fluid phase was active during the vein formation. CO_2 rich fluid is entirely consistent in Archaean lode gold deposits (Pandalai et al., 2003; Mao et al., 2008; Coulibaly et al., 2008) and is quite distinct with respect to fluids encountered in other major classes of ore types (Rainaud et al., 2003; Sharma 2006; Yudovskaya et al., 2006, Baidya et al., 1999)

The compositions of type-1 and type-2 inclusions are similar to auriferous fluids reported from other Archaean Au deposits in southern part of India (Table 7.1) and can be considered as the mineralizing fluids for gold deposition. Type-3 inclusions (CO_2 monophase, gas rich) are considered unlikely to represent the auriferous fluid as auriferous fluids are typically interpreted to have a significant

aqueous component (Phillips and Evans, 2004). Fluid inclusion petrography and field relations of quartz veins indicate type-4 and type-5 inclusions are not related to mineralization.

7.4.1 Fluid Source

In order to constrain genetic models for gold-quartz veins and source of fluid, it is necessary to understand the relations among regional and local structures, tectonics, age of metamorphism of host rocks, and fluid characteristics. The tectonic history of Attappadi includes: (1) regional metamorphism and shearing during 2500 Ma (Gosh et al., 2004) (2) exhumation and retrogression of high-grade rocks during the Neo-Proteorozoic (Ghosh et al., 2004).These tectonic events indicate that Attappadi greenstone belt experienced initial crustal thickening followed by crustal thinning/exhumation. The type1, type 2 and type 3 aqueous inclusions are related to retrogression during later uplift of the region or formed by equilibration of earlier formed fluid. This is indicated by the following observations: (1) type 2 inclusions are aligned on trails cutting quartz grains (2) they are most abundant in quartz and mylonites (3) morphological characteristics and microthermometric results of fluid inclusion indicate type 1 and type 2 inclusions and type3 inclusions present in mineralized vein and quartz biotite gneiss are similar (Figure 7.1), 4) discrete gold grain in mineralized vein and 5) fracture filled sulfide minerals in mineralized vein and quartz-biotite gneiss. Thus fluid inclusions present in studied samples certainly represent a mineralizing event and can be attributed to the remobilization of earlier formed minerals (sulfides and gold). However, less saline and H_2O-CO_2 fluids in inclusions present in quartz veins have relatively consistent composition throughout Attappadi region suggesting a regional uniform, homogeneous fluid source related to metamorphism (Dube and Gosselin, 2004)

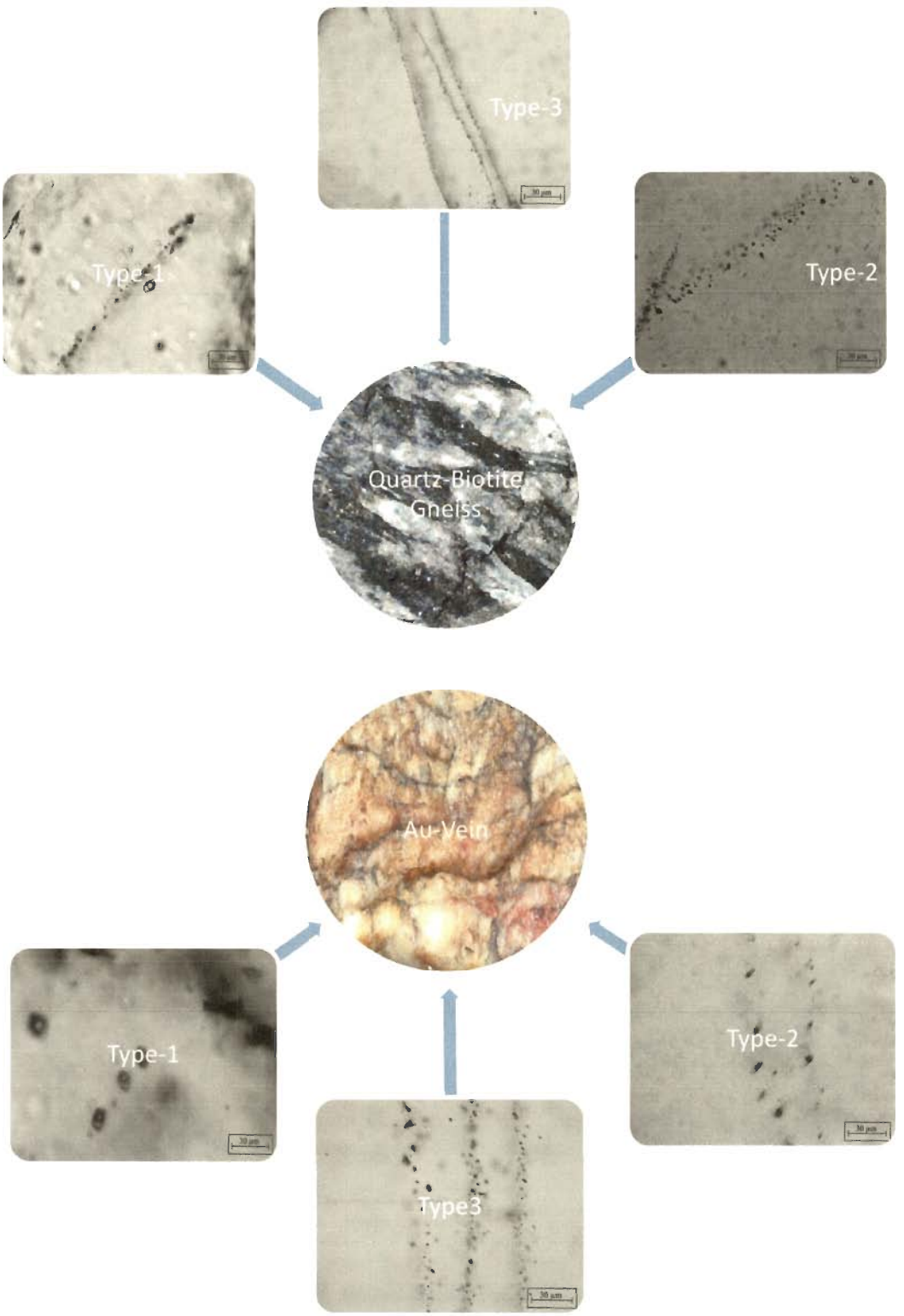

Fig ure 7.1 The fluid inclusions in quartz vein and Quartz biotite gneiss

Table 7.1- Summary showing relation among host rock types, metamorphic grades structural styles and fluid inclusion characteristics of metamorphic gold-quartz vein deposits in South India

Location	Host rock	Age of the host rock	Metamorphic grade	Structural style	Fluid inclusion types	Characteristics of fluids	References
Kolar schist belt India	Metavolcanics granitoids	Archaean	Middle amphibolite facies	Quartz reef in shear zones	Primary (Aqueous Bophase, Polyphase, Monophase Aqueous H_2O-CO_2	H_2O-CO_2 120 to 420 °C (<7 wt.% to <50 wt.% NaCl equivalent)	(Mishra and Panigrahi, 1999)
Hutti-Maski belt India	Metavolcanics metasediments	Archaean	Upper greenschist to lower amphibolite	Quartz veins that are controlled by shearing	Primary, psedo secondary, secondary along grain boundaries H_2O-CO_2 and aqueous H_2O-CO_2	CO_2–H_2O 240-360 °C <0–8 wt% NaCl eq: 1.5-3.5kb	(Pal and Mishra ; Pandalai et al., 2003)
Ramagiri	Metavolcanics	Archaean	Upper greenschist to lower amphibolite	Quartz reef in shear zones	H_2O-CO_2-CH_4-NaCl ($\pm H_2S$)	Low saline 1.45-1.7 kb	(Mishra, 2007)
Wynad gold filed India	Migmatized hornblende gneiss, amphibolites, granitic gneiss granulite-grade metapelites	Proterozoic	Granulite facies	Quartz veis in shear zones	Carbonic and aqueous H_2O-CO_2	H_2O–CO_2 300 to491°C (2–14 wt% NaCl equiv.) 0.5 and 2.9 kbars.	(Binu-Lal et al., 2003)
Attappadi India	Metavolcanics Hornblende gniess Quartz biotite gniess	Archaean	Greenshist to amphibolite	Quartz vein in shear zones	Carbonic and aqueous H_2O-CO_2	H_2O-CO_2 200-300	Present research

The earlier mineralizing fluids originally must have formed from metamorphic dehydration reactions. It is believed that such metamorphic environments were pervasive throughout Attappadi. Extensive research on the Archaean lode gold deposits the world over shows that auriferous low salinity H_2O-CO_2 fluids were channeled up in trascrustal shear zones during the late stage of greenstone belt deformation and metamorphism (Perring et al, 1987; Groves et al., 1988; Groves and Foster, 1991). Thus during the late stage of Attappadi greenstone belt deformation and metamorphism, the circulating hydrothermal fluids (H_2O-CO_2 fluid) were responsible for the breakdown of ferromagnesian minerals and release of silica which along with gold from the tholeiite rocks formed the quartz veins within the shear zones. This is correlated to the higher gold content available in the mafic rocks and also corroborated by the spatial proximity of the auriferous quartz veins to them.

Magmatic fluid can be another possible source for vein-type gold deposit in Attappadi, mainly because of the widespread distribution of granitic intrusive in the supracrustals. A case can be made for distal magmatic source of fluids due to characteristics of fluid inclusions in the veins- such as low saline, CO_2 rich fluids. In felsic magmas partial melting of CO_2 rich minerals can produce low salininity and CO_2 rich fluids at depth (Burnhan, 1979).

Summing up the source of fluids, the Attappadi greenstone belt constitutes orogenic gold deposits that formed by metamorphic fluids from accretionary processes and generated by prograde metamorphism and thermal re-equilibration of subducted volcano-sedimentary terrains.

7.4.2 Pressure Temperature conditions of mineralization

The average values of Th CO_2 from the histogram of fluid inclusions (H_2O-CO_2 system equation given by Kerrick and Jacobos, 1981) were used in the

MacFlinCor programme to obtain isochors for type-1 and type-2 inclusions (mineralizing fluids).

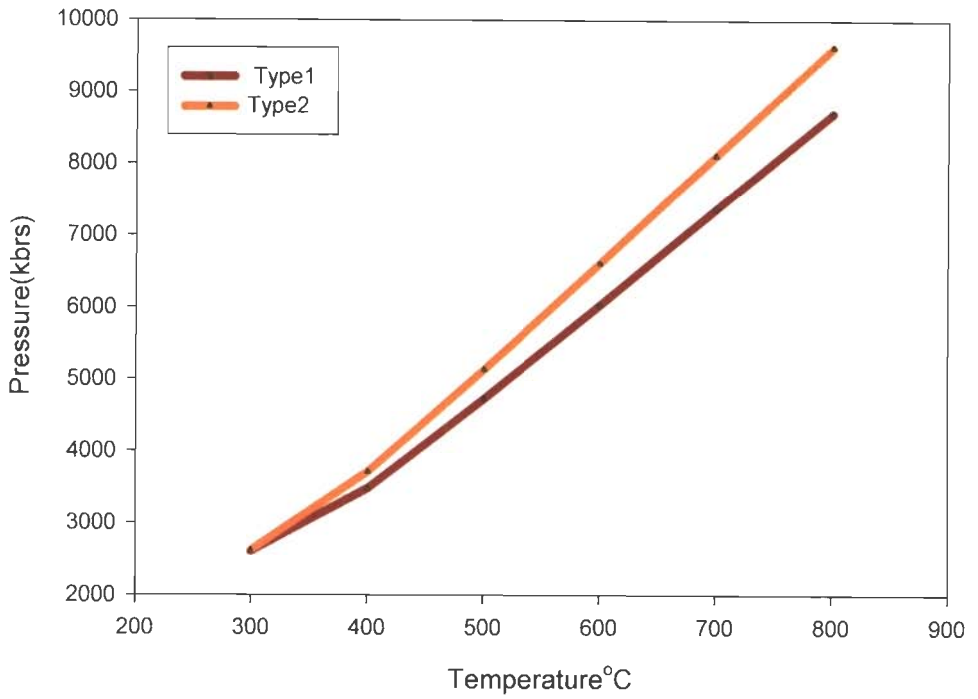

Figure 7.2 Isochors for Type1 and Type 2 inclusions from Attappadi greenstone belt

H_2O-CO_2 inclusions provide the best approximation of the P–T–X of the mineralizing fluid. The highest homogenization temperature of these inclusions (300°C) could therefore provide a minimum temperature of the original trapping conditions. At this temperature, the isochors of the H_2O-CO_2 inclusions indicate a pressure of approximately 2.5 kbar (Figure 7.2). Spread of the isochors and pressure data may account for pressure fluctuations, a common feature in the shear zone-hosted gold deposits, in which fluid pressure often exceeds the lithostatic conditions (Sibson 1987; Robert and Kelly 1987; Cox et al. 1995). This suggests that during the development of BSZ, pressure and temperatures decreased with time, as a result of upliftment. The homogenization temperature had to be taken as the minimum temperatures of ore formation which is 300 °C, and the maximum pressure of 2.5 kb

calculated from fluid inclusion isochors. Any mineralized zone controlled by shear zone ore forming fluids act as open system and thus the pressure correction should be addressed. The correction to the homogenization temperature would be roughly 15°C (Rodder, 1984). Hence, the minimum temperature of formation of gold from mineralizing fluids at Attappadi was 300 ± 15°C.

7.4.3 Gold Transport Mechanism

In order to evaluate potential reasons for gold deposition in the Attappadi greenstone belt, we first have to consider how gold is transported. Gold can only be transported in significant concentrations in solutions as complexes (Seward, 1984). Several theories have been put forth for the transportation and deposition of gold from solution. Hydroxide, chloride, bromide, iodide, sulfide, sulfate, cyanide, arsenic, antimony and telluride complexes have all been postulated as possible transporting agent for gold (Romberger, 1984). Gold is usually transported as gold sulfide/bisulfide and gold chloride complexes. Thermodynamic calculations by (Mikucki, 1998) and recent experiments by (Loucks and Mavrogenes, 1999) suggested that gold sulfide complexes are the most probable candidate for most of the orogenic and metamorphic hosted lode gold deposits. The solubility of gold in aqueous solutions is a function of temperature, pH, and pressure and sulfide concentration. Seward, (1973) indicated that $Au_2 (HS)_2 S^{2-}$, $AuHS^0$ and most importantly, $Au (HS)_2^{1-}$ are dominant sulfide complexes. . In Attappadi deposit, the temporal and spatial association of gold with pyrite and low salinity fluid inclusions is consistent with the conclusion that bisulphide complexes were responsible for gold transport.

7.4.4 Mechanisms of Gold Precipitation

Changes in fluid chemistry and the subsequent deposition of gold can occur due to several reasons like large-scale temperature and pressure gradients along the fluid pathways, phase separation in response to pressure fluctuations, reaction of the fluid with wall rocks or mixing of two or more fluids. All of these above processes are thought to be important gold precipitation mechanisms of different lode gold deposits (Mikucki and Ridley, 1993; Mikucki, 1998). Microthermometric data do not show conclusive evidences for mixing of fluids, so such a mechanism can be ruled out

7.4.5 Wall Rock Interaction

Fluid wall rock interactions involving solutions carrying gold complexes may cause gold precipitation. Hydrothermal reactions destabilize the gold transporting complex and gold is deposited from the solution. The auriferous veins in the Attappadi greenstone belts are associated with very limited hydrothermal alteration. The gold-quartz veins in the Attappadi greenstone belts are associated with very limited hydrothermal alteration. Wall rock alteration is restricted to Kottathara prospect where Type-4 inclusions are present which is recognized as formed from pegmatite intrusion. So, the wall rock reactions, leading to gold deposition in Attappadi if at all was active might have been on a localized scale, and can only be considered as a minor.

7.4.6 Fluid immiscibility

Pressure decrease could have caused fluid immiscibility, resulting in a sharp drop of fluid temperature, increase in fO_2 and pH. All of these are conducive for gold deposition (Naden and Shepard, 1989; Bowers, 1991). Fluid immiscibility has been proposed as the principle mechanism for gold deposition in Archaean gold vein systems (Guha et al, 1991; Smith and Kessler 1985; Robert and Kelly 1987). The

changes in pressure and temperature, due to the introduction of the fluid into shear zones, might also cause phase separation of an original immiscible fluid, which is an important cause for the Attappadi gold deposition. This is in conjunction with other Archaean lode gold deposits (Robert and Kelly, 1987; Walsh et al., 1988; Mikucki and Groves, 1990; Guha et al., 1991; Mao et al 2007; Coulibaly et al., 2008). The phase separation due to the lowering of lithostatic pressure during regional upliftment is well correlated with the geological history of BSZ. Type-1 and type-2 inclusions likely represent the CO_2 rich phase after the immiscibility of auriferous fluids. The proposed interpretation requires coexisting of H_2O rich fluids but aqueous inclusions were not observed together with Type 1 and Type 2 inclusions in high grade Au veins of Attappadi greenstone belt. The absence of aqueous inclusions suggest the differential trapping of H_2O following phase separation owing to the higher mobility of H_2O or CO_2 (Santosh et al., 1991).

7.5 Genetic model

Based on the preceding discussions on geological setting, nature of vein system, geochemical characterestics of lithologies and fluid inclusion data the following genetic model has been developed for gold mineralization in Attappadi.

The auriferous quartz veins of Attappadi are associated with metamorphosed rock sequences of mafic volcanic-sediments and BIF and felsic plutonic rocks. The mineralized veins are confined to zones of high strain that are manifested as ductile-brittle deformation. Gold mineralization in such an environment was possible with a convergent plate margin where crustal thickening, deformation, metamorphism and syn-orogenic magamatism played important role in fluid generation. The primary gold mineralization in Attappadi can be explained by the genetic model given by Robb (2005) as given below.

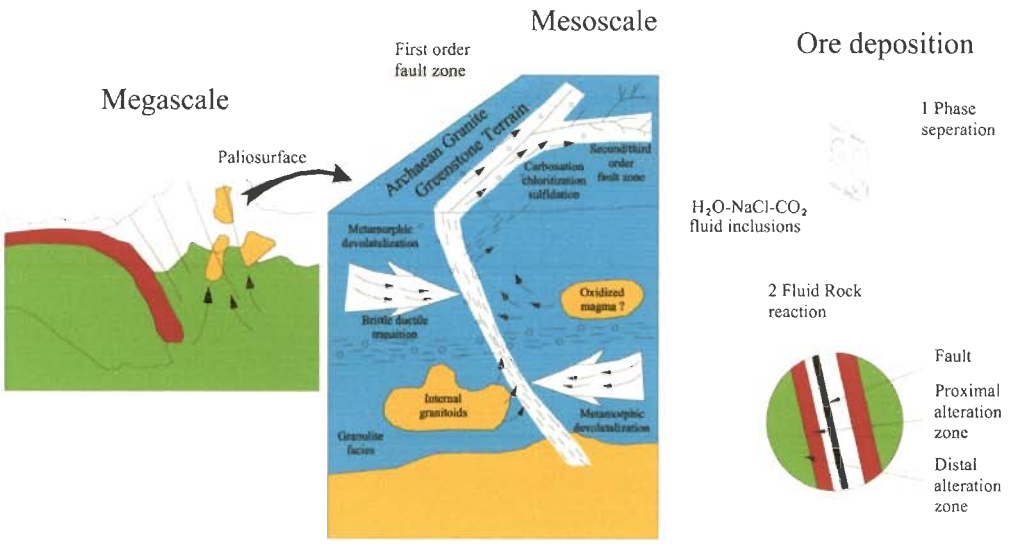

Figure 7.3 Schematic illustrations showing the principal features of Archaean orogenic gold deposits.

Major parts of the fluid (H_2O-CO_2 rich) responsible for mineralization appear to have derived from devolatalization during regional metamorphism of mafic volcanic rocks. Derivation of mineralizing fluids from granitic masses is also considered likely due to close spatial relationship between auriferous quartz veins and granitic gneisses. High gold content in Fe-rich tholeiite rocks of Attappadi metavolcanics indicate a gold rich source. The circulating hydrothermal fluid leached gold from mafic rocks and the fluids were focused along major structural discontinuities. These fluids preferably transported gold as $Au(HS)_2^-$. Primary gold deposition must have taken place due to destabilization of the dissolved gold complexes in fluid either due to wall rock alteration or phase separation. Fluid inclusion data of auriferous quartz veins clearly indicate a deformational event of early formed quartz veins. During this stage gold present in pyrite got remobilized and deposited as discrete gold grains along with other sulfide minerals within the quartz veins.

Conclusions

The results and interpretations of the filed, petrographic, ore microscopic, geochemical and fluid inclusion study presented above have a number implications for genetic and models for lode-gold vein system in Attappadi and other regions

- ✓ The assemblage of rock types such as metapyroxinite, talc-tremolite-actinolite schist, amphibolites, BIF, sillimanite/kyanite bearing quartzite and fuchsite quartzite in Attappadi represent a greenstone belt setup
- ✓ The mineralized zones typically occur within or in the vicinity of regional, crustal-scale deformation zones with a brittle to ductile type of deformation
- ✓ Gold is intimately associated with sulfide minerals, including pyrite, pyrrhotite chalcopyrite and galena in quartz veins. One or possibly two mineralizing events appear to have deposited gold in Attappadi greenstone belt. The first stage gave rise to a mineral assemblage consisting of simultaneous pyrite and gold deposition and followed by a late stage deposition of chalcopyrite and galena filling microfractures in quartz.
- ✓ The metavolcanics are low K and Fe-rich tholeiite .The overall enrichment of LREE in Fe-rich tholeiite reflects the composition of an enriched source EMORB or related to metasomatic enrichment in a hydrothermal system. A major part of the volcanism of the Attappadi supracrustal sequence must have evolved in a spreading center tectonic setting.
- ✓ The BIFs show LREE enrichment with a striking positive Eu anomaly and negative Ce anomalies. These patterns have been attributed to chemical

precipitation from solutions that were mixtures of seawater and hydrothermal input (Fe) from the spreading centers(volcanogenic in marine environment)

- ✓ The protoliths of gneisses are of mozodiorite in composition, have intruded into the Attappadi supracrustals during the melting of lower crust in a convergent tectonic setting and crustal thickening possibly associated with a subduction related processes
- ✓ Fe-rich tholeiite possibly under different physical conditions must have provided required sulfur and gold to hydrothermal fluid in Attappadi greenstone belt
- ✓ Fluid inclusion study of gold-quartz veins in Attappadi area provide good evidence of fluid chemistry, depositional environment, and origin of mineralizing fluids in this deformed terrain. The mineralizing fluids have relatively low salinity (3-6wt%NaCl eq.), consistent density of CO_2 (0.6-0.7 g/cm^3) and H_2-O-CO_2 rich. The combination of the fluid inclusion and other data suggest a pressure-temperature range of ore formation of the order of 250-300°C and 2.5 kb.
- ✓ The close association of gold with sulfide minerals within quartz veins indicates that gold was transported as bi-sulfide complexes.
- ✓ The phase separation due to the lowering of lithostatic pressure during regional upliftment caused fluid immiscibility which has been proposed as the principle mechanism for gold deposition in Attappadi greenstone belt.
- ✓ Attappadi greenstone belt constitutes orogenic gold deposit that formed by metamorphic fluids from accretionary processes and generated by prograde metamorphism and thermal re-equilibration of subducted volcano-sedimentary terrains.

References

- Ahmad T, Harris NBW, Islam R, Khanna PP, Sachan HK and Mukherjee BK(2005) Contrasting mafic magmatism in the Shyok and Indus Suture Zones: Geochemical constraints. Himalayan. Geology 26:33-40
- Alibert C, McCulloch MT (1993) Rare earth element and neodymium composition of the banded iron formations and associated shales from the Hamersley, Western Australia. Geochim. Cosmochim. Acta 57: 187–204
- Anderson DL (1989) Theory of the Earth. Bal ckwell scientific publications.
- Anglin CD, Jonasson IR, Franklin JM (1996) Sm-Nd dating of scheelite and tourmaline: implications for the genesis of Archean gold deposits, Val d'Or, Canada. Econ. Geol. 91: 1372-1382
- Appel PWU (1983) Rare earth elements in the early Archean Isua iron formation, West Greenland. Precam. Res. 20: 243–258
- Baidya TJ, Mondal SK, Balaram V, Parthasarathy R, Verma R, Mathur PK (1999) PGE Ag-Au mineralization in a Cu-Ni-Fe Sulfide rich brecia zone of the Precambrian Nuasahi ultramafic-mafic complex Orissa, India. Journal of geological Society of India 54: 473-482
- Balakrishnan S, Hanson GN, Rajamani V (1990) Pb and Nd isotope constraints on the origin of high Mg and tholeiitic amphibolites, Kolar Schist Belt, South India. Contributions to Mineralogy and Petrology 107: 279-292
- Barley ME, Eisenlohr BN, Groves DI, Perring CS, Vearncombe JR (1989) Late Archean convergent margin tectonics and gold mineralization: A new look at the Norseman-Wiluna belt, Western Australia. Geology 17: 826-829
- Barnicot AC, Fare RJ, Groves DI, McNaughton NJ (1991) Synmetamorphic lode-gold deposits in high-grade Archean settings. Geology 19: 921–924

- Bhasker Rao YJ, Janardhan AS, Vijayakumar T, Narayana BL, Dayal AM, Taylor PN, Chetty TRK (2003) Sm- Nd model ages and Rb -Sr isotopic systematic of charnockites and gneisses across the Cauvery Shear Zone, Southern India: Implications for the Archaean Neoproterozoic Terrane Boundary in Southern Granulite Terrain. Geol. Soc. India. 50: 297-317
- Binu-Lal SS, Sawaki T, Wada H, and Santosh M (2003) Ore fluids associated with Wynad gold mineralization, Southern India: evidence from fluid inclusion microthermometry and gas analysis. Journal of Asian Earth Sciences 22: 171-187
- Bowers T (1991) The deposition of gold and other metals: pressure induced fluid immiscibility and associated stable isotopic signatures, Geochim. Cosmochim. Acta 55: 2417–2434
- Boyle RW (1979) The geochemistry of gold and its deposits. Bull. Can.Geol. Surv. 280: 584
- Burnham CW (1979) Magmas and hydrothermal fluids, in Barnes, H.L.,ed. Geochemistry of hydrothermal ore deposits, 2nd.Wiley-interscience, New York. 71-136
- Burrows DR, Wood PC, Spooner ETC (1986) Carbon isotopic evidence for a magmatic origin for Archean gold- quartz vein ore deposits. Nature 321: 851-854
- Cameron EM (1988) Archean gold: relation to granulite formation and redox zoning in the crust. Geology 16: 109-112
- Cameron EM, Hattori Keiko (1987) Archean gold mineralization and oxidized hydrothermal fluids Economic Geology. 82(5): 1177-1191

- Campbell AC, Palmer MR, Klinkhammer GP, Bowers TS, Edmond JM, Lawrence JR, Casey JF, Thompson G, Humphris S, Rona P, Karson JA (1988) Chemistry of hot springs on the Mid-Atlantic Ridge. Nature 335: 514-519
- Card KD (1990) A review of the Superior Province of the Canadian Shield, a product of Archean accretion. Precambrian Res. 48: 99-156
- Chetty TRK (1996) Proterozoic Shear zones in Southern granulite Terrain, India. Gondwana Research Group Memoir (Ed. Santhosh M, Yoshida M). 3: 77-89
- Chown EH, N'dah E, Mueller WU (2000) The relation between iron-formation and low temperature hydrothermal alteration in an Archean volcanic environment. Precam. Re. 101: 263–275
- Colvine AC (1989) An empirical model for the formation of Archean gold deposits: Products of final cratonization of the Superior Province, Canada, in Keys, R.R., Ramsay, W.R.H., and Groves , D.I. eds., The Geology of Gold Deposits: The Perspective in 1988. Economic Geology Monograph 6: 37-53
- Colvine AC, Andrews AJ, Cherry ME, Durocher ME, Fyon AJ, Lavigne, MJ, MacDonald AJ, Marmont S, Poulsen KH, Springer JS, Troop DG (1984) An integrated model for the origin of Archaean lode gold deposits. Ontario.Geol. Surv. Open-file report 5524, 98p.
- Colvine AC, Fryon JA, Heather KB, Marmont S, Smith PM, Troop DG (1988) Archaean lode gold deposits in Ontario. Ontario Geol.Survey Misc. paper 139, 136p
- Coulibaly Y, Boiron MC, Cathelineau M, Kouamelan AN (2008) Fluid immiscibility and gold deposition in the Birimian quartz veins of the Angovia

deposit (Yaouré, Ivory Coast) Journal of African Earth Sciences 50 (2-4): 234-254

- Craw D, Koons PO, Zeitler PK, Kidd WS (2001) Fluid evolution and thermal structure in the rapidly exhuming gneiss complex of Namche Barwa-Gyala Peri, eastern Himalayan syntaxis. Journal Of Metamorphic Geology 23 (9): 829-845
- Crawford AR (1969) Reconnaissance Rb-Sr dating of the Precambrian rocks of Southern Peninsular India. Jour. Geol. Soc .India 10: 117-166
- Crawford ML (1981) Fluid inclusions in metamorphic rocks-low and medium grade. In short course on fluid inclusions: Applications to petrology, eds. Hollister, L.S. and Crawford, M.L. Mineralogical association of Canada 6: 157-181
- Crocket JH (1974) Gold. In: Wedepohl, K.H., ed.: Handbook of geochemistry: Berlin, Springer v. 2/5
- de Ronde CEJ, Faure K, Bray CJ, Whitford DJ (2000) Round Hill shear zone-hosted gold deposit, Macraes Flat, Otago, New Zealand: evidence of a magmatic ore fluid. Econ. Geol. 95: 1025-1048
- de Wit MJ (1998) On Archean granites, greenstones, Cratons and Tectonics, does the evidence demand a verdict? Precambrian Research 91: 181-226
- Derry LA, Jacobsen SB, (1990) The chemical evolution of Precambrian seawater: Evidence from REE in banded iron formations. Geochim. Cosmochim. Acta 54: 2965–2977
- Donnelly K.E, Goldstein SL, Langmuir CH, Speigelman M (2004) Origin of enriched ocean ridge basalts and implications for mantle dynamics, Earth and Planetary Science Letters, 226: 347-366

- Drury SA, Harris NBW, Holt RW, Reeves-Smith GJ, Wightman RT (1984) Precambrian tectonics and crustal evolution of South India. Journal of Geophysics 92: 3–20
- Dubé B And Gosselin P (2004) greenstone-hosted quartz-carbonate vein deposits (orogenic, Mesothermal, lode gold, shear-zone-related quartzcarbonate Or gold-only deposits) Geological Survey of Canada, Current Research 1-13
- Eisenlohr BN, Groves D, Partington GA (1989) Crustal-scale shear zones and their significance to Archaean gold mineralization in Western Australia Mineral. Mineralum Deposita 24: 1-8
- Foster RP (1985) Major controls of Archaean gold mineralization in Zimbabwe. Trans.Geol.Soc. S.Afr. 88: 109-133
- Foster RP (1985) Archaean gold mineralization in Zimbabwe: implications for metallogenesis and exploration. Economic Geology Monograph 6: 54-70
- Fryer BJ (1977) Rare earth evidence in iron formations for changing Precambrian oxidation states. Geochim. Cosmochim. Acta 41:361–367
- Ghosh JG, Davidek K, Hawkins D, Janadhan AS, Bowring S, De Wit MJ (1996) Geochronology Of the rocks from the Bhavani Shear Zone, South India. Implication for India Madagascar Reconstruction In: Santhosh M, Yoshida M (Eds.), Gondwana Research Group Misc. Pub. 4: 91-93
- Ghosh JG, Maarten J. de Wit, Zartman RE (2004) Age and tectonic evolution of Neoproterozoic ductile shear zones in the Southern Granulite Terrain of India, with implications for Gondwana studies Tectonics 23: 1-38
- Giritharan TS, Rajamani V (1999) Geochemistry of the metavolcanics of the Hutti - Maski Schist Belt: Implications to gold metallogeny in the eastern Dharwar craton. Journal of Geological Society of India 51: 583-594

- Giritharan TS, Rajamani V (2001) REE Geochemistry of ore zones in the Archean auriferous schist belts of the eastern Dharwar Craton, south India .Proc. Indian Academy of Sciences. (Earth Planetary Sciences) 110 (2): 143-159
- Goldfarb RJ, Groves DI, Gardoll D (2001) Orogenic gold and geologic time: A global synthesis: Ore Geology Reviews 18: 1-75
- Goldfarb RJ., Hart, C., Miller, M., Miller, L., Farmer, G.L.,Groves, D.I., (2000). The Tintina Gold Belt—a global perspective. The Tintina Gold Belt: Concepts, Exploration, and Discoveries. British Columbia and Yukon Chamber of Mines, Vancouver, 5–34
- Goldfarb RJ, Miller, L.D, Leach DL, Snee LW (1997) Gold deposits in metamorphic rocks of Alaska. Economic Geology Monograph 9: 151-190
- Goldfarb RJ, Newberry RJ, Pickthorn WJ, Gent CA (1991) Oxygen, hydrogen, and sulfur isotope studies in the Juneau gold belt, southeastern Alaska: Constraints on the origin of hydrothermal fluids. Econ. Geol. 86: 66-80
- Goldfarb RJ, Phillips GN, Nokleberg WJ (1998) Tectonic setting of synorogenic gold deposits of the Pacific Rim. Ore Geology Reviews Special Issue 13: 185-218
- Golding SD, Wilson AF (1987) Oxygen and Hydrogen isotope relationships in Archaean gold deposits of the Eastern gold fields Province, Western Australia: Constaints on Source of Archaean gold-bearing fluids. Univ. of W.Australia. Publ. 11: 203-214
- Gottfried D, Rowe JJ, and Tilling RI (1972) Distribution of gold in igneous rocks: U.S. Geological Survey Prof. Paper 727:42 p.
- Govett, GJS(1966) origin of banded iron formation. Geological Society of America Bulletin : 77 1191-1212

- Groves DI (1993) The crustal continuum model for late-Archaean lode-gold deposits of the Yilgarn Block, Western Australia. Mineral Deposita 28: 366-374
- Groves DI, Foster RP (1991) Archean lode gold deposits. In: Foster RP. (Ed.), Gold Metallogeny and exploration, Blackie and Son Ltd London
- Groves DI, Foster RP (1993) Archaean lode gold deposits In: Foster RP. (Ed.), Gold Metallogeny and Exploration, Chapman and Hall, London 63-103
- Groves DI, Goldfarb RJ, Gebre-Mariam M, Hagemann SG, Robert F (1998) Orogenic gold deposits: A proposed classification in the context of their crustal distribution and relationship to other gold deposit types. Ore Geology Reviews. Special Issue 13: 7-27
- Groves DI, Goldfarb RJ, Robert F, Craig JRH (2003) Gold Deposits in Metamorphic Belts: Overview of Current Understanding, Outstanding Problems, Future Research, and Exploration Significance. Economic Geology 98: 1–29
- Groves DI, Golding SD, Rock NMS, Barley ME, McNaughton NJ (1988) Archaean carbon reservoirs and their relevance to the fluid source for gold deposits. Nature 331: 254-257
- Groves DI, Phillips GN, Ho SE, Houston SM, Stand-ing CA (1987) Craton scale distribution of Archean greenstone gold deposits: predictive capacity of the metamorphic model. Economic Geology 82(8): 2045-2058
- Guha J, Lu H-Z, Dube B, Robert F, Gagnon M, (1991) Fluid characteristics of vein and altered wall rock in Archean mesothermal gold deposits. Economic Geology 86: 667–684.
- Hagemann SG, Brown PE (1996) Geobarometry in Archean lode-gold deposits. Eur. J. Mineral. 8: 937-960

- Hagemann SG, Cassidy KF (2000) Archean orogenic lode gold deposits, Gold in 2000, eds. S.G. Hagemann, P.E. Brown, Littleton, Co., Society of Economic Geologists 13: 9-68
- Hagemann SG, Gebre-Mariam M, Groves DI (1994) Surface-water influx in shallow-level Archean lode-gold deposits in Western Australia. Geology 22: 1067-1070
- Ho SE, Groves DI eds. (1987): Recent advances in understanding of pre-cambrian gold deposits. Gold.dept.Univ. Of W. Australia, publ. 11: 239-264
- Hodgson CJ, Hamilton JV (1989) Gold mineralization in the Abitibi greenstone belt: end-stage result of Archean collisional tectonics? Econ. Geol. Monograph 6: 86-100
- Hofmann AW and Hémond C (2006) The origin of E-MORB, Geochimica et Cosmochimica Acta Volume 70, Issue 18: A257
- Irvine, TN and Baragar WRA (1971) A guide to the chemical classification of the common volcanic rocks. Canadian Journal of Earth Sciences, 8: 523-548
- Isley AE (1995) Hydrothermal plumes and delivery of iron to banded iron formations. J. Geol. 103: 169–185
- Isley AE, Abbott DD (1999) Plume related mafic volcanism and the deposition of banded iron formation. J. Geophys. Res. 104: 15461–15477
- Jacobsen SB, Pimentel-Klose MR, (1988) A Nd isotopic study of the Hamersley and Michipicoten banded iron formations: thesource of REE and Fe in Archean oceans. Earth Planet Sci. Lett. 87: 29–44
- Kato Y, Kawakami T, Kane T, Kunugizat K, Swamy NS (1996) Rare-earth element geochemistry of banded iron formations and associated amphibolite

from the Sargur belts, South India Journal of Southeast Asian Earth Sciences 14 (314):161-164

- Keays RR, Scott RB (1976) Precious metals in ocean-ridge basalts: implications for basalts as source rocks for gold mineralization. Econ. Geol. 71: 705-720
- Kerrich R (1986) Archaean lode gold deposits of Canada, Part 1: Chararacterestics of hydrothermal systems and models of origin. Economic Geology Research Unit. Univ.of Witwatersand, Joganesburg, Inform, circ.183.34
- Kerrich R, and Cassidy KF (1994) Temporal relationships of lode gold mineralization to accretion, magmatism, metamorphism and deformation - Archean to present: A review: Ore Geology Reviews 9: 263-310
- Kerrich R, Fryer BJ (1979) Archean precious-metal hydrothermal systems, Dome mine, Abitibi greenstone belt. REE and oxygen isotope relations. Canadian Journal of Earth Sciences 16: 440-458
- Kerrich R, Goldfarb R, Groves D, Garwin S (2000) The geodynamic of world-class gold deposits: characteristics, space-time distribution and origins. SEG Reviews 13: 501-551
- Kerrich R, Wyman DA (1990) Geodynamic setting of mesothermal gold deposits: an association with accretionary tectonic regimes. Geology 18: 882-885
- Kerrick DM, Jacobs GK (1981) A modified Redlich-Kwong equation for H_2O, CO_2 and H_2O-CO_2 mixtures at elevated pressures and temperatures. American Journal of Science 281: 735-767

- Krogstad E.J, Balakrishnan, S, Mukhopadhyay, DK., Rajmiani V and Hanson, G.N. (1989). Plate tectonics. 2.5 billion years ago: Evidence at Kolar, South India. A report. Science 243:1337-l340
- Kusky TM, Polat A (1999)Growth of granite–greenstone terranes at convergent margins, and stabilization of Archean craton, Tectonophysics 305: 43–73
- Le Bas MJ and Streckeisen A (1991) The IUGS systematics of igneous rocks. Journal.of Geological. Society. London 148
- Loucks RR, Mavrogenes JA (1999), Gold solubility in supercritical hydrothermal brines measured in synthetic fluid inclusions. Science 284: 2159–2163
- Malathi MN, Srikandappa C (2005) Composition and evolution of fluids and timing of gold mineralization in the Malapuram-Gudalur and Bhavani shear zone, Nilambur, Kerala. Journal Geological Society of India 65: 689-702
- Mani G (1965) Report on the systematic mapping and mineral survey of Attappadi valley and adjacent hill tracts, Palakkad district, Kerala state. Unpublished progress report geological survey of India
- Mao J, Wang Y, Li H, Pirajno F, Zhang C , Wang R (2008) The relationship of mantle-derived fluids to gold metallogenesis in the Jiaodong Peninsula: Evidence from D–O–C–S isotope systematic. Ore Geology Reviews 33: 361–381
- McCuaig TC, Kerrich R (1998) P-T-t-deformation-fluid characteristics of lode gold deposits: evidence from alteration systematics. Ore Geol. Rev. 12: 381-453
- Meissner B, Deters P, Srikantappa C, Kohler H (2002) Geochronological evolution of the Moyar, Bhavani and Palghat Shear Zones of southern India:

Implications for East Gondwana correlations, Precambrian Research 114: 149-175

- Michard A and Albarede F (1986) The REE content of some hydrothermal fluids. Chem. Geol. 55: 514
- Mikucki EJ (1998) Hydrothermal transport and depositional processes in Archean lode-gold systems: a review. Ore Geology Reviews 13: 307-321
- Mikucki EJ (1998) Hydrothermal transport and depositional process in Archean lode gold systems: a review. Ore Geology Reviews 10: 31–50
- Mikucki EJ, Groves DI (1990) Genesis of primary gold deposits: gold transport and depositional models. Geology Department and University Extension, The University of Western Australia Publication 20: 212–220
- Mikucki EJ, Ridley JR (1993) the hydrothermal fluid of Archean lode gold deposits at different metamorphic grades: compositional constraints from ore and wallrock alteration assemblages. Mineralium Deposita 28: 469–481
- Misra KC (2000) Understanding mineral deposits. Kluwer Academic Publishers, Netherlands p845
- Morasse S, Wasteneys HA, Cormier M, Helmstaedt H, Mason R (1995) A pre-2686 Ma intrusion-related gold deposit at the Kiena mine, Val d'Or, Québec, southern Abitibi Subprovince. Economic Geology 90: 1310-1321
- Moritz R, 2000, What have we learnt about orogenic lode gold deposits over the past 20 years? A GEODE-GeoFrance 3D workshop on orogenic gold deposits in Europe with emphasis on the Variscides, Orleans, France, 7-8 November 2000, Extended abstracts 17-23

- Moritz RP, Crocket JH, Dickin AP (1990) Source of lead in the gold-bearing quartz- fuchsite vein at the Dome mine, Timmins area, Ontario, Canada. Mineral. Deposita 25: 272-280
- Morris RC (1993) Genetic modelling for banded iron formation of the Hamersley Group, Pilbara Craton, Western Australia. Precambrian Research 60: 243–286
- Mukhopadhyay, D. (1986), Structural pattern in the Dharwar Craton, J. Geology, 94, 167 – 186
- Naden J, Shepherd TJ (1989) Role of methane and carbon dioxide in gold deposition, Nature 342: 793–795
- Nair MM, Nair RVG (2001) Strategies for gold exploration in virgin high grade terrains of Attappadi valley, Kerala. Geol. Surv. India spec. pub. 58: 181-190
- Nair NGK, Santosh M, Mahadevan R (1987) Lateralization as a possible contributor to gold placers in the Nilambur Valley, Southwest India. Chemical Geology 60: 309–315
- Nair RVG and Rao , VG (1990) Report on search for sheelite mineralization in parts of Attappadi, palakkad District, Kearala, Progress report Geological Survey of India
- Nair RVG (1993) Primary gold mineralization in Attappadi valley Palakadu district, Kerala. Geological Society of India 41: 387
- Nair RVG, Maji AK (1995) Targeting gold prospects by panning and soil sampling from Attapadi Valley, Kerala. Indian Minerals. 49: 131-142
- Nair RVG, Nair MM (2004) Attappadi Supracrustals-A probable Greenstone belt in the Southern Granulite terrain. Indian minerals 58 (3-4): 143-156

- Nair RVG, Nair MM, Maji AK (2005) Gold mineralization in Kottathara prospect Attappadi valley, Kerala, India; A primary appraisal. Gondwana Research Group 8(2) : 203-212
- Nair RVG, Nair MM, Subramanian CS (1996) Gold mineralization in Puttumala area of Attappadi valley, Kerala. Geological Survey of India Special Publication 40: 155-167
- Nambiar AR (1982) Report on the geological mapping and geochemical exploration of precious metals in parts of Attappadi area, Palakkad district, Kerala state. Unpublished progress report geological survey of India
- Nawaratne SW, Dissanayake CB (2001) Gold occurrences in Madagascar, South India and Sri Lanka: significance of a possible Pan-African event. Gondwana Research 4(3) 367-375
- Nesbitt BE (1991) Phanerozoic gold deposits in tectonically active continental margins. In: Foster RP (Ed.), Gold metallogeny and exploration, Blackie and Son, Glasgow and London 104-132.
- Nesbitt BE, Muehlenbachs K (1989) Origins and movements of fluids during deformation and metamorphism in the Canadian Cordillera. Science 245: 733–736
- Nesbitt BE, Murowchick JB, Muehlenbachs K (1986) Dual origins of lode gold deposits in the Canadian Cordillera. Geology 14: 506-509
- Neumayr P, Groves DI, Ridley JR, Koning CD (1993) Syn-amphibolite facies Archaean lode gold mineralisation in the Mt. York District, Pilbara Block, Western Australia. Mineral. Deposita 28: 457-468
- Panchapakesan V, Pandalai HS, Srivasthava RK, Krishnamurthi R, Jadhav GN (1996) A note on fluid inclusions in mesothermal gold deposits of Archaean

greenstone belts. In National workshop on Gold resources of India, held at N.G.R.I, Hyderabad 274-280

- Pandalai HS, Jadha GN, Mathew B, Panchapakesan V, Krishnam Raju K, Patilm ML (2003) Dissolution channels in quartz and the role of pressure changes in gold and sulfide deposition in the Archean, greenstone-hosted, Hutti gold deposit, Karnataka, India. Mineralium Deposita 38: 597–624
- Pearce JA (1982) Trace element characteristics of lavas from destructive plate boundaries. In Andesites: Orogenic Andesites and Related Rocks (R.S. Thorpe, ed.). John Wiley & Sons, Chichester, U.K. 525-548
- Pearce JA, Harris NBW and Tindle AG (1984) Trace element discrimination diagrams for the tectonic interpretation of granitic rocks. Journal of Petrology, 25: 956-983
- Penczak RS, Mason R (1997) Metamorphosed Archean epithermal Au-As-Sb-Zn-(Hg) vein mineralization at the Campbell mine, northwestern Ontario. Econ. Geol. 92: 696-719
- Perring CS, Groves DI, Ho SE (1987) Constrains on the source of auriferous fluids for Archaean lode gold deposits. Univ.W.Australia publ.11: 287-306
- Peters SG, Golding SD, Dowling K (1990) Mélange and sediment-hosted gold-bearing quartz veins, Hodgkinson Gold Field, Queensland, Australia. Econ. Geol. 85: 312-327
- Pettke T, Diamond LW, Kramers JD (2000) Mesothermal gold lodes in the north-western Alps: A review of genetic constraints from radiogenic isotopes. Eur. J. Mineral. 12: 213-230
- Peucat JJ, Mahabaleshwar R, Jayananda M (1993) Age of younger tonalitic magmatism and granulite metamorphism in the south Indian transition zone,

Krishnagiri area, comparison with older Peninsular gneiss from the Gorur-Hassan area. J Metamorphic Geol 11: 879–888

- Peucat JJ, Vidal P, Bernard-Griffiths J, Condie KC (1989) Sr, Nd, and Pb isotopic systematics in the Archean low- to high-grade transition zone of southern India: syn-accretion versus post-accretion granulites. J Geol 97: 537–550
- Phillips G N, Powell R (1993) Link between gold provinces. Economic Geology 88(5): 1084-1098
- Phillips GN (1986) Geology and alteration in Golden Mile, Kalgoore. Econ. Geol. 81: 779-808
- Phillips GN (1993) Metamorphic fluids and gold, Mineralogical Magazine 57: 365–374
- Phillips GN, Evans KA (2004) Role of CO2 in the formation of gold deposits. Nature 42: 860-863
- Phillips GN, Groves DI (1983) The nature of Archaean gold bearing fluids as deduced from the deposits of Western Australia. Geol.Soc. Aus.J. 30: 25-39
- Phillips GN, Groves DI (1984) Fluid access and fluid wall-rock interaction in genesis of Archaean gold-quartz vein deposit at Hunt mine, Kambalda, Western Australia. In Gold'82: The Geology, Geochemistry and Genesis of Gold Deposits, ed. Foster RP, Balkema, Rotterdam 389-416
- Poulsen KH, Card KD, Franklin JM (1992) Archean tectonic and metallogenic evolution of the Superior Province of the Canadian Shield. Precambrian Res. 58: 25-54
- Poulsen KH, Robert F, Dubé B (2000) Geological classification of Canadian gold deposits. Geological Survey of Canada, Bulletin 540: 106p.

- Radhakrishna BP, Curtis LC (1999) Gold in India Bangalore: Geological Society of India
- Radhakrishna BP, Naqvi SM (1986) Precambrian continental crust of India and its evolution. J. Geol. 94: 145 – 166
- Radhakrishna T, Pearson DG, Mathai J (1995) Evolution of Archean southern Indian lithospheric mantle:A geochemical study of Proterozoic Agali – Coimbatore dykes. Mineral. Petro. 121: 357-363
- Rainaud C, Master S, Armstrong RA, Robb LJ (2003) A cryptic Meso-Archaean terrane in the basement to the Central African Copperbelt. Journal of the Geological Society 160 (1): 11-14
- Raith MM, Srikantappa C, Buhl D, Kaehler H (1999) The Nilgiri enderbites, south India: Nature and age constraints on protolith formation, high grade metamorphism and cooling history. Precambrian Res. 98: 129-150
- Ramakrishnan M (2003) Craton mobile belt relations in southern granulite terrain. In: Mem.Geol.Soc.India (Ed. Ramakrishnan M) 50: 297-317
- Ramakrishnan M. (1993) Tectonic evolution of the granulite terrain of southern India. Geol. SOC. India, Mem. No. 25: 35-44
- Ramakrishnan M and Vaidyanadhan R (2008) Geology of India. Geological Society of India, Volume 1, 556p
- Rao DR. and Rai H (2006) Signatures of rift environment in the production of garnet-amphibolites and eclogites from Tso-Morari region, Ladhakh, India: A geochemical study.
- Ridley JR, Diamond LW (2000) Fluid chemistry of orogenic lode gold deposits and implications for genetic models, in Gold in 2000. Reviews in Economic Geology 13: 141-162

- Robb L (2005) Introduction to ore-forming processes Blackwell publishing company USA 373p
- Robert F, Kelly WC (1987) Ore-forming fluids in Archean gold-bearing quartz veins at the Sigma Mine, Abitibi Greenstone Belt, Quebec,Canada. Economic Geology 82: 1464–1482
- Rock NMS, Groves DI, Perring CS, Golding SD (1989) Gold, lamprophyres, and porphyries: what does their association mean? Econ. Geol. Monograph 6: 609-625
- Rock NSM, Groves DI (1988) Can lamprophyres resolve the genetic controversy over mesothermal gold deposit? Geology 16: 538—541
- Rodder E (1984) Fluid inclusions: Mineralogical Society of America. Reviews in Minerology 12: 644p
- Rogers JJW, Giral RA (1997) The Indian Shield, in Greenstone Belts, Oxford Monogr. Edited by de Wit M, Ashwal L Geol. Geophys. Oxford Univ. Press, New York. 35: 620 – 635
- Romberger, S.B. (1984) Transport and deposition of gold in hydrothermal systems at temperatures up to 300°C. Geol. Soc. America Abstracts with Programs 14:602
- Saager R, Meyer M, Muff R (1982) Gold distribution in supracrustal rocks from Archaean greenstone belts of southern Africa and from Palaeozoic ultramafic complexes of the European Alps: metallogenic and geochemical implications: Econ. Geol. 77:1-24
- Saini NK, Mukherjee PK, Rathi MS,Khanna, PP and Purohit KK (1998) A new geochemical reference sample of granite (DG-H) from Dalhousie, Himachal Himalaya. Journal of Geological Society of India 52: 603-606

- Sangurmath P (2005) Geology and gold mineralization in Buddini gold deposit, Hutti-Maski Greenstone Belt, Karnataka. Journal Geological Society of India 66: 552-560
- Santosh M, Nadeau S, Javoy M (1995) Stable isotopic evidence for the involvement of mantle-derived fluids in Wynad gold mineralization, South India. Journal of Geology 103: 718–728
- Santosh M, Omana PK, Yoshida M (1990) Gold grains in laterite weathering profiles of Nilambur, South India and a model for the genesis of supergene gold deposits. Journal of Mineralogy, Petrology & Economic Geology 85: 416-423
- Santosh M, Yoshida M (1991) Fluid phase petrology of Antarctic charnockites from the Lützow-Holm Bay, implications for carbonic metamorphism. Mineralogy Journal 15: 175–181
- Sawarkar AR (1980) Geological and geomorphological features of Nilambur Valley, Kozhikode district, Kerala, with special reference to the alluvial gold deposits in the area. Geol. Surv. India Spec. Publ. 5: 29–38
- Seward TM (1973) Thio complexes of gold and the transport of gold in hydrothermal ore solutions. Geochimica et Cosmochimica Acta 37: 370-399
- Seward TM (1984) The transport and deposition of gold in hydrothermal systems: Gold'82': the geology, geochemistry and genesis of gold deposits: proceedings of symposium gold '82'
- Shabeer KP, Satish Kumar M, Armstrong R, Buick IS (2004) Constraints on the timing of Pan-African granulite-facies metamorphism in the Kerala Khondalite Belt of southern India: SHRIMP mineral ages and Nd isotopic systematics Journal of Geology 113(1): 95-106

- Sharma R (2006) Nature of fluids and regional implications for lesser Himalayan carbonotites and associated mineralization. Journal of Geochemical Exploration 89: 363-367
- Shelton KL, So C-S, Chang JS (1988) Gold-rich mesothermal vein deposits of the Republic of Korea: Geochemical studies of the Jungwon gold area. Econ. Geol. 83: 1221-1237
- Shimizu H, Umemoto N, Masuda A, Appel PWU (1990) Sources of iron formations in the Archean Isua and Malene supracrustals, West Greenland: Evidence from La-Ce and Sm- Nd isotopic data and REE abundances. Geochim. Cosmochim. Acta 54: 1147–1154
- Sibson RH, Robert F, Poulsen KH (1988) High angle reverse fault, fluid-pressure cycling and mesothermal gold-quartz deposits. Geology 15: 701-704
- Sibson, R.H., Robert, F and Poulsen, K.H (1987): High angle reverse fault, fluid-pressure cycling and mesothermal gold-quartz deposits. Geology, 15, 701-704
- Sivasiddaiah N, Rajamani V (1989) The geologic setting, mineralogy, geochemistry and genesis of gold deposits of the Archaean Kolar Schist Belt, India. Econ. Geol. 84: 2155–2172
- Sivasiddaiah N, Rajamani V (1994) Rare Earth Element evidence for syngenetic origin of an Archean Stratiform gold sulfide deposit, Kolar Schist Belt, South India. Economic Geology 89: 1152-1566
- Smith T.J.and Kesler S.E., (1985). Relation of fluid inclusions geochemistry to wall rock alteration and lithogeochemical zonation at the Hollinger-McIntyre gold deposit, Timmins, Ontario, Canada. Canadian Institute of Mining Metallurgical Bulletin 34, 35–94

- So C-S, Yun S-Y (1997) Jurassic mesothermal gold mineralization of the Samhwanghak Mine, Youngdong area, Republic of Korea; constraints on hydrothermal fluid geochemistry. Econ. Geol. 92: 60-80
- Spooner ETC, Bray CJ, Wood PC, Burrows DR, Callan NJ (1987) Au-qtz vein and Cu-Ag-Mo-anhydrite minreralizations, Hollinger-McIntyre Mine, Timmins, Ontario. δ 13Cvalues, fluid inclusion gas geochemistry, pressure estimation and H2O-CO2 phase separation as a precipitation and dialation mechanism. Onatio Geol. Surv.Mis.Paper 136: 36-56
- Srikantappa C, Srinivas G, Basavarajappa HT, Prakash Narasimha KN, Basavalingu B (2003) Metamorphic evolution and fluid regime in the deep continental crust along the N-S geotransect from Vela to Dharmapuram, Southern India, in Mem.Geol.Soc.India (ed Ramakrishnan M), 50: 319-373
- Sun S and McDonough, WF (1989) Chemical and isotopic systematics of ocean basalts: implications for mantle composition and processes. In: A.D.N. Saunders, M.J. (Editor), Magmatism in the Ocean Basins. Geological Society of London Special Publication. Geological Society of London 313-345
- Sylvester PJ, Harper GD, Byerly GR, Thurston PC, (1997) Volcanic aspects. In: de Wit, M., Ashwal, L.D. (Eds.), Greenstone Belts. Oxford Monogr. Geol. Geophys. 35: 55–90
- Thurston PC, Chives KM (1990) Secular variation in greenstone sequence development emphasizing Superior Province, Canada. Precambrian Res. 46: 21-58
- Tilling RI, Gottfried D, Rowe JJ (1973) Gold abundance in igneous rocks: bearing on gold mineralization. Econ. Geol. 68:168-186

- Vearncombe JR, Barley ME, Eisenlohr B, Groves DI, Houstoun SM, Skwarnecki MS, Grigson MW and Partington GA (1988) Structural controls on mesothermal gold mineralization; Examples from the Archaean terrains of south Africa and western Australlia. In Bicentennial Gold'88, Extended Abstracts Oral Programme. Geol.Soc.Aust.Inc.Abstr. 22: 19-23
- Viswanathan TV, Gopalakrishnan K, Genesan TM, Raman R (1990) .Cauvery suture zone :its implications, extended abstract group discussion on sututre zone young and old Abstract, Wadia Institute of Himalayan geology, Dehradun.
- Walsh JF, Kesler SE, Duff D, Cloke PL, (1988) Fluid inclusion geochemistry of high-grade vein-hosted gold ore at the Pamour Mine, Porcupine Camp, Ontario. Economic Geology 81: 681–703
- White RS and McKenzie DP (1989) Magmatism at rift zones: the generation of volcanic continental margins and flood basalts. Journal of Geophysical Research 94:7685-7729. Streckeisen A(1976) To each plutonic rock its proper name, Earth Science Review 12:1-33
- Witt WK, Knight JT, Mikucki EJ (1997) A synmetamorphic lateral fluid flow model for gold mineralization in the Archaean southern Kalgoorlie and Norsemen terranes, Western Australia. Economic Geology 92: 407–437
- Yudovskaya MA, Distler VV, Chaplygin IV, Mokhov AV, Trubkin NV, Gorbacheva SA (2006) Gaseous transport and deposition of gold in magmatic fluid: evidence from the active Kudryavy volcano, Kurile Islands Mineralium Deposita 40: 828–848
- Zachariah J K (1992) Geochemistry and petrogenesis of amphibolites from Ramagiri Gold Fields, Dharwar Craton, south India. Jawaharlal Nehru University, New Delhi, India

- Zachariah JK, Hanson GN, Rajamani V (1995) Post crystallization disturbances in the Nd and Pb isotope sys- tems of metabasalts from the Ramagiri schist belt, south India. Geochimica Cosmochimica Acta 59: 3189-3203
- Zachariah JK, Mohanta MK, Rajamani V (1996) Accre- tionary evolution of the Ramagiri schist belt, eastern Dharwar craton. J. Geol. Soc. India 47: 279-291
- Zhang Y, Frantz JD (1989) Determination of homogenization temperature and densities of supercritical fluid in the system NaCl–KCl–CaCl2–H2O using synthetic fluid inclusions. Chemical Geology 64, 335–350